JNMM
Journal of Nuclear Materials Management

JNMM

Journal of Nuclear Materials Management
Winter 2005, Volume XXXIII, No. 2

Topical Papers

Institute News

Departments

INMM
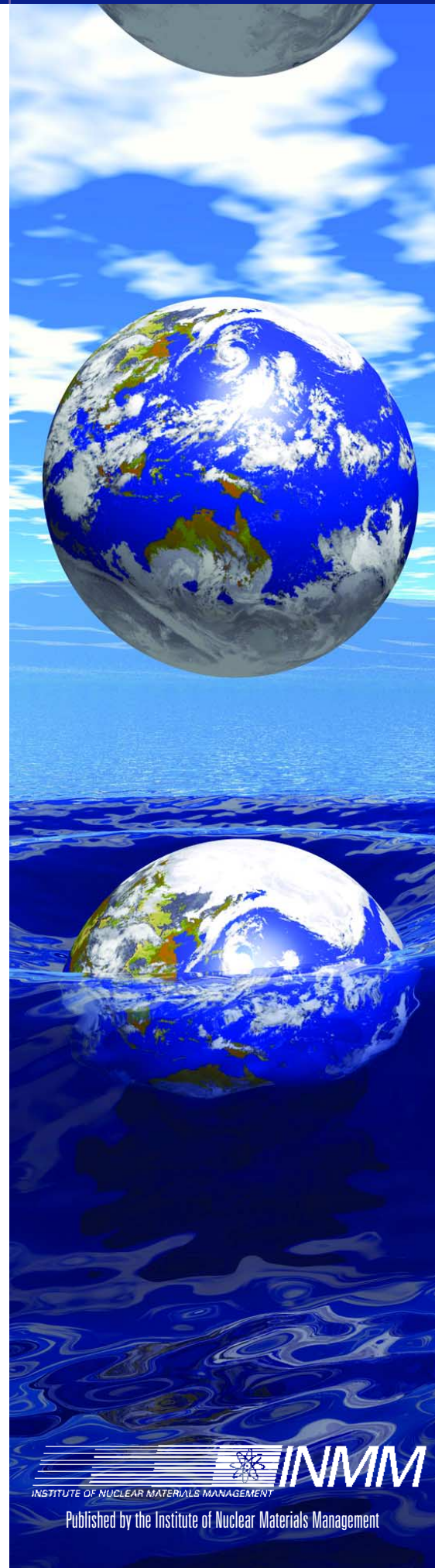*INSTITUTE OF NUCLEAR MATERIALS MANAGEMENT*

Geometrically Controlled Partially Filled Interrogation Volume: A Nontraditional Approach to ^{235}U Enrichment Measurement by Portable Germanium Spectrometer

J. Brent Montgomery
United States Enrichment Corporation, Paducah, Kentucky U.S.A.

Abstract

Enrichment measurements to determine ^{235}U content in UF_6 for nuclear material control and accountability (NMC&A) are easily performed via the gamma spectrometry enrichment meter method for large cylinders containing a wide range of enrichments. In this work, the same method has been applied to measuring small sample cylinders. The prohibitively large negative bias imposed by the incomplete filling of the detector's view has been overcome by calibrating with the same type of cylinder as that containing the sample. Normally, the system is calibrated with sources such as the NBS-SRM-969 U_3O_8 standards. Viewed from the end by a small diameter Germanium detector, these standards are essentially infinitely thick and wide with respect to the 185.7 keV gamma peak due to the self-shielding of the U_3O_8. In other words, the entire view of the detector is filled. This requires that the geometry of the sample be such that it covers the entire region of interrogation of the detector or a calculation to offset the void area is performed. The latter proves to be very cumbersome.

In this work, calibration was performed using UF_6 standards with certified ^{235}U enrichments contained in type 1S cylinders. The samples measured were also contained in 1S cylinders. Even though a significant portion of the detector's view was void of UF_6, the geometry of the material was held constant for the standards and samples resulting in highly successful measurements. A positioning device was utilized to couple the cylinder to the detector face, resulting in geometrical reproducibility. The result was an extremely low bias and standard deviation of the enrichment measurements while maintaining the speed of the enrichment meter method.

Introduction

Recent world events, specifically related to terrorism, have brought more sharply into focus the imperative nature of tight controls on fissile material. Nuclear material control and accountability (NMC&A), verification, or confirmatory, measurements of enriched uranium, and their accuracy have thus become increasingly important. Nuclear criticality safety (NCS) concerns have also increased with an ever-changing uranium enrichment industry in the United States and the demands imposed by a more competitive market as well as an aggressive campaign to convert highly enriched weapons grade uranium into reactor fuel. These factors have led to a significant increase in receipts of uranium hexafluoride (UF_6) as well as an increase in the ^{235}U enrichment of material received at the processing facility. Sample cylinders (type 1S) of the incoming UF_6 are also received and must have confirmatory analysis to verify the enrichment of the sample for NCS controls and as a pre-confirmation of the parent cylinder. At the Paducah Gaseous Diffusion Plant (Paducah, Kentucky), a facility with an U.S. Nuclear Regulatory Commission (NRC) license to operate at or below 5.5 wt percent ^{235}U, the NCS procedures require that a sample cylinder must be confirmed (including all measurement uncertainty) to contain UF_6 at or below that level. If the cylinder contains 5.0 wt percent, adding the known bias and required uncertainty (2 relative standard deviations) to measured results can easily surpass 5.5 wt percent if the bias and precision of the method are poor. The result of these factors is the need for nondestructive enrichment measurement capability for sample cylinders that is highly precise and accurate without sacrificing speed of analysis.

The Multigroup Gamma Analysis for Uranium (MGAU) method[1,2] produces accurate results and is well suited for the thin cylinder wall of the type 1S cylinder. However, it can only be used for UF_6 in which the ^{238}U and ^{234}Th (daughter of ^{238}U) has attained equilibrium. This requires several months after processing and thus is not useful for samples received only a few weeks after filling. Utilization of the enrichment meter method[3-5], relying solely upon the 185.7 keV peak, with a germanium detector has proven to be a reliable method for confirmatory analysis. The IMCA (Inspection Multi-Channel Analyzer), a highly portable system developed by Canberra, specifically the Portable Multi-Channel Analyzer with Germanium detector (PMCG)[6] has demonstrated improved performance in confirmatory measurement.[7] The setback of the enrichment meter method is that the system traditionally relies upon calibration with standards of infinite thickness with respect to the detector field of view (interrogation volume) in the 185.7 keV region, assuming that the interrogation volume will be filled when analyzing samples, as well. This is not the case when analyzing sample containers such as type 1S cylinders. In this case, because of the small diameter of the container, a significant portion of the interrogation volume is

outside the cylinder wall resulting in a large negative bias in the calculated enrichment. Also, a reduction in measured gamma counts results from an effective increase in the metal thickness traversed by gamma rays from the outer edge of the interrogation volume due to the curvature of the cylinder. Calculations to compensate for these factors could be performed but would lead to added uncertainty in the measurement. More recently, small coaxial high-purity germanium (HPGe) detectors were used with FRAM isotopic software[8] to supplement the enrichment meter method. The analysis time was greater than that desired for rapid determination of large sample batches of the 1S's mentioned above. The precision and accuracy of all methods thus discussed proved to be lower than that needed for the described analysis.

The PMCG, however, has been utilized successfully in this work by controlling the geometry of the measurement system such that the filled and unfilled portions of the interrogation volume remain constant for both standard and sample analysis. This was accomplished through the use of traceable UF_6 standards in the same type cylinders (1S) as the samples to be analyzed. Cylinder positioning reproducibility was ensured through the use of simple positioning hardware, the Axis Linking EXtension (ALEX). ALEX is nothing more than a cross-drilled polymer pipe, fabricated in-house, that slides over the detector head to hold the sample cylinder perpendicular to the detector. Rigor employed in cylinder thickness measurements was also imperative to the precision needed for this work. Benefits to this method include the following:

- Allows use of the enrichment meter method, quicker and less rigorous than use of the broad spectrum for gamma analysis
- A relatively short analysis time as compared to destructive methods normally utilized for sample cylinders such as gas source mass spectrometry (GS-MS) or thermal ionization mass spectrometry (TIMS). Also, in this work, the UF_6 was not allowed to be released to the laboratory until the confirmatory analysis was complete, ensuring that the ^{235}U enrichments were < 5.5 wt percent.
- There is no calculation for the conversion from U_3O_8 to UF_6 necessary since the standards and samples are both UF_6. This reduces uncertainty in the measurement.
- There is no absorber used in the calibration such as a known thickness of metal to mimic the cylinder wall since the standard is contained in a cylinder. This results in higher analytical counts and reduced uncertainty in the measurement.
- It is not necessary to correct for the standard container since it is the same composition as the sample cylinder. This reduces uncertainty in the measurement.
- ALEX utilized for reproducible cylinder positioning makes setup extremely quick and easy.

This work demonstrates that the enrichment meter method utilized for partially filled interrogation volumes generates results that far surpass uncertainty requirements. Hence, small sample cylinders may be quickly and nondestructively analyzed for ^{235}U

enrichment with confidence in high precision and accuracy.

Measurement System

The measurement system used in this work is the Canberra Industries IMCG (inspection multi-channel analyzer with germanium detector), an all-in-one system comprised of the Inspector Multi-Channel Analyzer, germanium detector, and the associated software. Three of these systems were utilized, configured as follows:

Detector	Low-energy germanium (LEGe), 500 mm2 active area planar germanium, 25.2 mm diameter × 15 mm thickness; systems 1 and 2 operated at a bias of − 2000 V; system 3 operated at a bias of −1500 V
MCA	InSpector 2000 (IN2K) portable multi-channel analyzer (MCA), 4,096 channels, 185.7 keV peak centered at channel 2,476
Software	IMCA 2000 operated in the GENIE 2000 environment, communication with MCA via USB
Computers	IBM ThinkPad i Series 1400, Windows 98 (systems 1 and 2) HP Omnibook 6100, Windows XP (system 3)
Ultrasonic	Krautkramer Branson—Model DM4 DL
Thickness Gauges	Krautkramer—Model DM4 E
ALEX	Polymer pipe–Internal diameter (~75 mm) sized to slide over the detector head with a hole (~40 mm) drilled perpendicular to the lengthwise axis of the pipe to accept the 1S cylinder. Total length - ~ 4 s''. Polycarbonate and PVC were both utilized in this work.

The highly automated system included total computer control of the MCA[9] and automatic data storage and analysis through a preset region of interest containing the 185.7 keV peak. The software handled immediate calibration constants upon standard analysis or through the use of spectral files.

Calibration

Calibration was performed against a series of UF_6 standards contained in type 1S cylinders (Table 1). The standard ^{235}U enrichment values were assigned by the analytical laboratory at the Portsmouth Gaseous Diffusion Plant (Piketon, Ohio). They were analyzed using two independent gas mass spectrometers via the ASTM Double Standard Method with standard materials traceable to the National Bureau of Standards (NBS) and the National Institute of Standard Technology (NIST).

Each standard was analyzed five times during the calibration with a measurement time of five minutes. All measurements were included in the generation of the calibration constants. The standard cylinders (and later, sample cylinders) were all measured in the same orientation, valve arbitrarily toward detector to keep the interrogation area constant. This allowed for quick thickness measuring without the necessity of demarcating the cylinder each time. This reduced the possibility of performing the enrichment measurement in an area of the cylinder that was different from

Table 1: UF$_6$ standard data

Type 1S Cylinder #	Enrichment (wt percent ^{235}U)	UF$_6$ Mass (g)
973410	3.223 +/- 0.002	445.7
973694	3.999 +/- 0.002	436.1
973769	4.947 +/- 0.003	434.8
973735*	4.490 +/- 0.002	440.1

* Performance check standard

where the thickness was measured. It was convenient to use the area of the cylinder that is at the height of the detector window with the cylinder resting on the bench. Also, the curved bottom of the cylinder was avoided because the thickness is much greater and less homogeneous. Five thickness measurements were taken and averaged avoiding any area that displayed non-homogeneity.

The cylinders were held in reproducible geometrical alignment during analysis through use of the ALEX positioning device. Graphical representation (figures 1 and 2) of the detector interrogation volume with respect to the sample cylinder demonstrates the importance of this reproducibility. If the cylinder was not aligned reproducibly, the geometry of the filled and unfilled regions of the interrogation volume would change significantly resulting in variations in the 185.7 keV peak. Both PVC and polycarbonate pipes were used as material to fabricate the ALEX, inconsequentially, since it is not inside the interrogation volume. It was not necessary to use an absorber since the standards were contained in the same type cylinder as the samples.

The software[10] automatically generated the calibration constant (K) for the determination of sample enrichment (E) according to the following equation:

$$E = K * R * CF_{mat} * CF_{mT}$$

Where: R = Net count rate @ 185.7 keV

CF_{mat} = Matrix material composition correction factor, tabulated values calculated relative to the calibration standard matrix material (internal to software)

CF_{mT} = Container wall correction coefficient = e^{mT}

m = Linear attenuation coefficient of the container

T = Container wall thickness

The IMCA 2000 software automatically applied a correction for container wall thickness. For this work, it was not necessary to correct for material matrix, container wall composition or for an

Figure 1. Graphical representation of the analytical setup with cutout view of the detector interrogation volume (shaded)
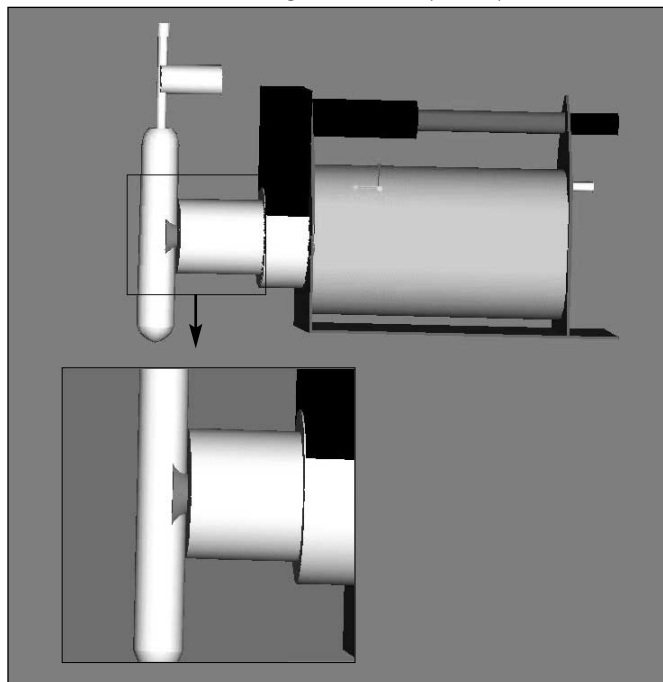
Figure 2. Graphical representation of the analytical setup from the end with the unfilled portion of the detector interrogation volume shaded
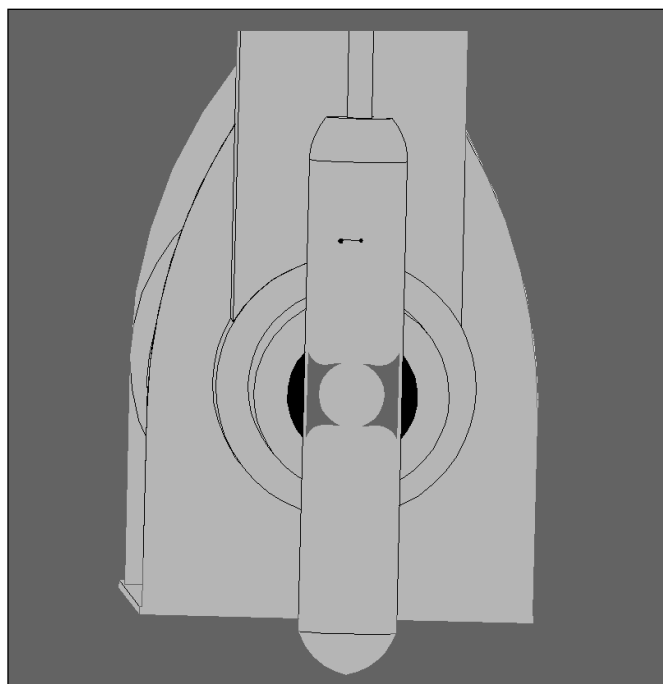
absorber used to simulate the sample container since the sample container was the same type as the standard container.

1S Cylinder Measurements

After calibration, a series of at least thirty measurements of the performance check standard were taken. From these, the standard deviation (σ) was determined and performance limits set up with the warning at the average +/- 2 σ and control at the average +/- 3 σ. The performance check standard was analyzed immediately before and after each sample measurement batch.

Multiple measurements (~120) of the standards were made to estimate the bias and precision of the system prior to analyzing samples. In order to maintain conservatism, the results of samples measured plus the bias and 2σ from the standard with the largest uncertainty had to be less than 5.5 wt percent in order to release samples. These uncertainty values were updated as results from sample analysis were generated and tag values confirmed by the GS-MS laboratory at the gaseous diffusion plant (PGDP) in Paducah, Kentucky.

The calibration and determination of performance limits, bias and σ were performed in the laboratory. Each sample measurement session was performed in the receiving area where the 1S cylinders were removed from the department of transportation (DOT) overpacks. The DOT overpacks were taken into account for NCS spacing requirements prior to removal. By analyzing the cylinders immediately upon removal from the overpacks, prior to intraplant transport, the possibility for interaction with other fissile material was limited until the enrichment had been verified. Cylinders, normally received in shipments of twenty to thirty-five, were routinely analyzed in two or more analytical batches with a defined maximum of twenty. These batches were analyzed simultaneously using two different instruments, each sample analyzed with a single five-minute measurement. The entire measurement apparatus during sample analysis is shown in Figure 3. The sample, as well as standard, cylinders (constructed of nickel) were ~8.5" (not including the valve) in length, ~1.5" in

Figure 3: Measurement system including the LEGe detector, MCA, computer, and sample cylinder. The sample cylinder is held in place with the ALEX attachment ensuring geometrical reproducibility.

diameter with ~1/8" wall thickness. The sample analysis setup was identical to that employed during the calibration session. All thickness measurements were made after either calibrating the thickness gauge or ensuring the accuracy thereof against a certified five step test block, traceable to NIST. The test block was also measured after analysis of the sample batch. The requirement was for these measurements to be +/- 0.003" of the certified value. Five measurements of each thickness were averaged, as during the calibration, to reduce uncertainty. The importance of accurate thickness measurements cannot be overstated. For example, an error of 0.1 mm on a thickness of 3 mm can bias a result as much as 0.1 wt percent (2 percent error relative to a 5 wt percent ^{235}U enrichment). For this reason, frequent thickness gauge calibration and calibration checks were performed followed by the averaging of multiple measurements for all cylinders.

Between the dates of June 12, 2002, and July 10, 2003, measurements were performed on 795 UF$_6$ samples contained in

Table 2: Measurement results summary

Number of cylinders measured	Accepted enrichment (wt percent ^{235}U)*	Measured enrichment (wt percent ^{235}U)*	Measured bias (wt percent ^{235}U)	Bias (percent of actual enrichment)	σ (wt percent ^{235}U)	RSD (percent)
40	3.2014	3.1395	- 0.0619	- 1.93	0.0576	1.84
17	3.6090	3.5315	- 0.0775	- 2.15	0.0673	1.90
235	4.0029	3.9383	- 0.0646	- 1.61	0.0782	1.99
152	4.4050	4.3132	- 0.0918	- 2.08	0.0784	1.82
351	4.9526	4.8762	- 0.0765	- 1.54	0.0900	1.85
Total 795	–	–	–	- 1.87#	–	1.88#

* Average of all values for a given enrichment range
\# Calculated as the average of the five biases, not weighted for the number of cylinders of each

1S type cylinders to determine the ^{235}U enrichment. The enrichments fell into five discreet values, or levels, between 3 percent and 5 wt percent ^{235}U. A summary of the results is presented in Table 2. At all enrichment levels, a negative bias was observed. The biases ranged between -1.5 percent and -2.2 percent of the actual enrichment. The average of the individual biases was only -1.87 percent. Bias correction can easily be performed to offset the negative effects to accuracy. The relative standard deviation (RSD) of the 5 levels ranged between 1.81 percent and 1.91 percent of the actual enrichment, the average of the individual RSD's being 1.88 percent. In all cases, the σ was <0.1 wt. percent. This is a fraction of the uncertainty exhibited by work performed using similar methods as discussed earlier. The accepted target value[11] for relative standard random uncertainty (u_r) is 4 percent for the PMCG method (including ultrasonic thickness gauge measurements) for determination of ^{235}U enrichment in the range measured. The results of this work yield less than half of this deviation. The target value for relative standard uncertainty of a systematic nature (u_s) is 2 percent, essentially equal to that demonstrated in this work.

A plot of the measured enrichment, as a percentage of the accepted values, is presented (Figure 4) along with the mean, 2σ and 3σ. The line representative of the average falls at 98.3 percent, depicting the bias after normalization to percent of actual values. The +/- 2σ range is exceeded by 41 of 795 points (5.2 percent). The +/- 3σ range is exceeded by 8 of 795 points (1.0 percent). This demonstrates a reasonable approximation of a gaussian distribution of data with no indication of errors specific to given batches of samples. Also, the measured value that was the least accurate was only 7.3 percent from the mean with an error of 0.35 wt percent on an accepted value of 4.003 wt percent.

Summary

It has been demonstrated that the ^{235}U enrichment measurement of small UF_6 sample cylinders may be performed with a high degree of precision and accuracy. Cylinders with a diameter that is too small to fill the interrogation volume of the detector have been measured with a small planar germanium detector via the enrichment meter method. Utilization of geometrical reproducibility to overcome the obstacle of an unfilled interrogation volume has proven to produce an extremely low uncertainty when the following criteria are met:
- Cylinder positioning is performed reproducibly
- Accurate thickness measurements are performed
- Standards utilized are of the same type as samples

The uncertainty of this measurement has proven to be much lower than that targeted by widely accepted standards and from

Figure 4. 1S sample results expressed as a percentage of the accepted value
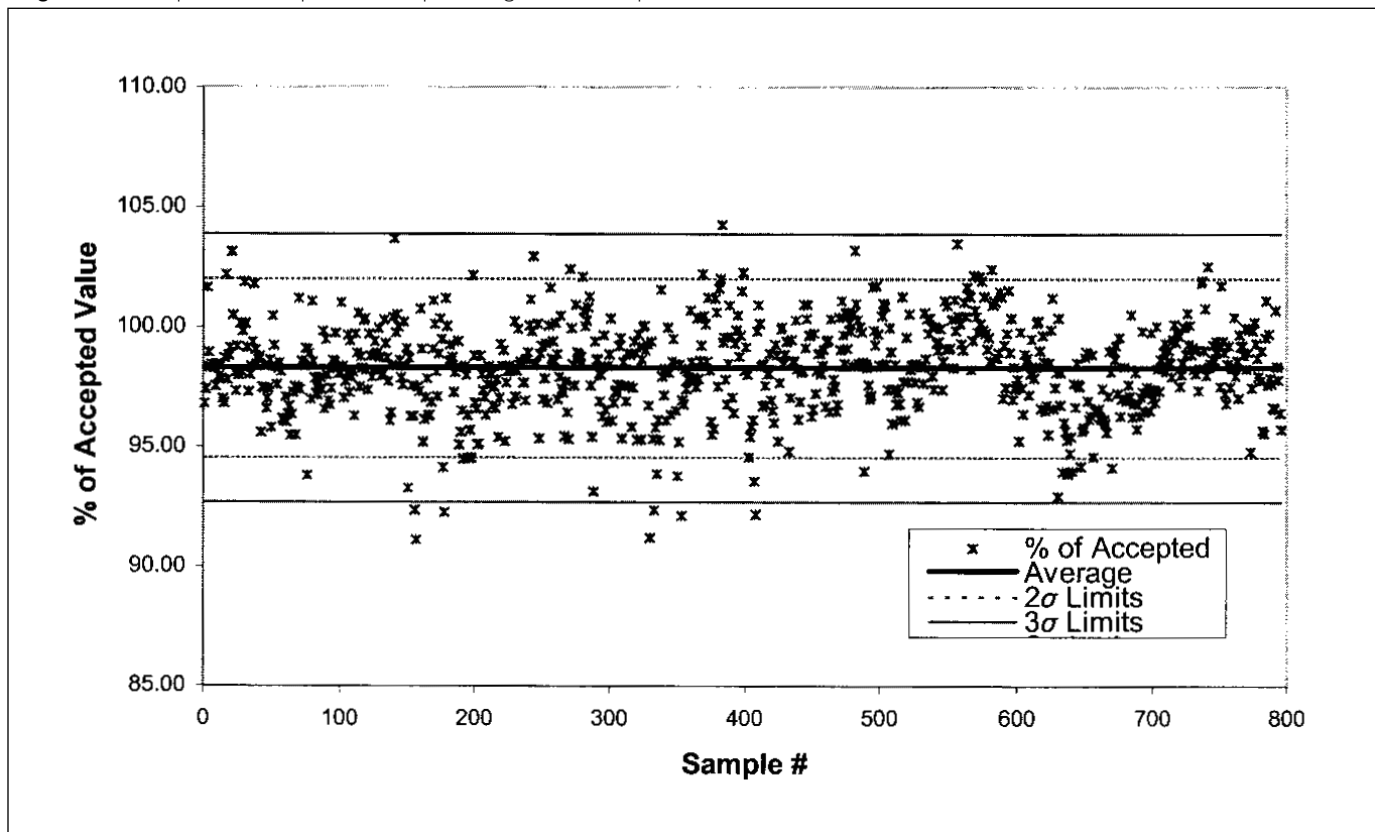
methods, both similar and differing from the method used in this work. With a bias and RSD both less than 2.0 percent and a count time of five minutes, the method provides an accurate, quick and easy analysis. Since the standards and samples are both UF_6 and contained in the same type cylinders, there is no matrix correction required and no absorber is necessary during calibration. The use of a simple positioning device makes setup quick and highly reproducible.

Future Developments

Future improvements to be considered are as follows:
- It is expected that a significantly shorter analysis time may yield similar results. The software updates the averaged calculated enrichment value to the laptop screen every few seconds during analysis. It appears that the value does not change dramatically after as few as ninety seconds. However, this is based only upon observation with no actual tabulated results from shorter times. Also, the precision and bias would be expected to suffer to some degree.
- If the low bias is due to problems associated with the specific standards utilized, then using multiple standards at each level of enrichment may lessen the effect by averaging. Also, if void areas in the UF_6 standards are causing the bias, liquefying and re-solidifying the standards may result in an improvement. Alternatively, analysis might also be performed in different areas of the standards. This might average out any effects of void areas, assuming that they would exist similarly in both standards and samples.
- The specification for type 1S cylinders for use with UF_6 is not specific to material composition between nickel and monel. While the cylinders are nickel, the software did not have nickel as an option for the container absorber. Monel was chosen for this option, the density being similar to that of nickel. While this does introduce error, it remains constant through the calibration and sample analysis. However, nickel should be added as a software option for future work.
- Extension of this work to other sample containers (2S cylinders, P-10 tubes, Hoke tubes, pinch tubes, etc.) is expected to yield similar results, providing a method of confirmation, if needed. However, the uncertainties associated with different container size and thickness would almost certainly vary.

Acknowledgements

Brent Montgomery began work at the Paducah Gaseous Diffusion Plant in Paducah, Kentucky, U.S.A., in 1989. He received an M.S. in chemistry from Murray State University in Murray, Kentucky, in 1993. He worked in the process analysis gas chromatography and infrared laboratories, becoming the supervisor in 1993, until 1998 gaining experience with UF_6 and other corrosive gases. At that time, he became the supervisor of the isotopic laboratories that specialize in ^{235}U enrichment in UF_6 as well as Uranium in waste, water, etc. In 2000, he became the section manager of the nondestructive assay laboratory where he worked until late 2003 focusing primarily upon confirmatory ^{235}U enrichment by gamma and process related deposit quantification by neutron. At that time, he became the manager of the radiochemistry group where he currently works.

References

1. Gunnink, R., W. Ruhter, P. Miller, J. Goerten, M. Swinhoe, H. Wagner, J. Verplancke, M. Bickel, and A. Abousahll. 1994. MGAU: A New Analysis Code for Measuring U-235 Enrichments in Arbitrary Samples, *IAEA Symposium on International Safeguards,* Vienna, Austria, March, 1994.
2. Abousahl, S., A. Michiels, M. Bickel, R. Gunnink, and J. Verplancke. 1996. Applicability and Limits of the MGAU code for the Determination of the Enrichments of Uranium Samples, *Nuclear Instruments and Methods in Physics Research,* A 368 (1996) 443-448.
3. Reilly, D., N. Ensslin, H. Smith, and S. Kreiner. 1991. *Passive Nondestructive Assay of Nuclear Material,* U.S. Nuclear Regulatory Commission, Washington, D.C.
4. 1974. Nondestructive Uranium-235 Enrichment Assay By Gamma-Ray Spectrometry. *United States Atomic Energy Commission Regulatory Guide 5.21.* April 1974.
5. Hagenauer, R. C., H. Y. Rollen, J. M. Whitaker, R. L. Mayer II, and T. Biro. 1998. Nondestructive Measurement of UF_6 Cylinders at the Portsmouth Gaseous Diffusion Plant, *Proceedings of the INMM 39th Annual Meeting.*
6. *PMCG: Measurement of UF_6 Enrichment and U-235 Mass,* International Atomic Energy Agency, SG-NDA-6, rev. 0, Vienna Austria.
7. Gardner, G. H., M. Koskelo, R. L. Mayer II, B. R. McGinnis, M. Moslinger, and B. Wishard. 1996. The IMCA: A Field Instrument for Uranium Enrichment Measurements, *Proceedings of the INMM 37th Annual Meeting.*
8. Verrecchia, G. P. D., M. T. Swinhoe, P. Schwalbach, J. Gustafsson, A. M. Anderson, J. Myatt, and B. Metcalf. 1999. Test and Evaluation of the FRAM Isotopic Analysis Code for EURATOM Applications, *Proceedings of the INMM 40th Annual Meeting*

9. Verplancke, J., P. Van Dyck, O. Tench, M. Koskelo, and B. Sielaff. 1995. The U-Pu Inspector System: A Dedicated Instrument for Assessing the Isotopic Composition of Uranium and Plutonium". Presented at the 17th ESARDA Symposium, May 9-11, 1995, Aachen, Germany.

10. Canberra Industries. 2001. *Model S572 IMCA 2000 Nuclear Safeguards Software User's Manual.*

11. Aigner, H., R. Binner, E. Kuhn, U. Blohm-Hieber, K. Mayer, S. Guardini, C. Pietri, B. Rappinger, B. Mitterrand, J. Reed, O. Mafra-Guidicini, and S. Deron. *International Target Values 2000 for Measurement Uncertainties in Safeguarding Nuclear Materials.* International Atomic Energy Agency, Vienna, Austria.

A Segmented Gamma Scanner for the Verification
of LEU Oxide Powders

A. Ravazzani, A. R. Jaime, M. Looman, P. Peerani, and U. Weng
European Commission, JRC, Ispra, Italy

P. Schillebeeckx
European Commission, JRC, Geel, Italy

Foglio Para
Politecnico di Milano, Nuclear Engineering Department, Milano, Italy

Abstract

The verification of the amount of U oxide powder and the ^{235}U/U abundance in typical fuel fabrication plant containers is described. Only gamma spectroscopy and direct calibration with standards are used. The measurements are performed scanning the container axis with a collimated detector. The spectrum energy considered covers the 1,001 keV region to estimate the ^{238}U mass and the 185.7 keV region to determine the ^{235}U/U abundance. The gamma spectra taken at different axial positions of the container verify the homogeneity level of the sample.

Introduction

Nuclear inspectors generally check the fissile content of low-enriched uranium (LEU) oxide powder samples in fuel fabrication plants using active neutron interrogation techniques. In this paper we propose a different approach entirely based on gamma spectroscopy using a segmented gamma scanner designed at JRC-Ispra.

The ^{238}U mass and the ^{235}U/U abundance are verified from a series of gamma spectra covering the full length of the supposedly homogeneous container. Two scanning profiles of interest are obtained with a collimated detector, one from the 1,001-keV and the other from the 185.7-keV photon net peak areas.

The ^{238}U mass is proportional to the integral of the net peak areas of the 1,001-keV photon. The mass is obtained by multiplying the integrated profile on the container fill height by a calibration constant. A correction procedure for the self-attenuation of the 1,001-keV photon in the container is included. The application of such a procedure requires the knowledge of the density and the U-factor of the powder. The density is calculated from the declared powder mass, the measured fill height, and the known section of the container. For the U-factor we use the operator's declaration. This can be considered a limitation of the technique, but it is considered acceptable for inspection purposes.

Since the 1,001-keV photon is emitted by ^{234m}Pa, the equilibrium between ^{234m}Pa and the ^{238}U is assumed. Non-compliance with this assumption results in an underestimation of the ^{238}U mass. The enrichment meter principle is applied for the verification of the ^{235}U/U abundance. Assuming infinite thickness conditions, the ^{235}U/U abundance is proportional to the net peak area of the 185.7-keV photon. The abundance is obtained multiplying the average of the corresponding profile plateau by a calibration constant. The amount of U oxide powder is verified with the measured ^{238}U mass, the measured ^{235}U/U abundance, and with the U-factor declared by the operator. The fill height of the container is calculated with an iterative weighted least square fit of the two profiles with an appropriate function.

Method for the Determination of ^{238}U Mass and ^{235}U/U Ratio

The homogeneous container is ideally considered as a parallelepiped sample divided by horizontal planes in a series of parallelepiped volume Np. Each volume presents a depth (d), a wall thickness (d_W), and a vertical square section (S) that matches perfectly with the collimator hole. The measurement of the Np volume is ideally considered in far-field condition since the sample-to-detector distance is supposed to be large compared to the depth. It means that only parallel beams from the emitting isotope in the volume reach the detector. Consequently the $1/r^2$ effect can be neglected and the detection efficiency is constant along d. Figure 1 illustrates the measurement configuration

The response of the detector is considered only when a full energy peak is given by the general expression:[1]
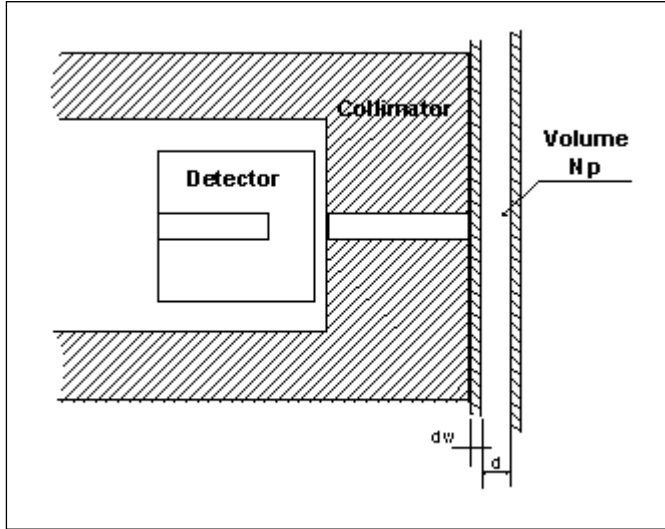
$$R_{ni} = \varepsilon(E_n)\beta_{ni}\lambda_i \frac{N_{Av}}{A_i}\alpha_i w_e \rho S d \frac{1-e^{-\mu(E_n)\rho d}}{\mu(E_n)\rho d} T_W(E_n) \qquad (1)$$

with:

$$\mu(E_n)\rho = \mu_e(E_n)\rho_e + \mu_m(E_n)\rho_m \qquad (1a)$$

and

$$T_W(E_n) = e^{-\mu_W(E_n)\rho_W d_W} \qquad (1b)$$

where R_n represents the net peak area per time unit (or full energy interaction rate or count rate) corresponding to the gamma ray of energy E_n emitted by the isotope i. The isotope i is distributed in the measured volume. The density of the isotope i is $\alpha w_e\rho$ where α, is the abundance of the isotope, w_e is the mass fraction of the nuclear element with i as isotope, ρ is the volume density. The specific emission rate (I) of the E_n gamma ray of the isotope i is then $\beta\lambda N_{Av}/A$, where N_{Av} is the Avogadro number, β is the emission probability of the considered photon, λ is the decay constant, and A the atomic weight of i. The full energy detection efficiency, $\varepsilon(E_n)$, includes the energy-dependent intrinsic detector efficiency and the measurement geometry (collimator and distance). The linear attenuation coefficient of the volume is $\mu(E_n)\rho$ and it is calculated with 1a where $\mu_e(E_n)$ and ρ_e are respectively the energy dependent mass attenuation coefficient and the partial density of the nuclear element and $\mu_m(E_n)$ and ρ_m are respectively the mass

attenuation coefficient and the partial density of the matrix. T_W represents the volume wall transmission calculated with 1b where $\mu_W(E_n)\rho_W$ is the linear attenuation coefficient and d_w is the wall thickness.

Considering the Np volume, Equation 1 is reduced to the quantities of interest ($M_{38}=\alpha_{38}w_U\rho Sd$ and α_{35}, respectively the ^{238}U mass and the $^{235}U/U$ abundance) in function of the associated photon count rate (respectively R_{38} and R_{35}). A basic calibration constant (K) is determined using standards and taking into account the volume self-attenuation. If needed, a calibration constant K' is calculated by multiplying K with correction factors including changes in matrix composition and wall thickness.

Considering the whole sample, the ^{238}U total mass (extensive quantity of interest) is equal, through K'_{38}, to the sum of the count rates from each elementary volumes Np. The $^{235}U/U$ abundance (intensive quantity of interest) is equal, through K'_{35}, to the average of the count rates from all the Np volumes.

In the following the determination of the two mentioned quantities of interest is described in detail. It is reported also the fill height calculation procedure used for density calculations and for the determination of the number of volumes Np.

^{238}U Mass
To compute the ^{238}U total mass, general expression 1 reduces to:

$$R_{38} = \varepsilon(1001)I_{38}M_{38}\frac{1-e^{-\mu(1001)\rho d}}{\mu(1001)\rho d}T_W(1001) \qquad (2)$$

where M_{38} is the mass of the ^{238}U present in the sample volume considered, I_{38} and $\varepsilon(1,001)$ are respectively the specific emission rate and the full energy detection efficiency of the 1,001-keV photon of ^{238}U. $\mu(1,001)\rho$ and $T_W(1,001)$ are respectively the linear attenuation coefficient calculated with (1a) and the wall transmission calculated with (1b) at the 1,001 keV energy.

Since M_{38} is the quantity of interest, we can write:

$$M_{38} = \left[\frac{1}{\varepsilon(1001)I_{38}}\right]\frac{1}{T_W}R_{38}\frac{\mu(1001)\rho d}{1-e^{-\mu(1001)\rho d}} \qquad (3)$$

where, assuming the transmission T = exp(-μ(1,001)ρd),

$$CF_{38}(T) = \frac{-\ln(T)}{1-T} = \frac{\mu(1001)\rho d}{1-e^{-\mu(1001)\rho d}} \qquad (3b)$$

is the correction factor of R_{38} that takes in account the self-attenuation of the volume. If multiplied by R_{38}, CF_{38} returns the corrected count rate (CR_{38}) that would have been observed if the sample volume were not self-attenuating. In this way CR_{38} is directly proportional to ^{238}U mass. Generally CF(T) is calculated as the ratio between the count rate that would be measured if the sample were totally non attenuating and the actual count rate from the sample. In this manner, the calculation takes into

account the position of the sample relative to the detector (inverse square dependence) and the geometrical shape of the sample. Only under far-field conditions and rectangular shape geometry can the CF(T) be expressed in the simple analytical form of 3b.

CF(T) is well determined only if the linear attenuation coefficient $\mu(E_m)\rho$ is single valued. The necessary assumptions are that both emitting element and matrix are homogeneous in composition and density and that the particles of material forming the volume have negligible self-attenuation. After calculating CF(T) the respect of these assumptions is generally more stringent than the respect of the far field condition. For M_{38} calculation a basic calibration constant K_{38} is determined using standards of the same shape of the volume and correcting R_{38} for the self-attenuation:

$$K_{38} = \left[\frac{1}{\varepsilon(1001)I_{38}} \right] \frac{1}{T_{WS}} \qquad (4)$$

where T_{WS} is the wall transmission of the standard. The calibration constant K_{38} takes into account the effects of detector efficiency, the measurement geometry ($\varepsilon(1,001)$) and the nuclear data (I_{38}). If the unknown sample volume has the same wall thickness of the standard then also the T_{WS} factor can be included in the basic calibration constant, otherwise it must be calculated with the unknown volume wall transmission T_{WM} to obtain the wall transmission correction factor T_{WS} / T_{WM}:

$$K'_{38} = K_{38} \frac{T_{WS}}{T_{WM}} \qquad (5)$$

The ^{238}U mass in the elementary volume can be determined by the simple relation:

$$M_{38} = K'_{38} CR_{38} \qquad (6)$$

where K'_{38} is the calibration constant obtained from standards and including an eventual correction factor, CR_{38} is the count rate of the sample corrected for its self-attenuation. Since we are considering a homogeneous sample ideally divided in a series of N volumes N_p and K'_{38} is constant, the ^{238}U total mass (M^T_{38}) is determined by:

$$M_{38}^T = \sum_{p=1}^{N} K'_{38} CR_{38p} = K'_{38} CF_{38} \sum_{p=1}^{N_p} R_{38p} \qquad (7)$$

where R_{38p} is the count rate of each volume N_p.

^{235}U/U Abundance

To compute the ^{235}U/U abundance the general expression 1 reduces to:[2]

$$R_{35} = \varepsilon(186)I_{35}\alpha_{35}\rho_U S \frac{1 - e^{-\mu(E_n)\rho d}}{\mu(E_n)\rho} T_W(186) \qquad (8)$$

where α_{35} is the abundance of the ^{235}U isotope, ρ_U is the partial density of U in the sample volume considered, I_{35} and $\varepsilon(186)$ are respectively the specific emission rate and the full-energy detection efficiency of the 186-keV photon. $\mu(186)\rho$ and $T_W(186)$ are respectively the linear attenuation coefficient calculated with (1a) and the wall transmission calculated with 1b at the 186 keV energy. If the volume thickness d is large enough, then the exponential term in 8 becomes negligible compared to 1 over a certain value (d_{IT}) of d. It means that the photons emitted beyond d_{IT} are absorbed and that the photon flux at the sample surface is independent of the sample thickness. Usually we define "infinite thickness" the volume depth that produces the 99.9 percent of the photon flux at the volume surface:

$$d_{IT} = \frac{-\ln 0.001}{\mu\rho} = \frac{6.91}{\mu\rho} \qquad (9)$$

This is the origin of the infinite thickness criterion on which the enrichment meter principle is based.

Usually, due to the high self-absorption values at the low energy considered, the depth of the volume visible by the detector is small. It implies that the assumed far field condition is easily verified if the visible depth is compared to the detector distance. Since E_{35} is the quantity of interest, combining Equation 8 in condition of infinite thickness and 1a, we can write:

$$\alpha_{35} = \left[\frac{\mu_U}{\varepsilon(186)I_{35}S} \right] \frac{1}{T_W} m(186)R_{35} \qquad (10)$$

where

$$m(186) = 1 + \frac{\mu_m(186)\rho_m}{\mu_U(186)\rho_U} \qquad (10b)$$

reflects the matrix attenuation effect. For α_{35} calculation a basic calibration constant K_{35} is determined using standards that verify the infinite thickness criterion:

$$K_{35} = \left[\frac{\mu_U}{\varepsilon(186)I_{35}S} \right] \frac{1}{T_{WS}} m_S \qquad (11)$$

where mS and T_{WS} are respectively the matrix attenuation and the wall transmission of the standard. The calibration constant K_{35} takes into account the effects of detector efficiency, the measurement geometry ($\varepsilon(186)$, S) and the nuclear data (I_{35}, μU). If the sample

has the same matrix composition and wall thickness of the standard then also m and T_{WS} factors can be considered in the basic calibration constant. On the contrary they must be calculated with the unknown volume matrix attenuation m_M and wall transmission T_{WM} to obtain the matrix correction factor m_M/m_S and the wall correction factor T_{WS} / T_{WM}:

$$K'_{35} = K_{35} \frac{m_M}{m_S} \frac{T_{WS}}{T_{WM}} \qquad (12)$$

The $^{235}U/U$ abundance in the elementary volume can be determined by the simple relation:

$$\alpha_{35} = K'_{35} \, R_{35} \qquad (13)$$

where K'_{35} is the calibration constant obtained from standards and including eventual correction factors, and R_{35} is the count rate of the unknown volume sample. This way for determining α_{35} is the so called enrichment meter principle.

The $^{235}U/U$ abundance of the homogeneous sample ideally divided in a series of N parallelepiped volumes Np is determined by:

$$\alpha_{35} = \frac{K'_{35}}{N} \sum_{p=1}^{N} R_{35p} \qquad (14)$$

where R_{35p} is the count rate of each Np volume.

Fill Height
The fill height of the whole sample is obtained from 186 and/or 1,001 keV scanning profiles. It is used for density calculations and for fixing the number N of parallelepiped volumes Np considered in equations 7 and 14. A well-known function returns the count rate measured by a non-collimated point detector moving along the z axis of a finite line source of height H:[3]

$$R(z) = \frac{eI}{D} \left(arctg\left[\frac{z-z_0}{D}\right] - arctg\left[\frac{z-(z_0+H)}{D}\right] \right) \qquad (15)$$

where e is the intrinsic efficiency of the detector, I is the intensity per unit length of the non attenuating source, D is the detector-source distance and z_0 is the bottom edge of the source. The formula easily fits also the profiles obtained with collimated detector along the z axis of the sample:

$$R(z) = \frac{R_p}{\pi} \left(arctg\left[\frac{z-z_0}{D}\right] - arctg\left[\frac{z-(z_0+H)}{D}\right] \right) \qquad (16)$$

where now π is the normalization constant for returning the plateau count rate R_p and D is the height resolution parameters of the system. D depends on the detector-source distance and the collimator geometry. The relation between D and the FWHM of the line-spread function is: FWHM = 2*D. The iterative

weighted least square fit of the axial profile results in the bottom edge z_0 and in the fill height H of the sample.

The region of the constant response profile can also be determined by a study of successive variances $\sigma^2(z_k)$ along the z axis:

$$\sigma^2(z_k) = \frac{1}{12} \sum_{i}^{k+2} (c_i - c_m)^2 \qquad (17)$$

where c_i is the value of the net peak area i and c_m the average of c_i in the interval considered. $\sigma^2(z_k)$ is function of the z-coordinate and shows two maxima. The difference between the two maxima can also be used to estimate the fill height (H) of the sample. In this example, the procedure will be used only for determining the initial guess values for fitting Equation 16. Because of the possible non-uniformity of the material surface slope at the top edge of the container, in the relation 16, D is considered different for the z_0 region (D_1) and the z0+H region (D_2).

Applicability of the Method
Geometry
The container to be measured is not an ideal parallelepiped sample, but a cylinder. During the scanning, a portion of the container is measured by a detector through a slit collimator. This allows approximating the elliptic cylinder segment geometrically seen by the detector with the parallelepiped volume considered in the previous paragraph. As illustrated in Table 1, we consider different types of cylindrical containers of different dimensions. For container type D-O are also present neutron absorbing resin and mousse that are reported in Table 1 as additional material.

Table 1. Dimensions of the containers considered in this exercise. The last column reports the distance between the detector window and the container axis.

Cont. ID (mm)	Ext. diam. (mm)	Int. diam (mm)	Wall Thick (mm)	Add. Mat. (mm)	Height (mm)	Dist. D-C (mm)
P-A	95	87	4	0	300	96
P-B	146	138	4	0	300	121
D-O	380	254	2	61	805	238

The measurement configurations that will be analyzed are shown in Figure 2. The container-detector distance is chosen as small as possible to minimise the counting time and to maximise the resolution in determining the fill height.

Infinite Thickness Condition
Due to the low energy of the186-keV photon, short paths in the elliptic cylinder segment are enough for a quasi-complete absorption. Only few sections of the segment seen by the detector at certain angles do not present a quasi-complete self-absorption beyond a certain point. In conclusion, with the adopted meas-

urement configurations, the infinite thickness condition for the 186-keV photon is verified within most of the whole viewing angle. The volume depth (d_{IT}) that produce the 99.9 percent of the 186-keV photon flux is obtained from equations 9 and 1a knowing the U-factor (U_f) and the density of the powder: $d_{IT}=6.91*\rho^{-1}*[\mu_U*U_f+\mu_m*(1-U_f)]^{-1}$. Typical values of d_{IT} for different compounds and densities are reported in Table 2.

Table 2. Volume depth producing the 99.9 percent of the 196 keV photon flux for different compounds and densities

Compound	U_f	μ at186keV (cm²/g)	ρ (g/cm³)	Depth (cm)
U	1	1.667	-	-
O	0	0.127	-	-
UO_2	0.881	1.484	1.0	4.7
			2.0	2.3
			3.0	1.6
U_3O_8	0.848	1.433	1.0	4.8
			2.0	2.4
			3.0	1.6

Figure 2. Measurement configuration of the containers. Side and horizontal sections are represented. For D-O container the additional material is reported too.
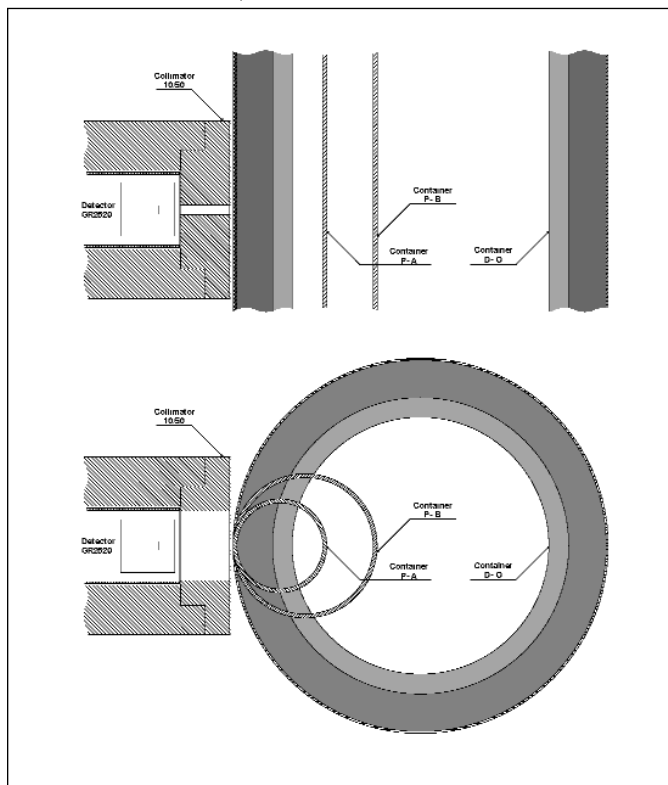
Far-Field Condition
The high absorption of the 186-keV photon implies that only a small part of the elliptic cylinder segment can be considered seen by the detector. The depth of the visible volume is small compared to the sample-detector distance. Consequently, it is possible to neglect the inverse square law effects. In the adopted measurement configurations, the far field condition for the 186-keV photon is respected.

Some doubts can arise about the far-field condition when considering the 1,001-keV photon. (In this case the transmission coefficient should allow the detector to see the whole elliptic cylinder segment volume). In the considered measurement configurations the sample to detector distance is not so small compared to the volume depth. This fact introduces the inverse square law effects in the calculation of CF in addition to the approximation regarding the volume shape. Fortunately the consequences of an imprecise CF have not a dramatic effect on the final result as demonstrated at the end of the next section of this paper.

Determination of CF for 1,001 keV photon
Generally speaking the correction factor (CF) for self-attenuation is a function of many parameters, listed here that in order of importance:
- The linear attenuation coefficient of the material
- The dimension and the shape of the sample
- The position of the sample relative to the detector
  Usually CF is represented as a function of the transmission $T = \exp(-\mu(E_n)\rho d)$. In our case CF(T) is calculated forcing the far-field condition and considering the volume as a parallelepiped. Under this last assumption we define an equivalent thickness d_e as the ratio between the area and the diameter of the cylinder section perpendicular to the axis. The mass-attenuation coefficient $\mu(E_n)\rho$ is variable and it depends on the matrix and the density of the sample.

In this case, the method is applicable only if the self-absorption let the detector see the whole sample volume. Usually the accuracy of the measurement becomes unacceptable for transmission values less than 0.01. In Figure 3 the 1,001keV photon transmission T is computed as a function of the diameter of the container. It is calculated for three different sample densities using the mass attenuation coefficient of the U_3O_8 powder. The arrows indicate the internal diameters of the containers considered in this work. It's clear that problems arise with densities higher than 2g/cm³ and diameters higher than 25cm, but this eventuality is rare for powder containers from fuel fabrication plants.

The two approximations on CF(T) (far-field condition and volume shape) do not introduce significant biases in the mass calculation. Let M^r_{38} and M^i_{38} the masses determined respectively with the real CF^r and the ideal CF^i (3b). Let T_M and T_S the transmissions respectively of the measured sample and the standard. The ratio of the masses determined with the real and the ideal CF is:

Figure 3. Transmission of the 1,001-keV photon in U_3O_8 for three different densities of the powder
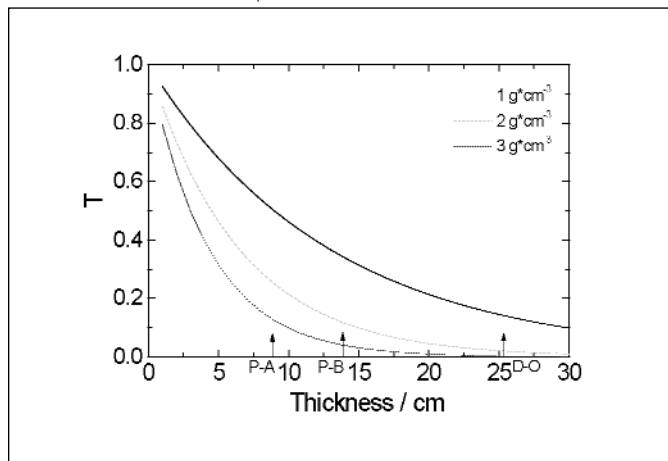
$$\frac{M^r}{M^i} = \frac{CF^r(T_M)\Big/CF^i(T_M)}{CF^r(T_S)\Big/CF^i(T_S)} \qquad (18)$$

This ratio does not depend directly on $CF^r(T_M)/CF^i(T_M)$, but only on a ratio of ratios. Finally, the CF(T) determination could be avoided if a set of calibration standards identical to the unknowns in composition, density, dimensions, and shape, are available. In this case the correction factor, equal for both measured samples and standards, can be included directly in the calibration constant. This procedure is applicable only when the characteristics of the assayed samples are fixed and well known.

Number of Standards

The ^{238}U mass and the $^{235}U/U$ abundance determined with equations 7 and 12 are linearly dependent to the count rates R_{38} and R_{35}. It implies that the calibration constant can be determined with a single standard in the range of the unknown quantities. In any event, the use of several standards of different mass, density, and enrichment is suggested. This procedure permits to validate the results.

Experimental Set Up

The segmented gamma scanning system is equipped with a detector positioned on a lifting unit, the acquisition electronics, a series of collimators, and a turntable for rotating the container. The container is measured into segments covering its full length. During each segment measurement the container is rotated by multiple of 2π and a complete gamma spectrum is acquired and stored. The two profiles of interest are obtained with an automatic procedure that calculates, for each spectrum, the net areas and the associated uncertainties of the 1,001-keV and 186-keV photon peaks.

Acquisition Chain

The acquisition chain is composed by the detector and the associated electronics. All settings used and the performance parameters as energy calibration and resolution are reported for a quick check of the instrumentation.

Detector

The detector is a germanium n-type coaxial, model GR2520 supplied by Canberra. It is 53.5 mm diameter and 55 mm length. Its distance from the Be window is 5 mm. The recommended bias voltage is –5,000 V. It is equipped with a preamplifier model 2002CSL. The resolution and the efficiency measured by the supplier are reported in Table 3.

Table 3. Detector characteristics measured by the supplier with a shaping time of 6ms

Isotope	^{57}Co	^{60}Co
Energy (keV)	122	1332
FWHM (keV)	0.969	1.98
Peak / Compton		53.2 : 1
Rel. efficiency (3"×3" NaI)		28.3 percent

Electronics

The electronics is a modular conventional NIM chain. The model, the supplier, and the main settings used of each NIM module are reported in Table 4. These settings are used for all the experiments.

Table 4. Model, supplier, and main settings of each NIM module of the chain

Module	Model	Supplier	Main Settings
High Voltage	459	EG&G	–
Amplifier	572	EG&G	500 oV
MCA	921	EG&G	2μs
Counter & Timer	776	EG&G	Manual 4k

Energy Calibration and Resolution

The acquired spectra cover an energy range 0–1200 keV. In laboratory conditions, the resulting energy calibration expressed in keV and calculated in function of channels, is:

$$E(P) = a_o + a_1 P \qquad (19)$$

with a_o = -0.44 keV and a_1 = 0.2736 keV/ch.

The resolution, defined by the full-width-at-half-maximum (FWHM), expressed in unit of channels and calculated in function of energy, is:

Collimator ID	Material	Thickness (mm)	Slit width (mm)	Slit height (mm)
10/25	Pb	25	70	10
05/50	Pb	50	70	5
10/50	Pb	50	70	10

$$FWHM^2(E) = b_0 + b_1 E + \frac{b_2}{E} \qquad (20)$$

with b_0 = 21.879 ch^2, b_1 = 0.0374 ch^2/keVand b_2 = 376 ch^2/keV. The first two parameters are physical, while the last one is an empirical correction for deviations from a straight line at low energy.

Collimators

The scanning system is equipped with a series of collimators with different thickness and slit dimensions summarized in Table 5. They have been tested in laboratory conditions for choosing the best measurement compromise.

In Figure 4 are reported respectively the scanning profiles of the 1,001-keV (a) and 185.7-keV (b) photons emitted from a test container positioned as shown in Figure 2.

Three different collimators have been tested and the 10/50 was found to be the most appropriate. The 10/25 is not thick enough for shielding the 1,001keV photon contribution from regions outside the viewing angle. The 05/50 and 10/50 are both appropriate, but 10/50 is chosen because gives higher count rates without significantly deteriorating the space resolution. Verification time is a stringent parameter during inspections. The 10/50 was then used for all the experiments.

Typical Spectra

Figure 5 shows two typical sum spectra. They are obtained summing each step contribution of the container fill height. They are referred respectively to a container type P-B containing U_3O_8 powder with $^{235}U/U$ equal to 0.98 percent (a) and to a container type D-O containing UO_2 powder with $^{235}U/U$ equal to 0.71 percent (b). The upper spectrum (a) has been collected in laboratory condition, the lower one (b) is from an in field inspection in a fuel fabrication plant. In the 200-keV region it is clearly visible the contribution of the scattered radiation.

Analysis Procedure

Fill Height

From the 186-keV scanning profile the fill height of the container is obtained with Equation 16 assuming D different for the two edge regions. The fill height is used for density calculation and for fixing the intervals of R_{38j} and R_{35j} integration respectively in equations 7 and 14. In case of R_{38j} the integration range includes the tails. Since E_{35} is an extensive quantity, in case of R_{35j} the interval is restricted to the central part of the plateau to apply the enrichment meter principle.

Figure 5. Two typical sum spectra measured in laboratory condition (a) and in field condition (b). They are normalized on 1,001-keV photon peak and (b) is reduced of a factor 10.
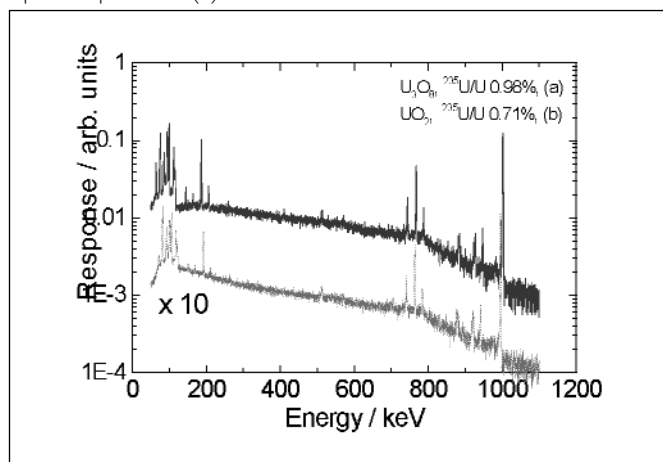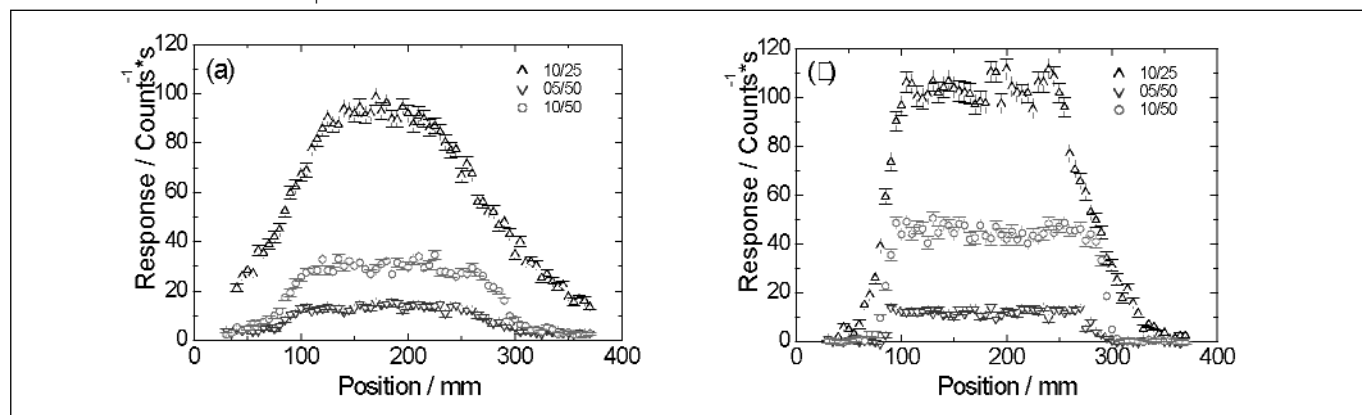

Figure 4. Scanning profiles of the 1,001-keV (a) and 185.7-keV (b) photon obtained using three different collimators and an acquisition live time of 10s for each 5 mm step

²³⁸U Mass, ²³⁵U/U Abundance and Oxide Powder Amount

The ^{238}U mass and the $^{235}U/U$ abundance are obtained from equations 7 and 14. The oxide powder amount (M^T_{OX}) is obtained from:

$$M^T_{OX} = \frac{1}{U_f} \frac{M^T_{38}}{1-a_{35}} \qquad (21)$$

where M^T_U is the uranium element mass and U_f is the operator declared U-factor.

Self-Absorption Correction Factor CF(T)

The correction factor for 1,001-keV photon self-attenuation, used for determining both the ^{238}U mass and the associated calibration constant, is calculated with Equation 3b. The mass attenuation coefficient $\mu(1,001)$ in Equation 3b is calculated with Equation 1a knowing the U_f of the powder: $\mu = \mu_U {}^* U_f + \mu_m {}^* (1-U_f)$. Typical values of $\mu(1,001)$ are reported in Table 6.

Table 6. Typical values of μ for 1,001- keV photon

Compound	U_f	μ at 1,001keV (cm²/g)
U	1	$7.896 {}^* 10^{-2}$
O	0	$6.372 {}^* 10^{-2}$
UO2	0.881	$7.715 {}^* 10^{-2}$
U3O8	0.848	$7.664 {}^* 10^{-2}$

The density ρ is calculated with: $\rho = (M^T_{OX})_{dec} / S_c {}^* H$ where $(M^T_{OX})_D$ is the operator declared powder amount, S_c is the internal section of the container and H is the fill height calculated with (16).

The equivalent thickness d_e is calculated with $d_e = \pi d_C/4 = S_C/d_C$ where d_C and S_C are respectively the internal diameter and the cross area of the container.

Calibration Constant and Correction Factors

The two basic calibration constants K_{38} and K_{35} are determined from equations 7 and 14. The matrix correction factor for K_{35} is the ratio between the two matrix attenuation coefficients (m_M / m_S) at 186 keV (12). The matrix attenuation coefficient $m(186)$ is obtained from (10b) knowing the U_f of the powder: $m = 1 + \mu_m {}^* (1-U_f)/\mu_U {}^* U_f$. Typical values of $m(186)$ are reported in Table 7. Usually small fluctuations of U_f in the same powder batch do not appreciably affect the matrix attenuation coefficient and can be neglected.

The wall correction factor for K_{38} and K_{35} is the ratio between the wall transmission coefficients (T_{WS} / T_{WM}) respectively at the energies of 1,001 and 186 keV (5, 12). The wall transmission coefficient T_W at the energy of interest is obtained from Equation 1b. Usually the sample container is the same used for calibration standards and there is no need to correct for the wall transmission coefficient.

Table 7. Typical values of m for 186-keV photon

Compound	U_f	m at 186keV
U	1	1
O	0	∞
UO₂	0.881	1.010
U₃0₃	0.848	1.014

Measurement Campaigns

Two measurement campaigns are reported. The first campaign is in laboratory conditions and involves standard samples with P-A and P-B type containers. The other campaign consists in an in-field inspection in a fuel fabrication plant and involves samples in D-O type containers. The CF(T) is calculated for each sample with the appropriate mass attenuation coefficient and density. There is no need to calculate the matrix and the wall correction factors for both the campaigns.

Laboratory Conditions Campaign

The measurements in laboratory conditions are performed in the PERLA laboratory at the JRC-Ispra. PERLA is a unique facility within the EU that houses an extensive collection of well-characterized nuclear reference materials.

In the reported campaign the acquisition live time used for each scan is 30s and the steps are 5 mm. An additional campaign involving the same samples is performed with the same step width and a new acquisition live time of 10s. The results agree with the previous ones and are not reported in this work.

The calibration constants are determined with a representative sample of the two container types. CF(T) is calculated for each sample with the relative calculated density and the mass attenuation coefficient of the U_3O_8 powder filling all the containers.

Fill Height and Density
The least square fitting for a typical 186-keV profile with Equation 16 and D variable for the two edge regions is shown in Figure 6. The sample fill heights obtained from the fittings are reported in Table A-I of Annex A. In Table A-I , the calculated sample densities are also reported as well.

²³⁸U Mass and ²³⁵U/U Abundance
In Annex A tables A-II and A-III report respectively the ^{238}U mass and $^{235}U/U$ abundance, with the associated uncertainties, for both declared and measured values of the ^{238}U mass and $^{235}U/U$ abundance for samples in the two PERLA containers. The accuracy in positioning the small P-A containers reflects in the results obtained. The measured ^{238}U mass and $^{235}U/U$ abundance show appreciable differences with the declared values. This fact is more evident in the $^{235}U/U$ abundance calculations where the infinite thickness condition is hardly fulfilled in the curvature of the container. The difference between the measured and the declared val-

Figure 6. Fitting of a typical 186-keV profile for container fill height determination.
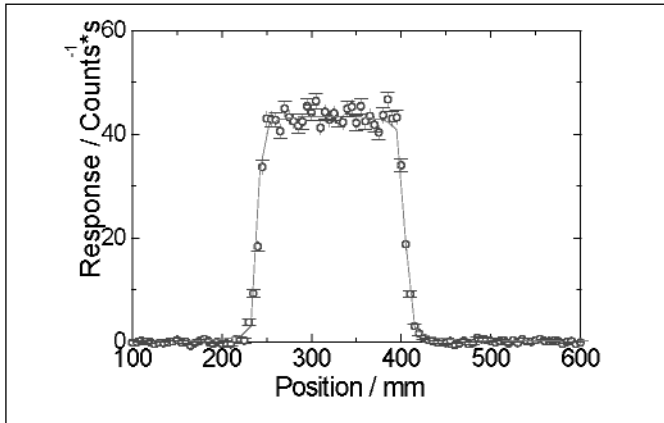
ues (d_{M-D}) with the corresponding uncertainty (s_d) is also shown. This form in presenting the results allows the inspector to check if the condition $d_{M-D}<3*s_d$ is respected. In the last column also the ratio between d_{M-D} and the declared value is reported in percentage.

Fuel Fabrication Plant Campaign

The campaign is performed in a typical fuel fabrication plant in EU during a routine inspection.

The acquisition live time is of 20s for each scan and the steps are 10 mm. The calibration constants are determined using three standards present in the fabrication plant. The standards cover the mass and the enrichment range of the UO_2 powder containers to be assayed. The self attenuation correction factor $CF_{38}(T)$ is determined for each standard and container with the relative calculated density and the mass attenuation coefficient of UO_2.

Table 8. Ratio and corresponding uncertainties between measured and declared ^{238}U mass for the fuel fabrication plant samples

Container	Sample ID	Date	$(M^T_{38})_M / (M^T_{38})_D$	
			(ratio)	(+ -)
D-O	X1-1	250701	1.03	0.02
D-O	X1-2	250701	0.97	0.02
D-O	X1-3	260701	0.97	0.02
D-O	X2-1	240701	0.98	0.01
D-O	X2-2	250701	0.98	0.01
D-O	X2-3	260701	1.00	0.01
D-O	X2-4	260701	0.99	0.01
D-O	X2-5	260701	1.00	0.01
D-O	X2-6	260701	1.00	0.01
D-O	X3-1	240701	1.01	0.01
D-O	X3-2	250701	0.99	0.01
D-O	X3-3	250701	1.02	0.01
D-O	X4-1	240701	0.66	0.01
D-O	X4-2	250701	0.74	0.01
D-O	X4-3	250701	0.70	0.01

Table 9. Ratio and corresponding uncertainties between measured and declared $^{235}U/U$ abundance for the fuel fabrication plant samples

Container	Sample ID	Date	$(\alpha_{35})_M / (\alpha_{35})_D$	
			(ratio)	(percent)
D-O	X1-1	250701	0.95	0.03
D-O	X1-2	250701	1.01	0.03
D-O	X1-3	260701	1.05	0.03
D-O	X2-1	240701	1.02	0.02
D-O	X2-2	250701	1.02	0.02
D-O	X2-3	260701	1.01	0.02
D-O	X2-4	260701	0.99	0.02
D-O	X2-5	260701	1.00	0.02
D-O	X2-6	260701	1.02	0.02
D-O	X3-1	240701	1.04	0.02
D-O	X3-2	250701	1.05	0.02
D-O	X3-3	250701	1.03	0.01
D-O	X4-1	240701	0.99	0.01
D-O	X4-2	250701	0.98	0.01
D-O	X4-3	250701	0.97	0.01

Table 10. Ratio and corresponding uncertainties between measured and declared U oxide powder amount for the fuel fabrication plant samples

Container	Sample ID	Date	$(M^T_{OX})_M / (M^T_{OX})_D$	
			(ratio)	(+ -)
D-O	X1-1	250701	0.99	0.03
D-O	X1-2	250701	0.98	0.04
D-O	X1-3	260701	0.98	0.03
D-O	X2-1	240701	1.00	0.02
D-O	X2-2	250701	1.01	0.02
D-O	X2-3	260701	1.02	0.02
D-O	X2-4	260701	1.01	0.02
D-O	X2-5	260701	1.03	0.02
D-O	X2-6	260701	1.02	0.02
D-O	X3-1	240701	1.04	0.02
D-O	X3-2	250701	1.02	0.02
D-O	X3-3	250701	1.05	0.02
D-O	X4-1	240701	0.69	0.01
D-O	X4-2	250701	0.76	0.02
D-O	X4-3	250701	0.73	0.02

Due to confidentiality reasons, we will not report the full information about the samples, but just the results of the verification. Four families of samples differing in the enrichment are identified. In tables 8 to 10, the ratio between the measured and the declared values of the ^{238}U mass, $^{235}U/U$ abundance and U oxide powder amount for the four families are reported with the corresponding uncertainty.

Samples of family X_4 present an underestimation of the ^{238}U contents. In Figure 7 the values reported in Table 8 are reported; the solid square points represent the X_4 family samples. Since X_4 containers are from a batch of *fresh* material such behavior is explained with the non-equilibrium between ^{234m}Pa and ^{238}U.

Figure 7. Graphic representation of Table 8 values. The square solid points refer to the X_4 family samples not in equilibrium.
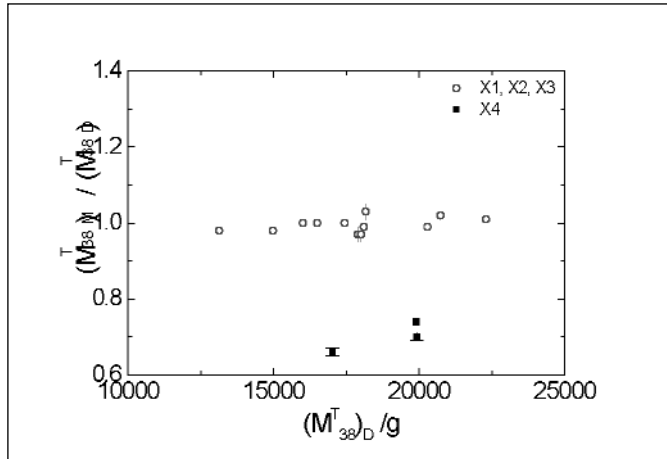
With the exception of samples of family X_4 for which the method is not applicable, all the samples measured in the fabrication plant show an excellent agreement between measurement and declaration. The results are even better of those obtained in laboratory conditions in PERLA. The reason of this is related to the larger container used in the fuel fabrication plant. This fact, even if from one side, makes the analysis much more sensitive to the self-attenuation correction, on the other hand allows meeting better the methodological assumptions, in particular the far-field and infinite-thickness conditions.

Conclusions

The proposed method for the verification of the amount of U oxide powder and the $^{235}U/U$ abundance with gamma spectroscopy has been discussed and applied. The approximations introduced in the calculations seem not to influence the results if in presence of large containers as the ones of a typical fuel fabrication plant. Good results are obtained both in laboratory condition measurement and in-field condition measurement. The only practical limitation is the non-applicability to freshly separated powders due to the condition of the equilibrium between ^{234m}Pa and the ^{238}U.

Another limitation is the fact that operator's declaration is used for the estimation of the powder density and U-factor used for the calculation of the self-attenuation factor. This limitation could be theoretically removed by developing an iterative procedure. We could use a typical value for density as first guess and then compute the self-attenuation factor to be used to obtain a first-iteration mass. With this new mass a better estimation of the density could be computed and therefore a second iteration would give a new value for mass. The process could be repeated until convergence. Nevertheless we preferred not to implement this iterative procedure and use the operator's declaration for the density in the calculation of the corrective factor in the development of the first prototype. For pure verification purposes this limitation is totally acceptable. In cases where the operator's declarations are not known *a priori,* the analysis software can be easily improved by implementing the iterative process described above. The method is based on direct calibration and the importance of using appropriate working standards is underlined. This method allows the verification of U mass and enrichment with an accuracy of a few percents, which is sufficient in most inspection conditions. Moreover the equipment is relatively cheap and easily transportable, making of this segmented gamma scanner a valid alternative to the existing techniques.

References

1. Kruger, G. M., P. Schillebeeckx, U. Weng. 1997. *Uranium Enrichment Verification by Gamma-Ray Spectroscopy, Introduction to the Measurement Technique.* ECSC-EC-EAEC, Bruxelles.
2. De Bievre, P., H. L. Eschbach, R. Lesser, H. Meyer, J. van Audenhove, and B. S. Carpenter. 1985. ^{235}*Uranium Isotope Abundance Certified Reference Material for Gamma Spectrometry. EC Nuclear Reference Material 171 Certification Report.* JRC, COM 4153.
3. Debertin, K., and R. G. Helmer. 1988. *Gamma and X-Ray Spectrometry with Semiconductor Detectors,* North Holland.
4. Nuclear Grade Sinterable Uranium Dioxide Powder, ASTM C 753-81.
5. Reilly, D., N. Ensslin, H. Smith Jr., and S. Kreiner. 1991. *Passive Nondestructive Assay of Nuclear Materials,* NUREG/CR-5550, LA-UR-90-732, 1991
6. Knoll, G. F. 2000. *Radiation Detection and Measurement.* John Wiley and Sons.
7. Guardini, S., F. Mousty, S. Nonneman, P. Schillebeeckx, J. Gerard, K. Vanaken, G. Bagliano, S. Deron, and H. Aigner. 1997. Procurement and Characterisation of LEU Special Nuclear Material Standards for Perla, *Proceedings of the 19th Annual Symposium on Safeguards and Nuclear Materials Management, Montpellier, France, 13–15 May, 1997,* ESARDA 28 pp. 307-312.

ANNEX A
Laboratory Condition Measurement of PERLA Samples

Table A-I. Sample fill height from the least square fitting and the calculated density for PERLA samples

Container	Sample	Date	Height (cm)	(+-)	(percent)	Density (g/cm3)	(+-)	(percent)
P-A	LU11	250601	11.8	0.1	1.0	2.84	0.03	1.0
P-A	LU12	220601	15.1	0.1	0.8	3.12	0.02	0.8
P-A	LU25	260601	16.4	0.1	0.4	2.87	0.01	0.4
P-A	LU42	260601	7.7	0.1	1.0	2.57	0.03	1.1
P-A	LU43	250601	10.9	0.0	0.4	2.52	0.01	0.4
P-A	LU44	220601	15.4	0.1	0.5	3.06	0.02	0.5
P-B	LU13	210601	16.1	0.1	0.7	2.93	0.02	0.7
P-B	LU26	260601	6.6	0.1	1.2	2.86	0.03	1.2
P-B	LU28	210601	9.3	0.1	0.6	2.88	0.02	0.7
P-B	LU30	200601	16.3	0.1	0.4	2.88	0.01	0.4
P-B	LU31	200601	18.8	0.1	0.5	3.02	0.01	0.5

Table A-II. Declared and measured ^{238}U mass for PERLA samples. d_{M-D} is the difference between the measured and the declared values and sd is the corresponding uncertainty. In the last column $100(M-D)/D$ represents, in percentage, the ratio between d_{M-D} and the declared value.

Container	Sample	Date	$(M^T_{38})_D$ (g)	(+-)	(percent)	(g)	$(M^T_{38})_M$ (+-)	(percent)	d_{M-D}	s_d	$100(M-D)/D$ (percent)
P-A	LU11	250601	1674.56	1.67	0.1	1639.79	31.08	1.9	-34.77	31.13	-2.1
P-A	LU12	220601	2349.69	2.35	0.1	2420.74	42.94	1.8	71.05	43.00	3.0
P-A	LU25	260601	2300.63	2.30	0.1	2351.20	40.38	1.7	50.57	40.44	2.2
P-A	LU42	260601	942.10	0.94	0.1	888.25	18.50	2.1	-53.85	18.53	-5.7
P-A	LU43	250601	1313.17	1.31	0.1	1249.05	23.55	1.9	-64.12	23.59	-4.9
P-A	LU44	220601	2256.16	2.26	0.1	2308.86	40.34	1.7	52.70	40.41	2.3
P-B	LU13	210601	5912.15	5.91	0.1	5865.44	52.49	0.9	-46.71	52.83	-0.8
P-B	LU26	260601	2300.88	2.30	0.1	2236.84	32.73	1.5	-64.04	32.81	-2.8
P-B	LU28	210601	3288.35	3.29	0.1	3291.01	34.41	1.0	2.66	34.56	0.1
P-B	LU30	200601	5788.32	5.79	0.1	5805.19	45.33	0.8	16.87	45.70	0.3
P-B	LU31	200601	6967.30	6.97	0.1	6979.42	54.57	0.8	12.12	55.01	0.2

Table A-III. Declared and measured $^{235}U/U$ abundance for PERLA samples. d_{M-D} is the difference between the measured and the declared values and s_d is the corresponding uncertainty. In the last column $100(M-D)/D$ represents, in percentage, the ratio between d_{M-D} and the declared value.

Container	Sample	Date	$(\alpha_{35})_D$ (percent)	(+-)	(percent)	(percent)	$(\alpha_{35})_D$ (+-)	(percent)	d_{M-D}	s_d	$100(M-D)/D$ (percent)
P-A	LU11	250601	0.9799	0.0010	0.1	0.89	0.03	3.4	-0.09	0.03	-9.1
P-A	LU12	220601	0.9799	0.0010	0.1	1.03	0.02	2.3	0.05	0.02	5.4
P-A	LU25	260601	3.0839	0.0031	0.1	3.22	0.05	1.6	0.13	0.05	4.3
P-A	LU42	260601	4.9687	0.0050	0.1	4.90	0.10	1.9	-0.07	0.10	-1.4
P-A	LU43	250601	4.9687	0.0050	0.1	4.87	0.08	1.6	-0.10	0.08	-1.9
P-A	LU44	220601	4.9687	0.0050	0.1	5.29	0.08	1.6	0.32	0.08	6.4
P-B	LU13	210601	0.9799	0.0010	0.1	1.00	0.02	1.5	0.02	0.02	1.8
P-B	LU26	260601	3.0839	0.0031	0.1	2.99	0.06	2.0	-0.09	0.06	-3.0
P-B	LU28	210601	3.0839	0.0031	0.1	3.16	0.04	1.2	0.08	0.04	2.6
P-B	LU30	200601	3.0839	0.0031	0.1	3.09	0.03	1.1	0.01	0.03	0.2
P-B	LU31	200601	3.0839	0.0031	0.1	3.07	0.03	0.9	-0.01	0.03	-0.4

For the Storage of Plutonium Metal, Is a Surveillance Program for Pressurization Necessary?

William J. Crooks III, Dane R. Spearing, John A. Rennie, Laura A. Worl, and Thomas L. Burr
Los Alamos National Laboratory, Los Alamos, New Mexico U.S.A.

Abstract

As part of the U.S. Department of Energy's (DOE) Materials Identification and Surveillance (MIS) program, gas generation issues for Pu metal stored in DOE-STD-3013-2000 containers were evaluated. This study was prompted in part by problems with lid thickness variabilities of "3013 containers" during initial quality assurance evaluations and to address issues with baseline radiographs in trying to detect pressurization in such containers at DOE packaging and storage facilities. If it is found that there is a credible mechanism for pressurization, then a research effort to show that we can detect such pressurization should be undertaken. If no such credible pressurization mechanism is identified, then there should be no need to implement mechanisms for the detection of pressurization in Pu-metal bearing containers. Elimination or minimization of surveillance activities to detect pressurization of Pu metal stored in 3013 cans for the fifty-year storage period would result in a significant cost savings. This work analyzes the published literature on Pu metal reactivity, presents calculations of pressure rise under credible storage conditions, and evaluates the results of recent Pu metal surveillance experiments. Based on this analysis, we conclude that a regular surveillance program to detect pressurization for the fifty-year term storage of metal items is not necessary.

Impact of Lid Thickness Variability on the Radiographic Surveillance of Pu Storage Containers

In the United States the storage and packaging of plutonium-bearing materials are govern by the U.S. Department of Energy (DOE) as described in the Standard DOE-3013-STD-20001 (Standard) and surveillance requirements are described in the Materials Identification and Surveillance (MIS) program. All approved long-term storage containers at the various DOE sites are identified as "3013 containers," indicating that the container specifications required in the Standard have been met. Both the Standard and the MIS program require a surveillance program for storage containers bearing Pu metal, and the nondestructive method of choice is specifically identified as radiographic imaging.

To evaluate the need for the quantitative radiography requirement, gas generation mechanisms in DOE-STD-3013-2000 containers loaded with Pu metal were investigated. If it is found that there is a credible mechanism for pressurization, then the research effort to show that we can detect such pressurization should be undertaken. If no such credible pressurization mechanism is identified, then there should be no need to implement mechanisms for the detection of pressurization in Pu-metal bearing containers.

This work reviews the published literature relevant to helium (He) generation, Pu metal-air-water reactions, and Pu oxide-air-water reactions. In addition, plausible container pressurization mechanisms are evaluated. Calculations are made to illustrate the type and amount of reaction that would occur under credible conditions, and the impact of the reactivity, such as indicated by pressurization or corrosion. Finally, the results of an ongoing six-year surveillance program for Pu metal stored in 3013 containers that were modified with pressure sensors are evaluated.

Gas Generating Mechanisms Associated with the Storage of Pu Metal

In 1994, an assessment of plutonium storage safety issues at DOE facilities was published[2] in which the anticipated hazards associated with the storage of Pu-bearing materials were addressed. Pu metal, oxides, hydrides, nitrides, and carbides, and their interactions with air, water, and organic materials were examined. The plausible mechanisms that could lead to pressure generation were 1) He release from alpha (α) decay, 2) chemical reaction (e.g., Pu + H_2O), 3) radiolytic decomposition of water, and 4) thermal desorption of physisorbed components.

He release: Following the method developed by Martz,[3] the He pressure expected from α-decay was calculated for 4.4 kg of Pu metal with the maximum specific surface area allowed by the 3013 Standard (1 cm^2/g) with the He gas in the void volume at the conservatively bounding temperature of 250°C in a Hanford bagless transfer can (BTC), with an internal volume of 1698 cm^3. The isotopics were assumed to be 89 percent ^{239}Pu, 1 percent ^{238}Pu, and 10 percent ^{241}Am (this latter nuclide is present assuming complete decay of the ^{241}Pu content), which represents a worst-case scenario in terms of He generation for Pu metal expected to be stored. The Pu metal shape was assumed to be a right circular cylinder with a 3:1 diameter to height ratio. For Pu metal, He is known to be trapped as microscopic bubbles at grain boundaries and only He emitted near the metal surface escapes based on

experience from reactor fuels.[2,3] For the calculation, it was assumed that only the He generated from the outer 1µm (0.0001 cm) of the surface of the button would be released. He generation for each isotope was then calculated using the following equation:

$$N_{He}(t) = N_{An,0}(1 - e^{-\lambda t})$$

where $N_{He}(t)$ = moles of He generated at time t, $N_{An,0}$ = initial moles of Pu and Am isotopes, t is time in years, $\lambda = \ln 2/(t_{1/2})$, $N_{He}(t)$ was converted to P_{He} (kPa) using the Ideal Gas Law at T = 523 K (based on the maximum metal storage temperature (250°C) established in DOE-STD-3013-2000).

Based on these calculations, the total pressure rise for He escaping from the outer micron of the 4.4 kg of Pu metal with a specific surface area of 1 cm²/g was calculated to be ~1 kPa after fifty years and ~2 kPa after one hundred years (Figure 1). Fortuitously, most of the He generated from alpha decay is trapped within the metal at grain boundaries and very little escapes.[2] In contrast, He from the alpha decay of PuO_2 almost quantitatively escapes[2,3], and calculations indicate He will contribute >600 kPa after fifty years and >1,100 kPa after one hundred years (Figure 2).

Chemical Reaction: A review of the reaction kinetics of unalloyed plutonium metal with oxygen, water, and humid air was conducted by Haschke et al.[4] In this review, the reactions Pu + H_2O, Pu + O_2, Pu + O_2 + H_2O were examined. In all cases, the reactions were consistently gas-consuming reactions in which the gaseous species adsorbed and/or reacted with the Pu surface. In terms of reaction rates, the Pu + O_2 reaction was the slowest for a given temperature and gas pressure, followed by Pu + H_2O, and Pu + O_2 + H_2O as the fastest. Furthermore, it was concluded that when Pu + O_2 + H_2O were all present (i.e., moist air conditions), PuO_2 was the exclusive product. Only after all of the oxygen was consumed would PuH_2 begin to form from the Pu + H_2O reaction. In addition, it was demonstrated that PuO_2 acts as a catalyst for the $H_2 + O_2 = H_2O$ recombination reaction. Thus, any hydrogen formed as a result of the reaction Pu + $2H_2O$ = PuO_2 + $2H_2$ would be consumed by the recombination with any oxygen in the container to form water. Once all of the oxygen is consumed, the hydrogen will react with the Pu metal to form PuH_2. Plutonium hydrides are known to form during the corrosion of plutonium metal by moist air, and larger quantities form when the corrosion takes place in the absence of oxygen.[5] The issue of volumetric expansion of the Pu material from high-density metal to low-density hydrides or oxides is addressed below in the section Impact of Generating of Plutonium Corrosion Products. In conclusion, the reaction of unalloyed Pu metal with oxygen, water, or hydrogen is not expected to contribute to gas generation.

With the addition of alloying elements to stabilize the delta (∂) phase of Pu, the oxidation reaction rate of the metal is generally reduced. For example, gallium (Ga) stabilized ∂-phase Pu is known to react slower with air than with unalloyed Pu. Haschke[6] reported the oxidation kinetics of ∂-phase Pu alloy in dry and humid air at 35°C. Under these conditions, it was estimated that an exposure period of approximately thirty days would be required to form a 1 µm thick oxide layer on the alloy at 100 percent relative humidity. In earlier work, electron diffraction analysis of the oxide layer identified both Ga_2O_3 and PuO_2.[5] Using the

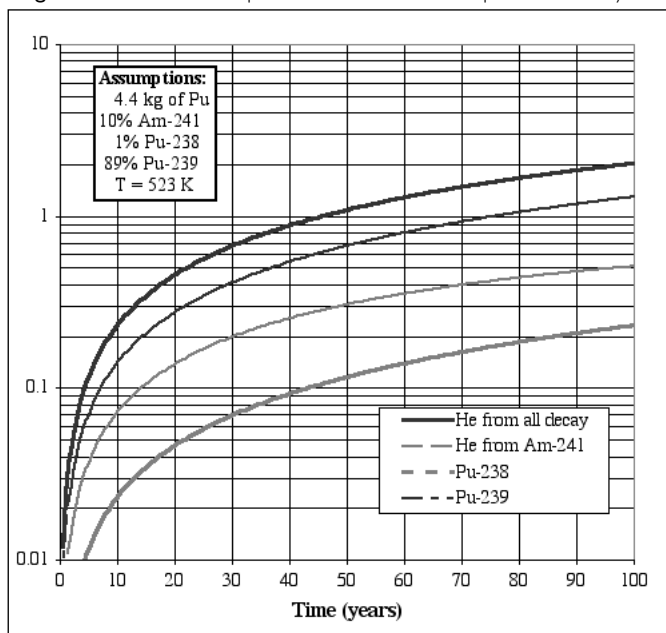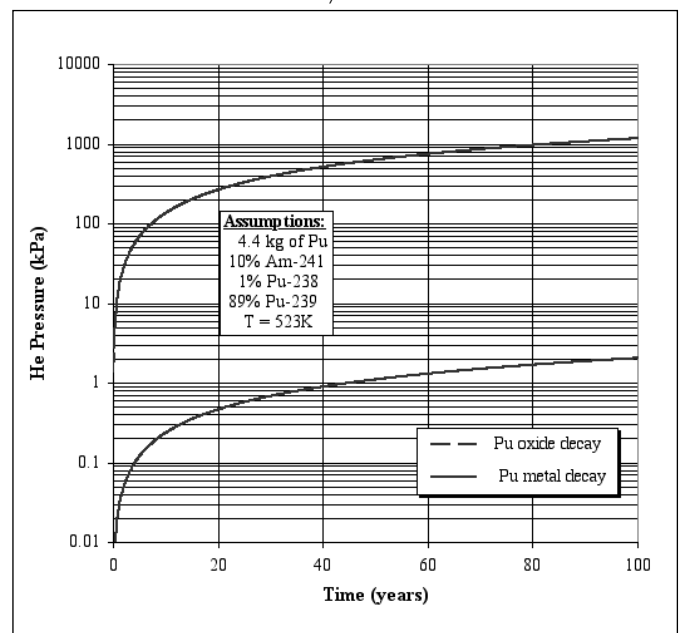**Figure 1.** Calculated He pressure rise vs. time for pu metal decay

Figure 2. Comparison of calculated He pressure rise vs. time for Pu Oxide and Pu metal decay

reaction kinetics data reported by Haschke *et al.*[4] for unalloyed Pu, we calculate that to form a 1 μm thick oxide layer on unalloyed Pu under similar temperature and humidity conditions would take only thirty-five hours. Thus, the reaction of alloyed ∂-Pu with moist air at 35°C is approximately twenty times slower than for unalloyed Pu. Nevertheless, these reactions are not indicative of any gas generation issues associated with the long-term storage of Ga stabilized ∂-Pu.

Other alloying elements have been added to Pu to enhance corrosion resistance and to stabilize crystallographic phases that have favorable chemical and physical properties. Unique alloy compositions7 that exist within the DOE inventory of metal items include the following: Pu/U, Pu/U/Mo (28:69:3 = "zipper alloy"), Pu/U/Fe, Pu/U/Zr, Pu/U/Th, Pu/U/Zr/Fe, Pu/U/Fs (where Fs = *fissium* = Zr, Mo, Ru, Rh and Pd), Pu/U/Fs/Ti.

To address the reactivity of these alloys, the reactivity of each individual alloying element is evaluated. For binary Pu/U alloys, the U addition is expected to have analogous atmospheric corrosion behavior to Pu. Both Pu and U components will be relatively inert to dry air but will react with atmospheric moisture, forming layers of oxide on the metallic surface.[5] As with unalloyed Pu, the alloy acts as a gas getter, and is not expected to generate gases or volatile compounds. Although not a gas generation issue during storage, finely divided Pu/U alloys are known to be pyrophoric,[8] and can contribute to safety concerns upon opening the sealed container. To address this safety concern, the DOE-3013-STD-2000 administratively precludes pyrophoricity issues by requiring metal pieces to be no less than 50 grams.[1]

Pu alloyed with Mo, Fe, Zr, or Th generally confers phase stabilization and corrosion resistance relative to unalloyed Pu. For each alloying element, the principal oxidation reaction products expected are MoO_3, Fe_2O_3, ZrO_2 and ThO_2, respectively. Analogously, for the suite of fission products defined as *fissium*, atmospheric corrosion is also expected to yield oxide products.

Therefore, for alloys, the Pu and alloying element compete to scavenge atmospheric gases. Although the scavenging reaction rates are generally slower (as evidenced by slower corrosion rates), simple calculations show that the metallic elements are still present in great excess relative to atmospheric reactants, and the gas-consuming reactions to form oxides are thermodynamically driven to completion. Therefore, under the nominal storage conditions of Pu metal within the 3013 containers that have been packaged according to the DOE-STD-3013-2000, the presence of alloying elements in Pu will not result in the formation of volatile or gaseous products.

Radiolytic Decomposition of Water: Water adsorbed on the surface of plutonium materials undergoes radiolytic decomposition to form hydrogen and oxygen gaseous products[9,10] according to the following reaction:

$$2H_2O \ (l) \rightarrow 2H_2 \ (g) + O_2 \ (g)$$

As a worst case, one could assume that the reaction proceeds 100 percent to completion. However, complete decomposition requires that all H_2O within the container is in close contact with Pu material. Models have been developed to predict the complex radiolytic and chemical processes that occur in the environment of Pu material, including the completeness of the H_2O decomposition reaction.[11,12] The Paffett-Kelly model of gas generation associated with plutonium oxide includes hydrogen and oxygen generation rates, and the rate for the recombination of hydrogen and oxygen back into water.[11] In this model, hydrogen and oxygen gas generation rates are controlled by dose rate and the amount of moisture present while the opposing recombination reaction to form water is a function of dose rate and power. For long time intervals, the model predicts that only 7 percent of the water is decomposed into hydrogen and oxygen. For the water that is radiolytically decomposed, subsequent reaction of the gaseous products with Pu trap the gases in the form of hydrides and oxides on the metal surface, resulting in no pressurization.

Thermal Desorption of Physisorbed Components: The introduction of water and organic matter on the Pu metal must be minimized by appropriate processing, material characterization, and quality control measures, as described in the Standard, DOE-3013-STD-2000. If water or organic matter is present in the storage container, the molecules can physically sorb to the surface of Pu metal, and some of these sorbents can be released by heating. For water, thermal desorption is expected to lead to a series of chemical reactions, as described earlier, and result in no pressurization. For organic material, thermal desorption and subsequent chemical and radiolytic reaction could result in the formation of noncondensible gases. At the time of packaging, the Standard requires metals to be "visibly free" of corrosion products, liquids, and organic matter. Therefore, for Pu metal that has been properly characterized and processed according to the storage Standard, thermal desorption of physisorbed components is expected to result in little or no pressurization.

Impact of Generating Plutonium Corrosion Products

As described above, for Pu metal that has been properly characterized, processed, and stored following the DOE-STD-3013-2000 storage standard, there is no credible pressurization mechanism. Of remaining concern is the formation of corrosion product, Pu oxide and/or Pu hydride, as a result of the reaction of Pu metal with any oxygen or water within the storage container, and whether the amount of oxide or hydride formed would present any hazard to the integrity of the container (e.g., volumetric expansion of the material resulting in mechanical pressure leading to vessel rupture). To address this issue, several calculations were done to assess the potential quantity of oxide and hydride formation under credible to bounding conditions, and these results were compared with observations of oxide formation on stored Pu metal samples.

Pu Metal–Moist Air Reaction: For the reaction of Pu metal with moist air, it was assumed that a clean 4.4 kg button of Pu metal was placed in a sealed 3013 container that contained air at 90 percent relative humidity at 30°C (a warm, moist day at the Savannah River Site (SRS), Aiken, South Carolina, U.S.A.). It was further assumed that the metal would radiolyze all of the water and react with all of the resulting hydrogen and oxygen, as well as the atmospheric oxygen. Based on these assumptions, it was calculated that this would result in the formation of approximately 5 g of PuO_2 and 0.7 g of PuH_2. Even if the PuO_2 and PuH_2 were of extremely low density (~ 3 g/cm^3), as would be expected for direct reaction with the metal, this would result in only 2-3 cm^3 of PuO_2/PuH_2 powder, which is such a small volumetric expansion of the material that the integrity of the storage container would not be compromised.

Pu Metal–Water Reaction: In addition to oxygen and water in the air, the presence of PuO_2 on a Pu metal sample prior to storage can also be an adsorption site for water that could react with the metal to produce additional Pu oxide and hydride. It has been well established that water readily adsorbs onto the surface of PuO_2.[13] Furthermore, current processing practices at the Hanford Plutonium Finishing Plant allow for up to sixteen hours between the time that a metal or alloy sample is brushed and when it is sealed within the storage container.[14] During this sixteen-hour exposure to glovebox atmosphere (nominally 20 percent to 50 percent RH), it was shown that up to 12 g of PuO_2 formed on a 2 kg Pu metal sample, and that for an off-normal exposure of >23 hours, up to 17.5 g of PuO_2 formed. Furthermore, brushing may not remove all adherent PuO_2 as some may remain in cracks and crevices. Figure 3 shows a 2 kg button that was removed from a SRS BTC at LANL in 1998. As is evident from the photo, the Pu button is covered by a thin layer of green PuO_2. Unfortunately, the mass and volume of the oxide on this button was not measured prior to its use in another experiment.

If it is assumed that PuO_2 is formed on the surface, it becomes saturated with respect to the humidity in the surrounding air (which has been measured[15] up to 50 mg H_2O / g PuO_2 at 25°C and 100 percent relative humidity), and that all of this water is radiolyzed and reacted with the metal, then for each gram of water-saturated PuO_2 placed in the container, calculations show that an additional 0.67 g PuH_2 and 0.38 g PuO_2 would form. Thus, if we assume an off-normal upper limit of approximately 25 g of PuO_2 (which would include remnant adherent oxide) that is saturated with water, and it is initially stored in the container with the Pu metal, then an additional 9.5 g of PuO_2 and 16.8 g of PuH_2 would form as a result of the reaction of the metal with the water. At 3 g/cm^3, this would represent a total volume of approximately 17 cm^3 of oxide and hydride powder.

Based on the above calculations of additional oxide and hydride formation as a result of water in the air and adsorbed onto an off-normal amount of PuO_2 in the container, it is apparent that the total volume of oxide and hydride powder formed

Figure 3. A 2-kg Pu metal button upon removal from SRS bagless transfer can

(even at relatively low densities of 3 g/cm^3) will result in such a small volumetric expansion of the material that the integrity of the storage container will not be compromised. The presence of up to 20 g of PuH_2 represents a pyrophoricity hazard upon opening such a container after storage, and appropriate safety precautions should be taken (e.g., open cans in an inert atmosphere). Proper brushing of metal samples and minimization of the time between brushing and subsequent packaging as per the DOE-STD-3013-2000 will reduce the potential for additional oxide formation as well as any adsorbed water associated with the oxide.

Results of the Ongoing Six-Year Surveillance Program for Pu metal at LANL

The lack of any gas generation mechanisms for packaged pure Pu metal samples is supported by recent surveillance experiments in which pressure sensing bellows were inserted into 3013 containers and then periodically inspected via radiography for any change in internal can pressure.[16,17] The results are shown in Figure 4. Over the course of six years, the largest observed pressure for a Pu-metal containing can was 25 kPa. Following these experiments, it was later determined that the error bars are on the order of ± 34 kPa due to errors in repositioning the cans for radiography. Bement et al.[18] noted that the bellows were not calibrated to measure less than 34 kPa because of a nonlinear response in the 0 to 34 kPa range. Our analysis, in view of previous calibration results, is consistent with the assumption that each of the monitored containers experienced a negligible pressure change. The lower limit of detection (LLD) is approximately 34 kPa and all measured values were beneath this LLD. More specifically, analysis of surveillance data on containers with bellows, together with bellows calibration results regarding how well the bellows measure pressure and over

what range,[18] are consistent with the assumption that the true pressure in each of these containers remained at or near 0 kPa. A pattern of positive measured pressures midway through the surveillance period is unlikely to have arisen by chance (less than 1 percent probability of arising by chance) so this remains an unexplained feature in this data, although the magnitudes are small and the positive bias at the mid-way time period is more likely due to measurement error than true pressure changes.

Thus, within error, these bellows experiments indicate no detectable change in pressures over four years within Pu-metal bearing 3013 cans. These surveillance results are consistent with findings in the literature and the conservative calculations presented in this work. Therefore, in a sealed container with an excess of Pu metal relative to the total amount of oxygen, water, and hydrogen, we would thus expect any pressure change to be zero or negative. Furthermore, *paneling* or partial collapse of *food pack* storage cans has been observed, which is indicative of a pressure *decrease* (partial vacuum).[19] As per the DOE-STD-3013-2000, the current packaging was designed to have sufficient mechanical strength to withstand a total internal vacuum (0 kPa).[19] Futhermore, no gas generation problems have been found in a DOE complex-wide information search.[19] With decades of favorable surveillance experience at the DOE sites, pressurization issues associated with metal storage should have been observed if they existed. Ongoing surveillance activities in the United States are preformed as part of the DOE Integrated Surveillance Program[20], which bins nuclear materials according to storage concerns. Metal items are binned under the lowest concern category called innocuous. According to the LANL surveillance program, ten samples will be randomly selected from the *innocuous* bin over ten years. Therefore, this program is likely to provide surveillance data on metal items, providing on-going assurance that Pu metal storage practices in the United States are safe.

Figure 4. Pressure change vs. time for Pu metal in 3013 cans measured via radiographic surveillance of internal bellows[21]
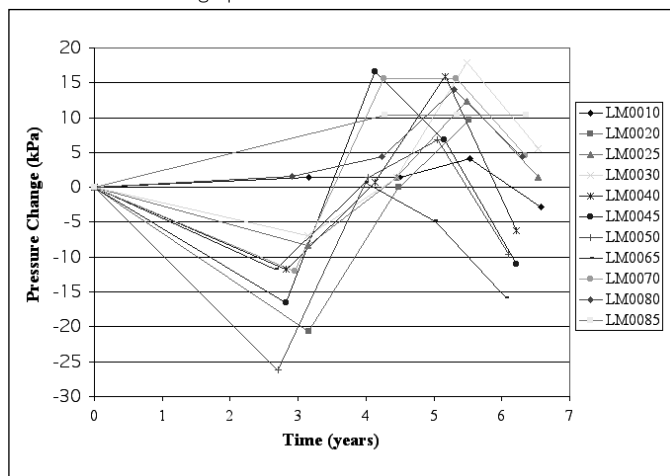
For the Storage of Pu Metal, Is There a Technical Basis to Eliminate a Surveillance Program for Pressurization?

Favorable attributes for the storage of Pu in the metallic state include the low surface area (which minimizes the sorption of water) and the ability to get gasses. Based on the literature review and analysis, the only credible gas generation mechanism with respect to pure Pu metal was He produced from α-decay of plutonium. Over a fifty-year storage interval, the calculated pressure rise in a DOE-3013 container due to α-decay of 4.4 kg of Pu metal equilibrated at 250ºC is less than 1 kPa. Thus, for the long-term storage of Pu metal packaged according to DOE-STD-3013-2000, He generation from a-decay will not make any significant contribution to pressurization. Finally, bellows experiments for Pu metal within DOE-3013 containers indicated no detectable change in pressures over four years.

As detailed in a recent summary of plutonium oxide and metal storage package failures,[18] the largest number of well-documented package failures involves the storage of Pu metal in non-airtight containers. In these cases, air leaking into the container lead to extensive oxidation of the metal accompanied by a large increase in the plutonium material volume which caused mechanical failure of the cans. As part of a corrosion surveillance program, radiography and weight gain are useful tools to identify oxide formation due to a containment failure, such as a failed weld. Thus, it is imperative that a certified process and/or inspection regimen for insuring leak-tight cans is in place. The presence of up to 20 g of PuH_2 on the surface of the Pu metal represents a pyrophoricity hazard upon opening such a container after storage, and appropriate safety precautions should be taken.

With no credible mechanism to pressurize sealed containers of Pu metal prepared and stored according to DOE-STD-3013-2000, and no experimental evidence of pressurization of such metal items, we conclude that a long-term surveillance program to detect pressurization for the fifty-year term storage of metal items is not necessary. Because 3013 container integrity is essential to the safe storage of Pu metal, control of corrosion and fabrication defects in containers must be attained with a rigorous quality assurance program for weld integrity and a corrosion surveillance program.

References

1. United States Department of Energy. 2000. *Stabilizing, Packaging, and Storage of Plutonium-Bearing Materials,* DOE-STD-3013-2000, September 2000, U.S. DOE, Washington, D.C.
2. United States Department of Energy. 1994. *Assessment of plutonium storage safety issues at Department of Energy Facilities,* DOE/DP-0123T, January 1994, U.S. DOE, Washington, D.C.

3. Martz, J. C. 1992. Analysis of Plutonium Storage Pressure Rise. LANL Memorandum, NMT-5:92-328, July 13, 1992.

4. Haschke, J. M., T. H. Allen, and J. L. Stakebake. 1996. Reaction Kinetics of Plutonium with Oxygen, Water and Humid Air: Moisture Enhancement of the Corrosion Rate. *Journal of Alloys and Compounds* 243, 23-35.

5. Wick, O. J. (ed.) 1980. *The Plutonium Handbook.* The American Nuclear Society, La Grange Park, Illionois, U.S.A.

6. Haschke, J. M. 1997. *Oxidation of Delta-Phase Plutonium Alloy: Corrosion Kinetics in Dry and Humid Air at 35°C.* Los Alamos National Laboratory, Report LA-13296-MS.

7. Schaade, J. 2003. Personal communication, Westinghouse Savannah River Company.

8. Waber, J. T. 1957. *The Corrosion Behavior of Plutonium and Uranium,* 2nd UN Geneva Conference, London: Pergamon Press, London.

9. Worl, L. A., J. M. Berg, F. C. Prenger, and D. K. Veirs. 2000. *Justification for Pressure and Combustible Gas Limitations in Sealed Instrumented Containers of Oxide Materials,* Los Alamos National Laboratory, Report LA-UR-00-1510.

10. Vladimirova, M. V., and I. A. Kulikov. 2002. Formation of H2 and O_2 in Radiolysis of Water Sorbed on PuO_2, *Radiochemistry* 44, 86-90.

11. Paffett, M. T., and D. Kelly. 2002. *The Essential Elements of Modeling Gas Generation From Well-Defined Plutonium Materials,* Los Alamos National Laboratory, Report LA-UR-02-4349.

12. Vladimirova, M. V. 2002. A Mathematical Model of Radiolysis of Water Sorbed on PuO_2. *Radiochemistry* 44, 501-505.

13. Haschke, J. M., and T. E. Ricketts. 1997. Adsorption of Water on Plutonium Dioxide, *Journal of Alloys and Compounds,* 252, 148-156.

14. Venetz, T. W., and R. W. Szempruch. 2002. *Plutonium Metal Preparations to Meet DOE-STD-3013-2000 in the Plutonium Finishing Plant,* Hanford Site, Washington, Report FH-0103610A R7.

15. Moseley, J. D., and R. O. Wing. 1965. *Properties of Plutonium Dioxide,* The Dow Chemical Company, Golden, Colorado, August 1965. US DOE Report RFP-502.

16. Rennie, J. 2001. Radiographic Surveillance of 3013 Nuclear Materials Storage Containers with Bellows. Los Alamos National Laboratory, Memorandum NMT-04-01-59.

17. Rennie, J. 2002. Radiographic Surveillance of MIS Items. Los Alamos National Laboratory, Memorandum NMT-04-02-62.

18. Bement, T.R., R.R. Picard, D.R. Horrell, V.D. Sandoval, and P.M. Jorgensen Jr. 1996. Analysis of Mini-Flex Prototype Bellows and Initial Production Data, Los Alamos National Laboratory, Report, LA-UR-96-1863.

19. Eller, P. G., R. W. Szempruch, and J. W. McClard. 1999. *Summary of Plutonium Oxide and Metal Storage Failures,* Los Alamos National Laboratory, Report, LA-UR-99-2896.

20. Dworzak, W., E. Kelly, and L. Peppers. 2003. *Integrated Surveillance Program Implementation Guide,* Los Alamos National Laboratory, Report LA-UR-03-5583.

21. MIS Program Review. 2002. Report, Los Alamos National Laboratory, LA-UR-02-6612.

The Effect of Standardizing Material Property Definitions on Nuclear Material Inventories in the U.S. Department of Energy

John R. Shultz
U.S. Department of Energy Office of Safeguards and Security Policy, Germantown, Maryland, U.S.A.

Abstract

In the United States, nuclear material of strategic concern is accounted for in a database called the Nuclear Materials Management Safeguards System (NMMSS). The U.S. Department of Energy (DOE) has for several decades issued policy guidance regarding how to report information to NMMSS. Furthermore, the DOE requires, through sunset provisions, that this policy must be revised on a periodic basis.

On October 1, 2003, a revised NMMSS policy was issued. The revised policy addressed a number of issues that have been raised by auditors and corrected some policy problems noted by users of the NMMSS, including the lack of nuclear material property standards. This paper discusses the process used to adopt nuclear material physical property definitions and consensus standards, and the effect of the adoption of these standards on the U.S. nuclear material inventory.

DOE Accounting Policy for Nuclear Material in the U.S. National Database— Some Historical Context

In the United States, nuclear material of strategic concern is accounted for in a database called the Nuclear Materials Management Safeguards System (NMMSS).[1] The U.S. Department of Energy (DOE) has for several decades issued policy guidance regarding how to report information to NMMSS.[2] Furthermore, the DOE requires, through sunset provisions, that this policy be reviewed and revised on a periodic basis.

In 1998, a DOE manual was published that provided policy guidance for reporting information to NMMSS.[3] Per the DOE policy sunset provisions, a review and revision of the 1998 manual began in fall 2002. The new NMMSS manual, which would be called DOE M 474.1-2A, 2003, was officially published on August 19, 2003, with an effective date of October 1, 2003.

The revised policy addressed a number of issues that have been raised by field facilities, auditors, the DOE headquarters policy staff, and others. In this paper, the selection of the National Nuclear Data Center (NNDC) at Brookhaven National Laboratory (BNL), as the source for nuclear material physical property definitions is discussed. Additionally, the effect of the adoption of data published by NNDC on the U.S. nuclear material inventory is presented.

What Does the DOE NMMSS Policy Require?

The NMMSS manual contains detailed instructions for reporting nuclear material shipments and/or performing physical and book inventory reconciliation. In addition, the NMMSS manual requires reporting of other information that affects inventories, e.g., radioactive decay and isotope in-growth, for the DOE accountable nuclear materials.[4]

As the revision of DOE M 474.1-2, 1998 progressed, it became apparent that there were a number of issues that would require resolution in DOE policy:

- Physical properties or *constants* were sometimes ill-defined. This left information regarding isotope decay half-lives, and what was mean by a *year* open to interpretation.
- The source of the radioactive decay constants could not be properly determined. For example, the decay constants in 1998 NMMSS manual were purportedly from the NNDC. However, when the source of the constants was checked, it was found that the half-lives were actually pulled from several sources, including an outdated American National Standards Institute (ANSI) standard.
- Agencies both within and outside of DOE had issued reports noting the need to standardize information for nuclear material accounting.[5]
- There were factual errors in calculating some material properties. For example, the conversion equation from volume to mass basis for some gaseous isotopes was improperly defined.
- In some instances, the shipper and receiver of nuclear material would use different decay values for the same material over the same time period.[6]

Nuclear Physics Affects the Quantities of Material in Inventory Over Time

The quantities of nuclear material actually in inventory changes over time due to fundamental physical processes such as radioactive decay. For example, Figure 1 shows that the quantity of some relatively short-lived isotopes decrease significantly over time. For Pu-241, 50 percent of the amount stated on the book inventory disappears after about fourteen years due to radioactive decay.

Therefore, if a measurement is made during a physical inventory in the fourteenth year, only half of the original quantity of Pu-241 would remain. This could certainly be alarming, if one
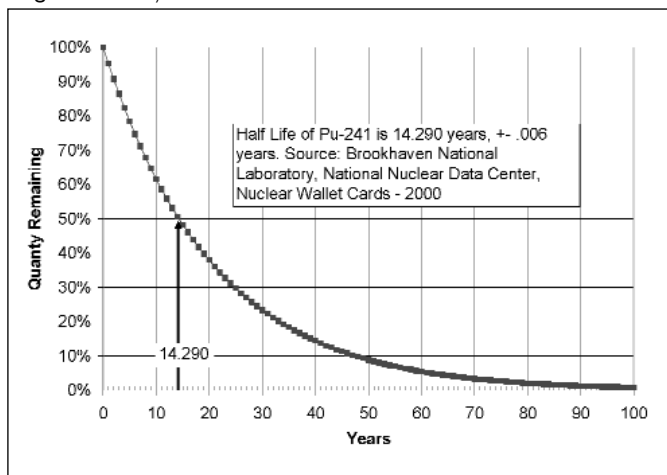
did not understand that the natural process of decay is constantly changing the quantities of nuclear materials in inventory, and therefore inventory records must be adjusted to reflect this physical reality. To ensure that the appropriate inventory adjustments are made, the 2003 NMMSS manual states:

> *Facilities will send data on reportable quantities of radioactive decay to the NMMSS on a DOE/NRC F 741 as per instructions in Chapter III of this manual.[7]*

This process ensures that both the book and site records are revised in concert and that material quantities physically on hand are neither over nor understated in the facility or NMMSS book inventories.

Table 1. Half-lives for 3 isotopes and their source

Element & Isotope	Half-Life (years)					
	ANSI N 15.22-1987	Standard Deviation	DOE M 474.1-2 Feb. 1998	Standard Deviation	BNL-Nuclear Wallet Cards Jan. 2000	Standard Deviation
Am 241	433.6	1.4	432.7	.6	432.2	.7
Pu 238	87.74	.04	87.74	.04	87.7	.3
Pu 241	14.348	.022	14.35	.1	14.290	.006

Figure 1. Decay of Pu-241 over time

purportedly are from Brookhaven National Laboratory,[9] but they appeared to come from a variety of sources including an old ANSI standard.[10] We felt this was unsatisfactory, and that the numbers published in the 2003 NMMSS manual should be clearly traceable back to their source.

Ambiguous Statements Can Lead to Diminished Nuclear Material Accountability

Another problem in the 1998 NMMSS manual regarding decay constants centers on an ambiguous statement that allowed too much room for interpretation of supposed *constants*. The statement read as follows:

> *"…However, a facility will have the option of maintaining its records of radioactive decay to a greater degree of precision than that required for reporting purposes."[11]*

This statement allowed facilities the option of choosing whatever decay constant they want, as long as they feel is has a "greater degree of precision..." than that published in the 1998 NMMSS manual. But, what is precision?

Most scientists would consider a measured value as better (more precise) when the variance is smaller (i.e., standard deviation squared is smaller). This also depends on the number of independent measurements and perhaps the quality of the laboratory doing the measurements, but it is a good rule of thumb. If the variance is used as a criterion for choosing between decay half-lives, then the decay constants would be chosen as follows:

As can be seen from Table 2, the information in the 1998 NMMSS manual was more precise, based on smaller variance, for Am-241 and tied with the 1987 ANSI standard for Pu-238. However, the 1998 NMMSS manual was the worst of the three information sources for the shortest lived isotope, Pu-241 and the 2000 BNL Wallet Cards data was best.

A Policy Question: Exactly How Long is an Isotope's *Half-Life*?

As mentioned above, nuclear decay affects the nuclear material inventory. One may think that an isotope's *decay constant*, or *half-life*, would not be open to interpretation or confusion. Actually, as is the case for most measured values that are used as *constants*,[8] an isotope's half-life depends to some degree on when, how, where, and by whom it is measured. Table 1 shows that isotope half-lives can vary depending on the source.

The Need for an Audit Trail for Constants Used in Reporting Nuclear Material

It is very important that the numbers used for accounting for nuclear material at the DOE be based on data from an acceptable source. In the case of the 1998 NMMSS manual, we did not have an audit trail backward in time to the source documents on which the decay constants are derived. For example, the radioactive decay constants used in DOE M 474.1-2, 1998, Figure IV-2,
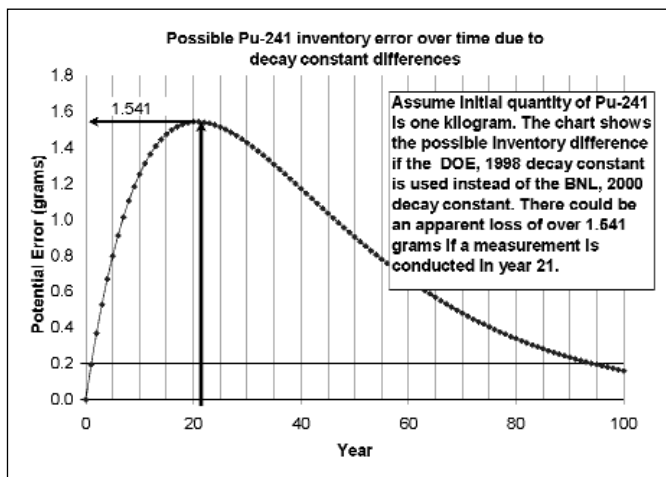
Table 2. Comparison of variance of decay constants from various sources

Element & Isotope	Ranking Based On Varience (using data from table 1)		
	ANSI 1987	DOE 1988	BNL 2000
Am 241	3	1	2
Pu 238	1	1	3
Pu 241	2	3	1

What could a facility do? If they were aware of all three data sources, they could possibly pick the 1998 NMMSS manual for Am-241 and Pu-238, and the 2000 BNL Wallet Cards for Pu-241. However, a second facility might not be as inquisitive. This facility may simply use the constants published in the 1998 NMMSS manual. A third facility might select an entirely different source for the constants, and for a reason other than a smaller variance.[12]

The problems created by allowing facilities this leeway are compounded when the chosen decay constants are hard-coded into facility software. Once this occurs, people at the facilities may not even be aware of what value they are using, or where it came from, if the required decay reporting information (the DOE/NRC F 741) is generated automatically via the software.

A reason for the concern regarding consistency can be seen from figures 2 and 3. The use of a decay constant from one organization versus another (1998 NMMSS manual versus 2000 BNL Wallet Cards) can lead to some significant errors over time. The figure shows that a bookkeeping loss (or gain) of 1.541 grams of Pu-241 could occur after twenty-one years (from an original quantity of one kilogram). The full set of comparisons in Figure

3 shows that the inventory could also be understated by 1.490 grams in year twenty-one.

How Many Days Are in a Year?

Another source of error in the inventory is due to an apparently simple item such as knowing how many days are in a year. But when calculating decay of nuclear materials, and subsequently updating inventory records for these materials, a year is not simply a year.

For example, non-leap year calendar year has 365 days,[13] a *Julian* year has exactly 365.25 days, a *tropical* year has 365.2422 days, and a *sidereal* year averages 365.2564 days.[14] A problem in the 1998 NMMSS manual is that what is meant by a *year* was undefined. This left the facilities using the decay constants listed in the manual the latitude to choose various *years* to perform decays calculations and update the quantities of material in inventory.

How Could Different Definitions of a Year Impact the Quantities of Material in Inventory?

The short answer is: not much impact. The half-lives for most of the isotopes of concern are long enough that the slight variation in the definition of a year does not have much impact on the amount decayed. If one chooses a sidereal versus a tropical year, the difference between the two years is only 44.64 seconds (365.2564 – 365.2422 = .0142 days). At the end of one hundred years, the time difference would be approximately 74.4 minutes. For all of the isotopes of concern in the NMMSS system, the decay half-lives are stated in years, so the potential change in the amount reported to the database (erroneously) due to different definitions of a year is very small.[15] Figure 4 shows that for a *short* year of 365 days versus a *tropical* year of 365.2422 days, the

Figure 2. Potential inventory error simply due to different decay constants


Figure 3. Potential inventory error due to three different decay constant source documents
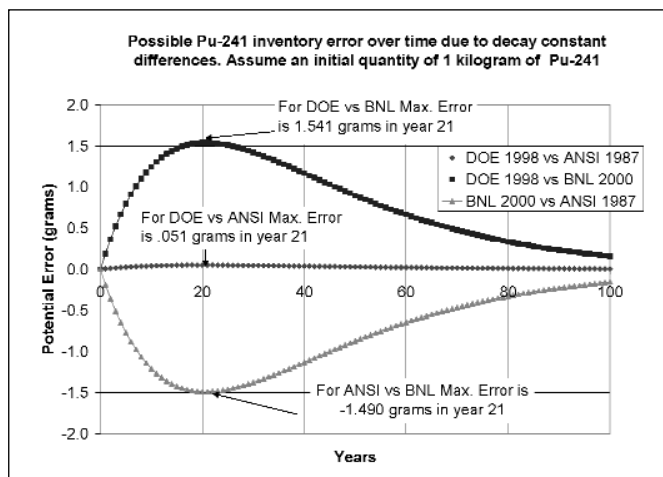
maximum potential error would be about .24 grams of Pu-241 per kilogram in inventory and this maximum occurs in year 20. For a tropical versus sidereal year, the maximum error is about .0006 grams of Pu-241 per kilogram in inventory and this maximum also occurs in year 20. The NNDC uses a tropical year to calculate nuclear decay, and that is the year adopted by DOE.

Potential inventory errors due to different definitions of a *year*
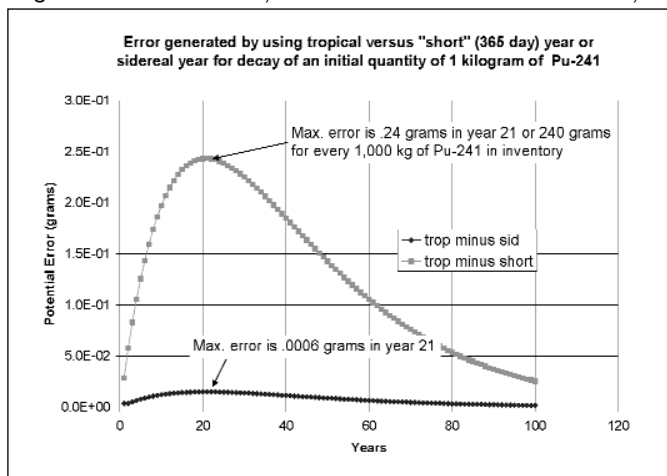
Consistency Should be a Priority in Accounting Systems

As shown in the examples above, a lack of consistency in sources of data can lead to perceived errors in the nuclear material inventory. If the decay calculation and subsequent write-down of inventory book values is as least consistent across DOE, then any calculation error that may be discovered can be corrected. However, if facilities throughout DOE are not consistent in the constants they use, it can be nearly impossible to fix some inventory errors in the future.

The Effort to Enhance Consistency and Traceability of Material Properties Across DOE

A search was conducted to find an organization that could operate as both the central point of contact and clearinghouse for the latest information on nuclear materials properties.[16] Since the earlier NMMSS manuals referred to BNL, this organization was considered a good starting point. After investigating other options, it was decided that the best, most widely accepted and used radioactive decay information is provided by the Brookhaven National Laboratory National Nuclear Data Center. Therefore, DOE adopted the BNL-2000 Nuclear Data Wallet Card decay data for nuclear material inventories.

Some facilities were concerned that wallet cards meant an abbreviated selection of isotopes and a small collection of data that would not include information they needed. The term *wallet cards* could not be more of a misnomer. The *wallet cards* are available online in a blown up version on 8 1/2-by-11-inch paper that is more than one hundred pages long. True *wallet cards* are available from the NNDC in a handy, smaller 3-by-5-inch booklet that still has fifty pages (printed front and back). What was meant by *wallet cards* is that this collection of information is still quite brief when compared to the Table of the Isotopes, which has around 3,000 tightly formatted pages.[17]

A key decision factor in choosing NNDC is seen in the information from the following information from the NNDC Web site:[18]

> *The National Nuclear Data Center (NNDC) is funded by the U.S. Department of Energy to:*
> * *provide information services in the fields of low- and medium- energy nuclear physics to users in the United States and Canada,*
> * *serve as contact for international data exchange.*
> *In particular, the Center can provide information on:*
> * *neutron, charged-particle, and photonuclear reactions,*
> * *nuclear structure, and radioactive decay.*
> *Extensive bibliographic, experimental data, and evaluated data files are available and may be accessed through the Internet. More general needs can often be satisfied by one of the Center's many publications.*
>
> *The information available to the users of NNDC services is the product of the combined efforts of the NNDC and cooperating data centers and other interested groups, both in the United States and worldwide. Services are generally free of charge.* [19]

The NNDC agreed to freeze the BNL-2000 Nuclear Data Wallet Cards and maintain them on its Web site at www.nndc.bnl.gov. The information is therefore available to DOE free of charge. A screen capture of the BNL Web site is shown in the following figures.

A Forward-Leaning (Proactive) Approach

An added benefit of adopting the BNL-2000 Nuclear Data Wallet Cards is that DOE has taken a proactive approach with respect to the NMMSS system. In the future, if additional nuclear materials must be tracked in NMMSS, the issue of decay and material property definitions is already resolved.

Figure 5. Screen capture of the NNDC Web site showing a hyperlink for wallet cards
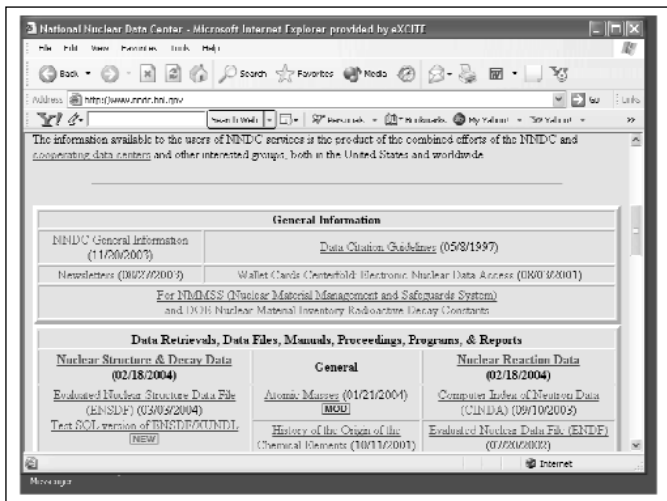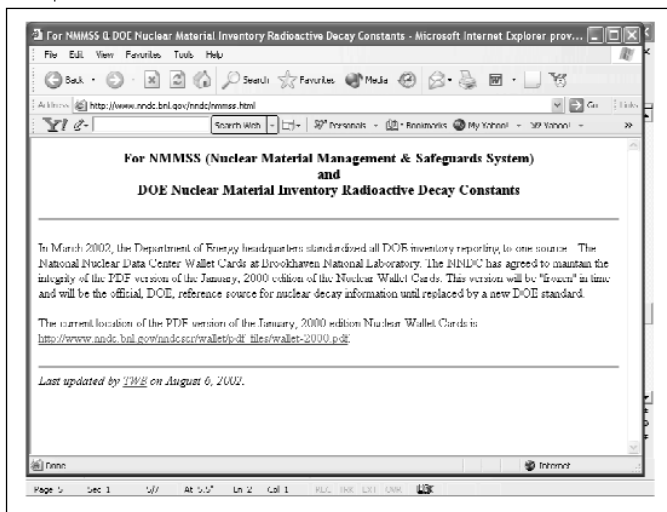

Figure 6. Screen capture of NNDC Web site with language regarding adoption of BNL-NNDC Wallet Cards

Acknowledgements

John R. Shultz is an engineer in the Office of Safeguards and Security Policy, Nuclear Materials Control and Accountability Program, Headquarters, U.S. Department of Energy. Shultz is responsible for writing and interpreting policy regarding the accountability of nuclear material at DOE sites throughout the United States. Before his current job, Shultz worked as a lead project engineer at the National Energy Technology Laboratory, Morgantown, West Virginia, U.S.A., and has consulted for the Mineral's Management Service, U.S. Department of Interior, on the risk of accidents or spills at offshore natural gas and oil production platforms, and performed greenhouse gas emissions accounting for the Northern Indiana, Public Service Company (NIPSCO), Merrillville, Indiana, U.S.A. Shultz has graduate degrees in mechanical engineering (M.S.) and engineering and public policy (M.S., Ph.D.) from Carnegie Mellon University — Pittsburgh, Pennsylvania, U.S.A., and has undergraduate degrees in mechanical engineering (B.S., magna cum laude, University of Alabama — Hunstville, Alabama, U.S.A.,) and business administration (B.S., University of the State of New York — Albany, New York, U.S.A.).

1. Not all nuclear material is accounted for in this system. Only materials of strategic concern to the U.S. (called Special Nuclear Material [SNM]) are included. The nuclear materials which constitute SNM are defined in the Atomic Energy Act of 1954 as amended and in government agency policy. The information contained in the NMMSS database is summary in nature. DOE facilities maintain highly detailed records on SNM and non-SNM nuclear material in their own databases, and provide summary data to the NMMSS. The Nuclear Regulatory Commission (NRC) also reports nuclear material information to the NMMSS pursuant to their rules (NUREG-006 and NUREG-007).

2. The NMMSS database began in approximately 1965. The policy governing submission of data to NMMSSS has evolved over this time period and is now published through the DOE Directives system

3. DOE M 474.1-2, 1998 *"Nuclear Materials Management and Safeguards System Reporting and Data Submission."* This document is commonly referred to in DOE as the "NMMSS Manual"

4. The NMMSS accountable elements for DOE (2004) are Americium, Berkelium, Californium, Curium, Hydrogen (as Deuterium and Tritium), Lithium, Neptunium, Thorium, Plutonium, and Uranium. Not all isotopes of the accountable elements are reported to NMMSSS.

5. DOE Inspector General, DOE Office of Assessment, Office of Management and Budget, Government Accounting Office, etc…

6. Source: personal conversation on March 24, 2004, with Bob Trivett, Westinghouse-Savannah River – LANMAS Project,

7. See DOE M 474.1-2A, 2003, page II-8. The DOE/NRC F 741 is the form-of-record for making corrections to the book inventory of the facility that is maintained in the national system (i.e., NMMSS). The facility is also responsible for updating their database/records to write-down the quantity of material that has decayed.

8. For example, the speed of light in a vacuum has undergone numerous revisions as measurement technology has improved.

9. For example, in DOE M 474.1-2, 1998, Footnote 1, page IV-5 states that the half-lives are from BNL. The key missing data is a reference year for the purported BNL data. This would have allowed us to determine if the constants were truly from BNL. For historical context, the half-life for Pu-238 is listed in the predecessor of DOE M 474.1-2 1998 (that is DOE 5633.5, 1987, Figure IV-2) as 87.74 $\pm$.3y. The source for the DOE 5633.5, 1987 Pu-238 decay constant is also supposedly BNL, but since a reference year is not given, one can not with confidence say that this statement is true.

10. ANSI N 15.22-1987 *"Plutonium-Bearing Solids Calibration Techniques for Calorimetric Assay."*

11. DOE M 474.1-2, 1998, page IV-4.

12. Perhaps an old version of the Table of the Isotopes that they have handy on their desk, or a CRC handbook, a college physics book, or the Internet.

13. For lack of a better term, I call a year with 365 days a short year.

14. From: Wikipedia, The Free Encyclopedia at http://en.wikipedia.org/wiki/Main_Page. A sidereal year is the actual period for the earth to complete on revolution of its orbit, as measure in a fixed frame of reference. The actual duration varies from year to year due to non-earth body gravitational influences. The tropical year is the period for the earth to complete one revolution with respect to the framework provided by the intersection of the ecliptic (the plane of the orbit of the Earth) and the plane of the equator (the plane perpendicular to the rotation axis of the Earth). Because of precession, this framework moves slowly backwards along the ecliptic with respect to the fixed stars; as a consequence, the Earth completes this year before it completes its full orbit as measured in a fixed reference frame. Therefore, a tropical year is shorter than the sidereal year.

15. Pu-241 was chosen for illustration purposes. The shortest lived isotope of concern in the DOE NMMSS database is Californium-252, which has a half-life of 2.645 +-.008 years. Shorter lived isotopes experience maximum possible error earlier in the isotope lifetime

16. Conducted by a member of the security policy staff within the DOE Office of Security (SO)

17. *Table of Isotopes,* 8th edition, Firestone, R. B. and Shirley, V. S., editors, John Wiley & Sons, New York, 1996. A two volume set with 3,000 pages available at a cost of approximately $200 U.S. (2004).

18. The U.S. Nuclear Data Program (USNDP) membership and organization: The USNDP includes nuclear data groups and nuclear data experts from national laboratories and Academia, including Argonne National Laboratory (ANL), Brookhaven National Laboratory (BNL), Georgia Institute of Technology, the Idaho group, Los Alamos National Laboratory, E.O. Lawrence Berkeley National Laboratory, Lawrence Livermore National Laboratory, Triangle Universities Nuclear Laboratory, McMaster University, and the National Institute of Standards and Technology. Source: http://www.nndc.bnl.gov/usndp/.

19. Source: http://www.nndc.bnl.gov/nndc/nndcinfo.html.

The Detection of Enrichment of Uranium System: A Portable System for Nondestructive Assay of TRIGA® Spent Nuclear Fuel

John J. King and Gary N. Hoggard
Global Technologies, Inc., Idaho Falls, Idaho U.S.A.

Abstract

The Detection of Enrichment of Uranium System (DEUS) is a portable nondestructive assay system capable of measuring the U-235 mass remaining in TRIGA® (Training, Research, and Isotope General Atomics) spent nuclear fuel (SNF). The DEUS is described and results from DEUS assay of irradiated TRIGA® fuel elements performed at the University of Texas Nuclear Engineering Teaching Laboratory (UT) and the Texas A&M University Nuclear Science Center (TAMU) are presented. These measurements were performed February 24-28, 2003, at TAMU and November 10-14, 2003, at UT. Irradiated fuel elements assayed at TAMU consisted of three 20 percent-enriched-U-235-by-weight uranium in an UZrH matrix, which are commonly called standard-plain (STD-PLN), and five 70 percent-enriched-U-235-by-weight uranium in an UZrHEr matrix, which are commonly called FLIP (Fuel Lifetime Improvement Program). The fourteen irradiated fuel elements assayed at UT were all STD-PLN. The U-235 mass solutions derived from these measurements are generally within ±5 percent of the declared U-235 mass values. Two FLIP elements measured at TAMU produce a reduced neutron interrogation response that may be associated with fuel-matrix damage. Monte Carlo Neutron Particle (MCNP) calculations show that when fissile materials are diverted from the STD-PLN fuel meat and replaced with non-fissile materials, the DEUS is able to detect this with definitive statistical significance.

Introduction

Beginning in the 1950s, as part of the Atoms for Peace program, the United States provided nuclear technology to foreign nations for peaceful application in exchange for their promise to forego the development of nuclear weapons. A major element of this program was the provision of research reactor technology and the enriched uranium needed in the early years to fuel the research reactors. The U.S. Department of Energy (DOE), in consultation with the U.S. Department of State, implemented a new foreign research reactor (FRR) spent nuclear fuel (SNF) acceptance policy on May 13, 1996. The purpose of the acceptance policy was to support the broad U.S. nuclear weapons nonproliferation policy calling for the reduction and eventual elimination of the use of highly enriched (weapons-grade) uranium in civil commerce worldwide. In accordance with this new policy, TRIGA® (Training, Research, and Isotope General Atomics) reactor fuel from FRR facilities that contains uranium enriched in the United States is transported to and managed at, pending ultimate disposition, the Idaho National Engineering and Environmental Laboratory (INEEL). Of this foreign SNF, an estimated 4,940 elements (1,033 kg of enriched uranium) are TRIGA® reactor SNF from various countries—some of which have already been shipped to the INEEL.[1]

The DOE-Idaho Operations Office (NE-ID) foresaw the need and provided funding for developing a nondestructive assay system to quantitatively determine the amount of U-235 that remains in TRIGA® reactor SNF upon its return to the United States As specified by NE-ID, the system would:
1) Non-intrusively interrogate TRIGA® SNF
2) Determine its uranium enrichment (in grams of U-235) with an acceptable degree of accuracy of ±5 percent, and
3) Meet portability and functionality requirements as necessary to be deployable domestically and/or internationally.

Since late 1999, the evolving Detection of Enrichment of Uranium System (DEUS) has performed fuel measurements at both domestic and international TRIGA® facilities (see Figure 1). This portable system has been tested domestically at the Texas A&M University Nuclear Science Center (TAMU) four times, Kansas State University (KSU), and the University of Texas Nuclear Engineering Teaching Laboratory (UT). The DEUS has also been successfully deployed internationally to the Instituto Nacional de Investigaciones Nucleares (ININ) near Salazar, Mexico. Each measurement trip was generally five working days at each facility with specific measurement priorities assigned depending upon the stage of development of the DEUS. In the case of the measurements at the ININ, the objective was to demonstrate that the DEUS could perform measurements at a facility outside the United States; and to establish requirements and protocols that would be applicable to other international deployments. DEUS modifications were evaluated through the repetition of measurements at TAMU. DEUS measurements on standard-plain (STD-PLN) fuel with low burnup were conducted at KSU to aid in the development of the current DEUS design.

Figure 1. The detection of enrichment of uranium system (patent pending)

The measurements at UT represent the last deployment of the DEUS to assay TRIGA® fuel. Only results from TAMU and UT are presented since each of those experiments was conducted with the latest and final DEUS configuration.

In the following sections, the subsequent topics are described: the TRIGA® reactor fuel in units commonly referred to as *elements,* the design and key components of the DEUS, the DEUS algorithm, the TRIGA® fuel assay results from UT and TAMU, the DEUS response to non-fissile surrogate fuel materials, and the conclusions concerning the progress to date. Any facilities, reactors, and reactor fuel discussed in the following sections are TRIGA® type unless otherwise specified. Also note that all discussed and reported errors presented in the following sections are at 1 sigma (68.3 percent confidence based upon Gaussian statistics).

TRIGA® Reactor Fuel Description

The development of the TRIGA® reactor began in 1956 with a goal of building a reactor that was inherently safe.[2] The prototype Mark I reactor was commissioned by General Atomics on May 3, 1958. Three reactors were placed in operation by the end of 1958. Today, an installed base of sixty-five reactors is found in twenty-four countries on five continents. These reactors have a range of power levels from 100 kW to 14,000 kW. The number of elements and the constituents in each element determine these reactor power levels.[3]

There are four basic types of TRIGA® fuel elements. These are aluminum-clad, stainless-steel-clad, Incoloy-800-clad, and

fuel-follower-control-rod (FFCR) elements.[4] The lengths of these elements can vary from 72.06 cm to 168.9 cm, and diameters can vary from 1.37 cm to 3.81 cm. These fuel elements contain fuel meat that is an UZrH-based alloy. The uranium U-235 enrichment at beginning of life (BOL) ranges from 20 percent to 93 percent by weight. The amount of uranium in the UZr alloy can vary from 8 percent to 45 percent by weight. The amount of natural Er in the fuel meat can vary from 0 percent to 1.6 percent by weight. The fuel meat within the element can have lengths that vary from 35.6 cm to 55.9 cm. These fuel element dimensions and associated end fitting types can vary based upon the reactor design, desired power, and associated cooling requirements. This is especially true for TRIGA® reactors that have been converted from material test reactors (MTR).

Figure 2. TRIGA® Standard-Plain fuel element and components
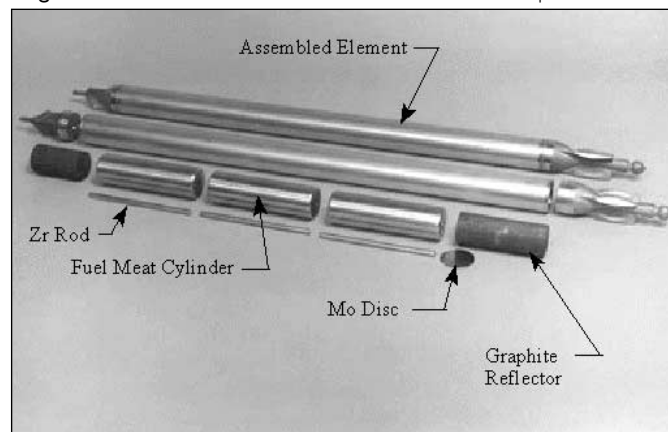

Figure 2 is a photograph of the components associated with a typical STD-PLN element. A STD-PLN element weighs approximately 3.4 kg and contains 8.5 percent total U by weight for the UZr alloy. The H/Zr atom ratio is typically 1.6 after the addition of H at an elevated temperature. After the H addition, a Zr rod (nominally 5.72 mm in diameter) is inserted axially into the radial center of each of the 12.7-cm-long UZrH fuel meat cylinders. The three-stacked UZrH cylinders are sandwiched by graphite reflectors. The small disc laying flat at the right side of the fuel meat is a thin molybdenum disc that normally resides between the fuel meat and the graphite reflectors. Each of these components is stacked inside the cladding and enclosed by two end fittings. At the BOL, the nominal gap between the fuel meat and cladding may be as small as 0.0038 cm. The cladding thickness is nominally 0.051 cm.

FLIP elements also contain 8.5 percent total U and 1.5-1.6 percent Er poison by weight for the UZrEr alloy. The Er is used as a neutron poison to flatten the neutron flux along the axial length of FLIP fuel. These elements are constructed the same as that described above and shown in Figure 2.

References 1-4 provide more details concerning other aspects of TRIGA® fuels.

DEUS Description

The successful development of the DEUS began with several fundamental concepts and concerns as necessary to meet the NE-ID specifications listed above for non-intrusiveness, accuracy, portability, and functionality. He-3 proportional counters would be used to detect neutrons from the U-235 fission induced by neutrons from an external source. The apparatus would be designed using the Los Alamos code, MCNP.[5] The portable design would incorporate simple materials (polyethylene and aluminum), simple electronics, and have a high degree of operational reliability. In order to approach the desired 5 percent accuracy, the DEUS had to perform measurements in air (i.e., not under water). The neutron interrogation response as well as the gamma-ray exposure rate generated by each fuel element would be predicted by modeling the burnup of each fuel element.

The He-3 proportional counters would be used for neutron detection, but it was unknown whether the large gamma-ray flux from SNF would allow for the proper measurement of neutrons. B-10 lined He-3 proportional counters were proposed to minimize these gamma-ray interactions.[6] In addition, other sources of neutrons due to spontaneous fission of transuranic nuclei and (α,n) reactions in the fuel meat were also of concern. However, initial investigations revealed that the zirconium (Z=40) matrix in TRIGA® fuel inhibits (α,n) reactions, and the maximum intensity of spontaneous fission neutrons measured to date translates to several neutron counts per second. Hence, neutron *singles* counting is allowed for the assay of TRIGA® SNF.

These fundamental concepts, concerns, and later experimental trials have led to the DEUS design as described in the following paragraphs.

Referring to figures 3 and 4, the DEUS apparatus consists of seven basic components that are needed for determining the amount of U-235 that remains in SNF. These components include: 1) a source holder that houses a Cf-252 neutron source placed within graphite/polyethylene concentric cylinders, 2) a neutron lens that consists of a polyethylene block having two apertures at opposite angles relative to the source axis and one cone of borated polyethylene, 3) a main fuel tube (MFT) consisting of an aluminum pipe to which an aluminum funnel is connected and on which a fuel-position sensing switch is installed, 4) a reflector plate consisting of polyethylene, 5) a detector package consisting of a block of polyethylene covered with cadmium sheet metal and three He-3 proportional counters on which preamplifier/amplifier/discriminator electronic modules are mounted, 6) an auxiliary fuel tube (AFT) consisting of a Cd-covered aluminum pipe to which an aluminum funnel is attached, and 7) an ionization chamber. The above components are mounted on a small table and centered approximately 38.10 cm above the floor surface as depicted in figures 3 and 4.

The Cf-252 neutron source consists of a stainless-steel capsule that contains a Cf/Pd-source pellet with a nominal 10 µg (2.3E+7 neutrons/second) of Cf-252. neutrons from this source

Figure 3. Front View of the DEUS apparatus
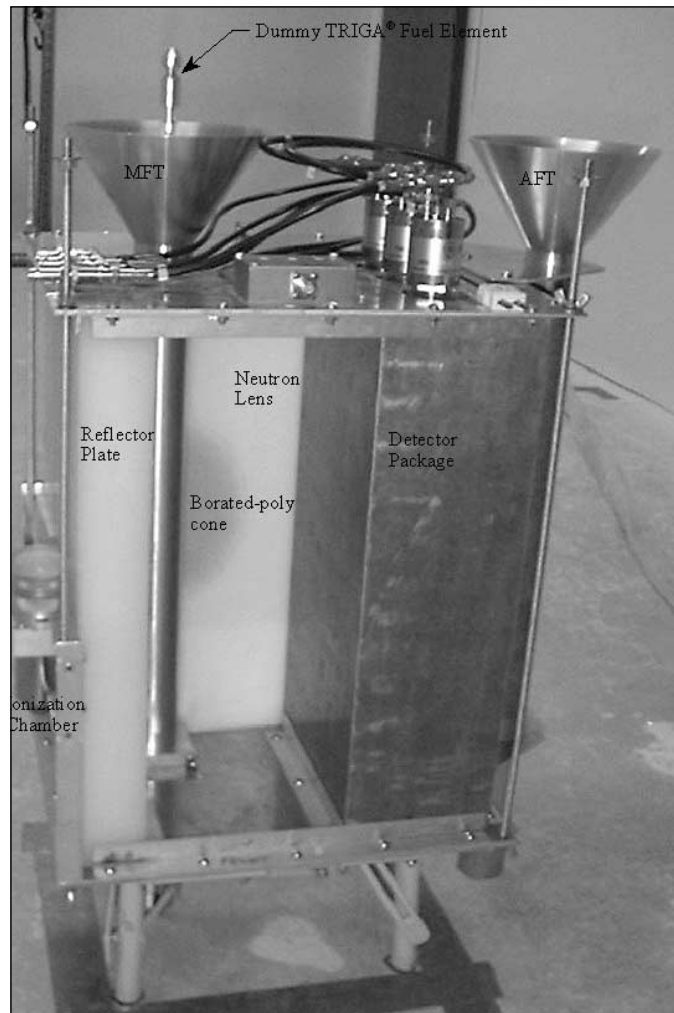
are produced by spontaneous fission of Cf-252 nuclei. The graphite cylinder and polyethylene cylinder associated with the source holder partially slow the Cf-252 fission neutrons and aid in directing them toward the neutron Lens.

The neutron lens moderates (slows) and spreads out the neutron beam leaving the Cf-252 source to ensure that the response over the nominal 38.10 cm fuel meat length of the fuel element is uniform. The polyethylene is used as the neutron moderating material. The borated-polyethylene cone is used as the neutron absorbing material that flattens the intrinsically-peaked distribution of neutrons coming from the source holder. The apertures (hidden by the MFT in Figure 3 and the source holder in Figure 4) allow for the transport of neutrons to the upper and lower sections of the fuel element meat section. This results in an equally weighted axial interrogation of the entire fuel element meat when the element is placed in the MFT.

During neutron interrogation, the fuel element rests within the MFT. The aluminum funnel is utilized for ease in inserting

Figure 4. Back view of the DEUS apparatus
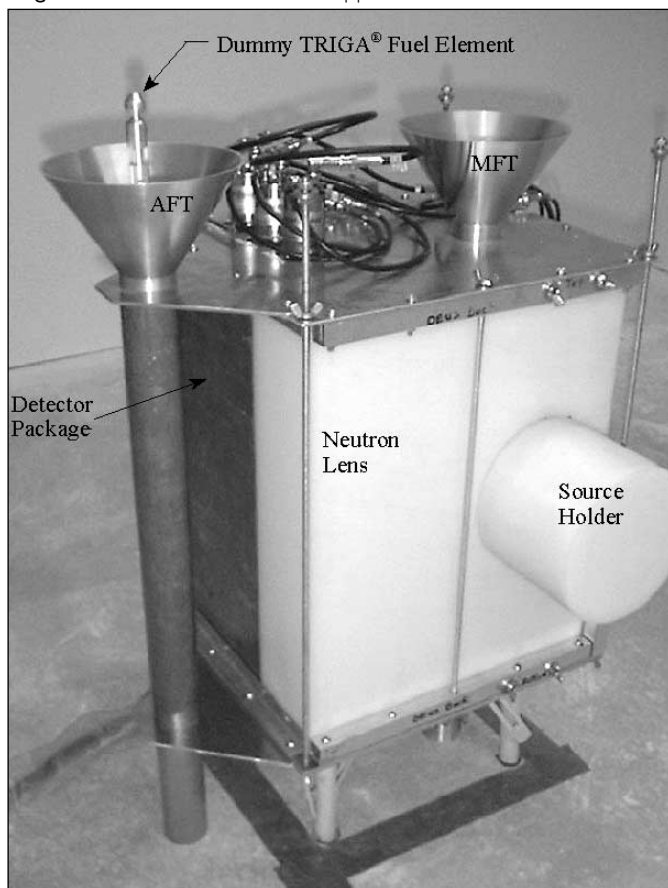
the fuel element into the MFT. The MFT positions the fuel element at a reproducible measurement location and a fuel-position-sensing switch provides the operator with a remote indication that the fuel element is fully inserted. neutrons exiting the neutron lens are incident on the fuel element to induce fission in the U-235 nuclei contained in the fuel. The number of fissions that occur is directly proportional to the mass of U-235 in the fuel element. This fission process produces more neutrons that go on to interact with other components of the apparatus.

Next to the MFT is a reflector plate that enhances the neutron economy of the apparatus by returning neutrons to the fuel element. These returning neutrons induce more fissions in the U-235 nuclei in the fuel element.

On the beam-left side of the MFT resides the detector package that holds three He-3 proportional counters. The detector package is a block of polyethylene that is surrounded by a thin layer of cadmium sheet metal. The design of the detector package optimizes the counting of fast neutrons that are created during the fission of U-235 nuclei within the fuel element meat. The He-3 proportional counters each have a diameter of 2.54 cm, an active length of 30.48 cm, a He-3 fill pressure of 405 kPa, and incorporate a B-10 lining to minimize gamma-ray interactions

(see Reference 6). The signals from the He-3 proportional counters are processed through attached preamplifier/amplifier/discriminator modules that send a logic pulse to a counter/timer unit located in a small NIM bin. The three He-3 proportional counters receive a positive operating voltage that is supplied by a high-voltage power supply, which is also located in the small NIM bin. All of the nuclear counting instrumentation associated with DEUS is commercially available.

On the backside of the detector package resides the AFT, which is used to hold fuel elements while performing background counting. The AFT is similar to the MFT, but it is covered with cadmium and does not have a fuel position-sensing switch installed. The presence of the fuel element in the AFT provides a radiation field during background measurements for the He-3 proportional counters that is equivalent to that produced when the fuel element is in the MFT during neutron interrogation. The equivalent gamma-ray-radiation field must be present during background measurements to ensure the He-3 proportional counters operate at the same efficiency as that during foreground measurements. Empirical data show that the efficiency of the He-3 proportional counters decreases as the gamma radiation field increases for a constant operating voltage (see Figure 7). The AFT is located off of the neutron beam line and is covered with cadmium, which inhibits induced U-235 fissions within the irradiated fuel element during the background measurement.

Referring to Figure 3, the ionization chamber is located on the outside of the reflector plate. It is used to measure the exposure rate (R/hr) that is produced from radioactive nuclei in the fuel element. The radioactive nuclei are direct and indirect products from the fission process. Therefore, the exposure rate from an irradiated fuel element is directly proportional to the U-235 mass that has been depleted for a given decay time. The ionization chamber centerline is 16.47 cm from the MFT centerline. This is the exposure-rate equivalent distance of that between the MFT centerline and the closest He-3 proportional counter centerline for a 662 keV gamma ray (from Ba-137m). Hence, the ionization chamber reading indicates the exposure rate at the He-3 proportional counter in the detector package nearest the MFT where the irradiated fuel element is measured. The ionization chamber is a stand-alone commercially available unit powered by small batteries that provides a direct readout in R/hr. This readout must be corrected for altitude since the ion chamber is unsealed (vented to the atmosphere).

Figure 5 is a photograph of the DEUS apparatus as it was configured for measurements at UT. A polyethylene *tent* covers the DEUS to protect it from dripping water from pool-stored fuel as well as any potential loose contamination. Polyethylene *socks* are also used in the MFT and AFT to isolate loose contamination. Figure 5 displays the openings for the MFT and AFT funnels with the tent in place. The apparatus dimensions with the tent installed are approximately 71 cm tall by 53 cm square. The DEUS currently has a 17-m long cable harness that separates the

Figure 5. DEUS apparatus covered with polyethylene *tent* during TRIGA® fuel transfer at UT
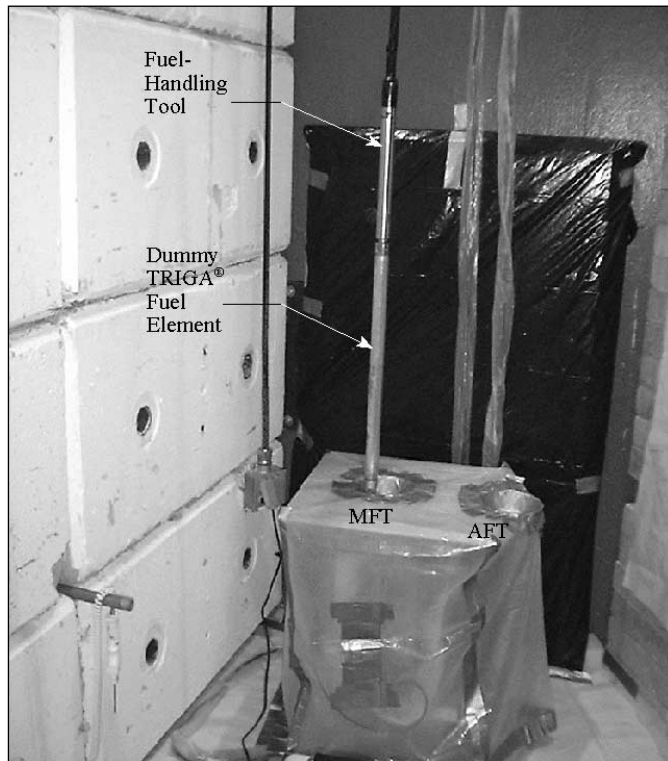
controlling electronics from the apparatus during fuel element measurements. This cable harness is covered with a polyethylene sleeve to prevent its contamination.

The above components are the basic physical building blocks of the DEUS. The exposure rate measurement, in concert with the net (foreground–background) neutron counting rate, provides information that relates to burnup of U-235 in fuel elements. The amount of U-235 remaining in the fuel element is directly measured by the net-neutron-counting rate as determined by neutron interrogation of the fuel element. The amount of U-235 consumed is indirectly determined by measurement with the ionization chamber. The combination of both measurements provides two nuclear attributes that constrain the amount of U-235 that remains in the fuel element. The total weight of the DEUS apparatus is approximately 45 kg. The DEUS packaged in five shipping containers has a gross shipping weight of 137 kg.

The DEUS has four key features that identify uniqueness for assaying TRIGA® SNF. They are that it:
1) Provides for axially uniform neutron detector response to fuel element meat (UZrH or UZrHEr) while interrogating the fuel with external Cf-252 neutrons. This uniform response is generated by means of the neutron lens. This uniform response allows for unbiased assay of fuel elements with variable axial burnup.
2) Uses active total neutron *singles* counting for U-235 assay of

fuel elements. No neutron coincidence counting is required. The net neutron signal for total singles counting is directly related to the quantity of U-235 remaining in each fuel element.
3) Uniquely corrects for radiation-field induced charge-collection deficit in He-3 proportional counters caused by significant gamma radiation fields emanating from fuel elements. This correction compensates for the reduced response of the He-3 proportional counters as the radiation field increases.
4) Incorporates an ionization chamber to measure the gamma radiation field (R/hr), which indirectly determines the amount of U-235 consumed in each fuel element

DEUS Algorithm Description: Assay Results from the University of Texas Nuclear Engineering Teaching Laboratory

The major components of the DEUS algorithm include those of computer modeling, operation, measurements, and analysis. The following sections provide an overview of each of these components.

The reactor at UT is a 1.1 MW (steady-state) Mark II with pulsing capability. This reactor was first taken critical in March 1992. It was preceded by a Mark I reactor (referred to as the Taylor Hall reactor) that operated from January 1963 to December 1988.

DEUS measurements were conducted on UT fuel November 10-14, 2003. The fuel was all low-burnup STD-PLN elements; one of which had the maximum declared burnup of 5.30 g of U-235 (14.0 percent of U-235 consumed). A total of fourteen irradiated STD-PLN elements were assayed, and three of the fourteen were assayed twice for reproducibility testing. Non-irradiated element 10809 was used as the standard of comparison.

The majority of the burnup for the fourteen UT elements occurred at other reactors in the 1960s, and these elements were transferred to UT in 1972. The maximum U-235 consumed at UT for any of the fourteen elements was only 0.2 g in the Taylor Hall reactor.[7] The elements ranged in length from 72.06 cm to 75.39 cm with a nominal outer diameter equal to 3.746 cm.

Modeling

Prior to performing SNF measurements with the DEUS, a series of computer calculations are conducted for measurement planning and data analysis purposes. Ideally, BOL values for the following parameters are needed to prepare the input files for these calculations. In practice, many of these parameters are not known but can be assumed based upon the general features of TRIGA® fuel. The parameters are:
• Element identification number
• Enrichment of the element (i.e., the initial mass of U-235)
• Total weight percent uranium

- Total weight percentage of neutron poison (erbium as applicable)
- H:Zr atom ratio
- Diameter of the inner zirconium rod
- Fuel annulus diameter and the cladding thickness
- Total length of the fuel
- Distance from the bottom of the fuel meat to the bottom of the lower end fitting

With this information, the mass and mass fractions for the constituents in the fuel meat are generated. This mass information, along with fuel dimensions, is input into the ORIGEN[8], MCNP (see Reference 5), and ISO-PC[9] codes.

The ORIGEN code uses single-group neutron cross-sections to simulate burnup of the fuel elements of concern based upon:
- Date of initial irradiation in a reactor
- Dates for significant core configuration changes
- Date of the final removal from the reactor
- Declared U-235 mass at final removal (or the specific element burnup in megawatt days)
- Similar information concerning prior irradiation at a different reactor

ORIGEN accommodates four modified PWR cross-section libraries for thirty-seven actinides: three libraries were specifically developed for STD-PLN (8.5 percent U weight), LEU (20 percent U weight), and Al Clad (8.0 percent U); and additional libraries were specifically developed for FLIP (8.5 percent U weight) fuel. The libraries contain BOL cross sections, which are appropriate for low-to-medium burnup of TRIGA® elements. They were developed using MCNP modeling of a Mark I TRIGA® reactor core.[10] Preliminary ORIGEN calculations with these libraries were benchmarked against ORIGEN calculations performed by Sterbentz.[11]

Initial ORIGEN calculations are conducted to irradiate the fuel element for the purpose of creating radioactive fission products and activation products. The output from these calculations is activities (Ci) of radionuclides that are used to generate a subset list of gamma-emitters for inclusion in ISO-PC. Fifteen isotopes bound the gamma-ray-emitting radionuclides that adequately represent the radiation field emitted from irradiated fuel that has been out of a reactor for at least nine months. ISO-PC is then used to model a uniform mixture of the selected radionuclides in the fuel meat in order to calculate a predicted exposure rate in units of R/hr. These calculations show that for a constant decay time, the exposure rate varies linearly with the mass of depleted U-235.

The estimated relative error in the UT predicted exposure rates is ±8 percent based upon all known power history information. The accuracy of these predictions depends mostly on the accuracy of the documentation for power history and the initial U-235 mass for each individual element. These errors are evaluated on a case-by-case basis.

A separate ORIGEN input file is also created that is used

specifically for providing masses of nuclides for MCNP produced by the fission and activation processes in the fuel meat and the cladding. This second ORIGEN calculation provides irradiation-altered constituents that are present in the irradiated fuel meat as an input to an MCNP file. The fuel-meat constituents are represented by eighty-five cross-section libraries for improved MCNP-memory management, which were developed from analyzing all constituents with masses exceeding 1E-7 g (or about 48 parts per trillion) for the FLIP element with the highest burnup found to date. The eighty-five cross-section libraries were reduced from a starting list of 213 nuclides, based upon the process of combining isotopes into a single element cross-section (when natural abundance was not altered), and the use of conservative surrogates for neutron cross-sections that are not yet represented in MCNP databases.

MCNP is used to calculate a DEUS gross and background response in units of neutrons detected per source neutron from neutron interrogation of fuel with the Cf-252 source. The MCNP models include the fuel elements of concern (with ORIGEN-calculated constituents) inserted in the DEUS apparatus and the geometry of the room in which the apparatus resides at the facility. The difference between the gross and background responses is the MCNP net responses shown in Figure 6.

Figure 6. MCNP net responses in units of neutrons detected per source neutron (n/n_s) vs. U-235 mass in units of grams for UT STD-PLN TRIGA®. A linear regression is calculated in Microcal™ ORIGIN® 6.0 using the MCNP net response errors as weight. The linear regression represents the MCNP net response function with associated fit parameters (A and B) and errors. R is the linear correlation coefficient that quantifies the goodness of fit where R = 1 for a perfect linear correlation.
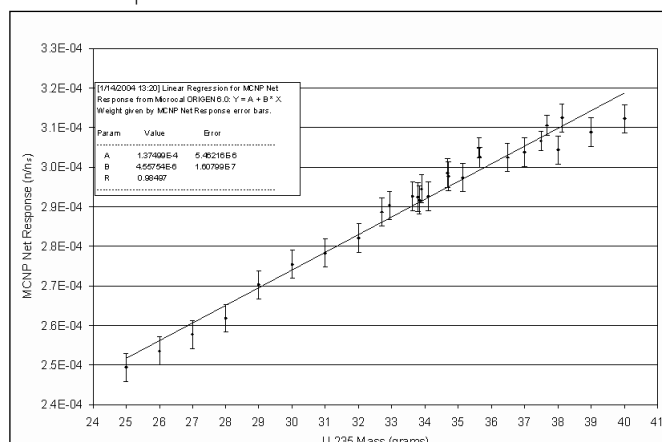
The MCNP net responses of the DEUS to the UT STD-PLN elements as a function of U-235 mass (grams) is shown in Figure 6. A linear regression is calculated using Microcal™ ORIGEN® 6.0[12] from these MCNP net responses weighted by the MCNP net response errors (< ±1.5 percent relative). The linear regression represents the MCNP net response function that is

normalized and then used to calculate the U-235 mass solution for an element using the measured net counting rate of that element. This solution is referred to as the neutron U-235 solution.

Operation

The use of He-3 proportional counters for neutron counting is normally performed in environments with minimal gamma-ray radiation fields. neutron counting is usually performed on the *plateau* of a counting curve, which can be developed by examining the counting-rate performance of a He-3 proportional counter at different operating voltages.

Figure 7. Relative neutron singles counting efficiency vs. operating voltage for the DEUS detector package
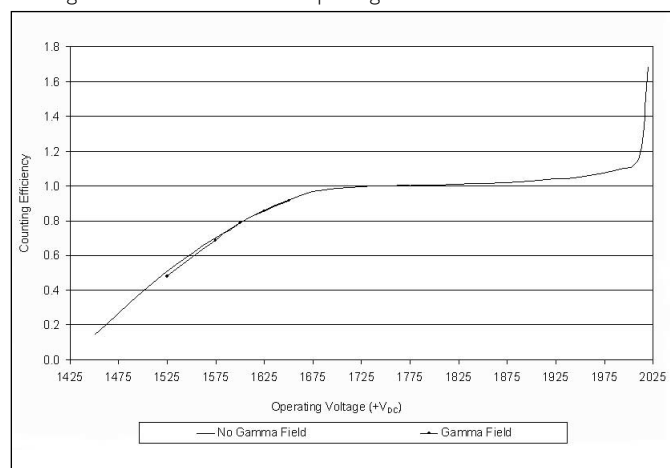

Figure 7 is a plot of the neutron singles counting efficiency for the detector package. Referring to the "No Gamma Field" series, the neutron counting efficiency is normalized (defined to equal 1.0) at +1750 V_{DC}, which is at the left end of the counting plateau. As the voltage is decreased below +1750 V_{DC}, the counting efficiency decreases as one proceeds down the *knee* of the curve. Concurrently, as the voltage reduction decreases the efficiency for counting neutrons from the (n,p) reaction in He-3, it also significantly decreases that for gamma rays. Hence, by operating the detector package at voltages below +1,750 V_{DC}, it is possible to eliminate pulse detection from gamma-ray interactions in the detector walls and He gas, but with the penalty that the neutron counting efficiency also decreases.

The neutron singles efficiency curve presented in Figure 7 was generated with a Cf-252 source present in the source holder and no irradiated fuel present. The gamma rays emitted from the Cf-252 source will not measurably impact the neutron efficiency curve, except at high operating voltages. The sharp increase in efficiency on the right side of the curve (>+2,000 V_{DC}) represents a point where the Cf-252 gamma rays and the detector electronic noise are amplified to the point of forming countable pulses.

Figure 8 is a plot of allowable radiation fields (gamma-free

neutron counting) as a function of operating voltage for the detector package. The phrase "allowable radiation field" is defined as that radiation field of which gamma rays emitted from irradiated fuel elements only generate several counts per second at a given operating voltage.

Figure 8. Measured exposure rate vs. *gamma-free* operating voltage for the DEUS detector package
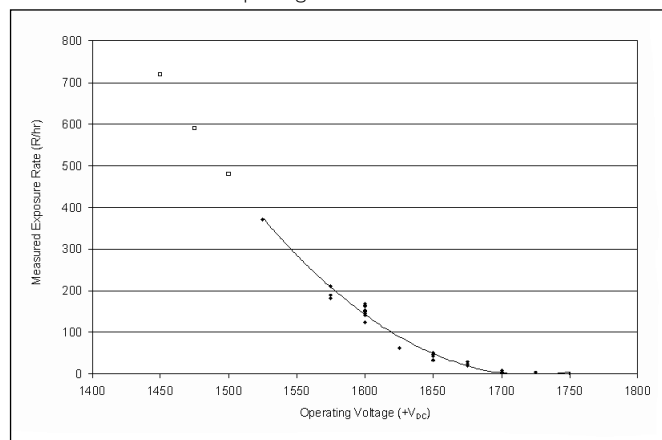
The Figure 8 plot data were acquired with irradiated fuel elements in the MFT and no Cf-252 source installed in the source holder. The operating voltage was reduced until the detector package counted only a few counts per second. The measured exposure rate was then recorded at that voltage. The same measured exposure rate values were then reproduced during fuel assay with the Cf-252 source present. Recall that the ionization chamber reading indicates the exposure rate at the He-3 proportional counter in the detector package nearest the MFT where the irradiated fuel element is measured.

As indicated in Figure 8, the largest measured exposure rate to date is 370 R/hr. The counting effects of this gamma-ray radiation field were removed by operating the detector package at +1525 V_{DC}. As shown in Figure 7, the neutron counting efficiency at +1525 V_{DC} ("No Gamma Field" series) is only about 50 percent as compared to that at +1,750 V_{DC}. However, a very subtle effect occurs concerning the counting of neutrons in a gamma radiation field. As the radiation field strength increases, the collection of charge associated with the (n,p) reaction in the He-3 gas suffers a charge-collection deficit that is proportional to the strength of the radiation field. This subtle effect is demonstrated in Figure 7 by the "Gamma Field" series, which is slightly offset below the "No Gamma Field" series.

The greatest charge-collection deficit, documented for the previously mentioned situation at +1525 V_{DC}, occurred for a 280 R/hr exposure rate for element 7526T at TAMU. The effect of this exposure rate was to reduce the apparent neutron counting efficiency 5.08 percent. When this difference is propagated, the measured net counting rate is reduced 36.1 percent. The charge

Measurements

The DEUS has not been calibrated with an appropriate set of *certified* standards. Therefore, measured net counting rates from a standard of comparison are used to normalize the MCNP net response function. The standard of comparison is a non-irradiated element for which the U-235 mass is assumed to be a known quantity within ± 0.85 percent relative error. This estimated error was established by independent agreement between General Atomics material flow data errors[13] and the statistical spread in U-235 content for fifty ININ FLIP elements.[14] Individual fuel records reviewed during this project have not noted uncertainties in fuel meat constituents.

Because no absolute measurement calibrations have been performed, the incremental deviation method (IDM) was developed to provide a technique for determining the remaining enrichment (U-235 mass) in a fuel element. *Incremental* refers to the selection of discrete fuel elements that have burnups that monotonically increase from very little burnup to the element that has the maximum burnup (all are elements that have been removed from the core for at least six months). By selecting a set of elements that span the range of fuel burnup found for a given core, one can acquire a general perspective of a degree of bias that may occur as to how the reactor staff estimated their fuel burnup (assuming all DEUS biases are properly corrected). The *deviation* portion of the IDM refers to the difference between the declaration of U-235 by the specific reactor staff and the DEUS U-235 solution. The IDM relies on the neutron U-235 solution and gamma U-235 solution to constrain the actual burnup of an irradiated fuel element. Currently, the data analysis that was conducted while performing measurements at a facility is limited to the IDM.

A DEUS neutron-interrogation measurement consists of three background and three gross counting rate measurements. Recall that the background measurements on irradiated fuel elements are conducted with said elements inserted in the AFT. The three measurements are used to calculate the means and standard deviations for the background and gross counting rates. The three measurements are taken as a minimum such that the standard deviation can be calculated to monitor for acceptable statistical behavior. Counting times for these are selected based upon the predicted net counting rate in an attempt to achieve a random statistical uncertainty in measured net counting rate of ±0.25 percent at 68.3 percent confidence (1σ). The measured net counting rate, which is the difference between mean gross and mean background counting rates, directly relates to the amount of U-235 in the fuel element. These measured net counting rates in units of counts per second (cps) require data reduction, effi-

ciency corrections and Cf-252 source decay corrections.

At UT, a 12.4 mg Cf-252 source (2.87E+7 n/s) was used in the DEUS resulting in background counting rates of 41,200 cps at +1,750 V_{DC} with 300-second counting times. The standard of comparison, element 10809, produced counting rates of 48,100 cps at +1,750 V_{DC}. The counting times for the irradiated elements increased proportionally to the relative counting efficiencies for their respective *gamma-free* operating voltages shown in figures 7 and 8, respectively.

The measured exposure rates are recorded with each neutron interrogation measurement and require data reduction, altitude corrections, and calibration corrections. The UT measured exposure rates ranged from 4.5 R/hr (element 2945) to 31.8 R/hr (element 5246). The relative errors for the measured exposure rates are based upon uncertainties from calibration, drift, and variability in radial burnup of the fuel element. This error is evaluated on a case-by-case basis. The relative errors for the UT measured exposure rates are ±3 percent. A U-235 mass solution is calculated from the measured exposure rate by linear extrapolation from the predicted exposure rate for a particular fuel element. This solution is referred to as the gamma U-235 solution in the following discussion.
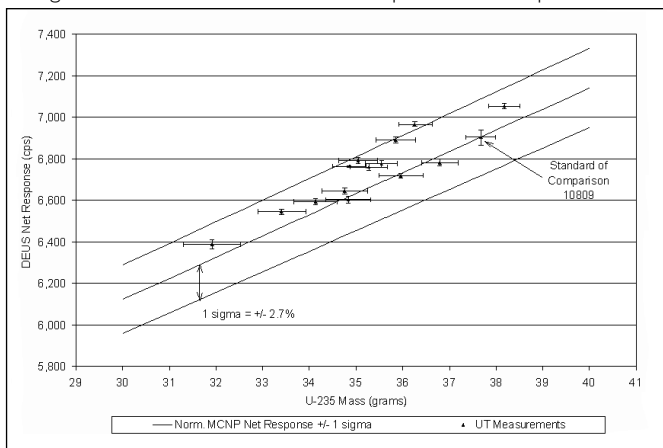
Analysis

Referring to Figure 9, the MCNP net response function is normalized to the measured net counting rate of the standard of comparison, element 10809. The assumed 0.85 percent relative error in U-235 mass and errors in measured net counting rate for the standard of comparison and the MCNP net response function fit parameters are propagated through the normalization calculation to produce the error bands for the normalized MCNP net response function in Figure 9.

Measured net counting rates (*UT Measurements* series) of the UT STD-PLN fuel elements measured November 10-14, 2003, are plotted in Figure 9. Errors in measured net counting rates are shown with y-error bars and are all < ±0.6 percent. These data are plotted at the gamma U-235 solution for each element assayed. The gamma U-235 solution is used instead of the facility declared U-235 mass because it is believed to be a more accurate value (see following paragraph for an explanation). All gamma U-235 solutions but one (element 6592) are within ±2.7 percent of the declared U-235 mass values. The outlier, element 6592, has a gamma U-235 solution that is 4.4 percent above the declared U-235 mass.

Errors in this gamma U-235 solution are shown in Figure 9 with x-error bars and are all < ±2 percent. Note that all measured results fall within the 1-sigma error bands of the normalized MCNP net response function. Hence, there is an excellent correlation between the gamma U-235 solution and the neutron U-235 solution. Historically, the gamma U-235 solution has supported the independently measured neutron U-235 solution

Figure 9. DEUS net response vs. U-235 mass for UT STD-PLN TRIGA® elements assayed November 10-14, 2003. The lines denote the normalized MCNP net response function (Norm. MCNP net response) with error bands at ±1 sigma. The MCNP net response is normalized to the decay- and efficiency-corrected measured net counting rate (UT Measurements) for the standard of comparison, element 10809. The UT Measurements series has errors in measured net counting rate (y error bars) and U-235 mass (x error bars). UT Measurements are plotted at the gamma U-235 solutions that are all within ±4.5 percent of the declared values. U-235 mass relative errors for gamma U-235 solutions are all < ±2 percent on this plot.

Figure 10. Column-type chart showing declared U-235 mass with ±0.85 percent relative errors and neutron, gamma, and weighted mean U-235 mass solutions in grams with associated errors for each UT STD-PLN TRIGA® element (element ID# on the x-axis). This chart shows the agreement between the neutron and gamma solutions even in cases where they differ significantly from the declared values such is the case for elements 3170 and 6592.
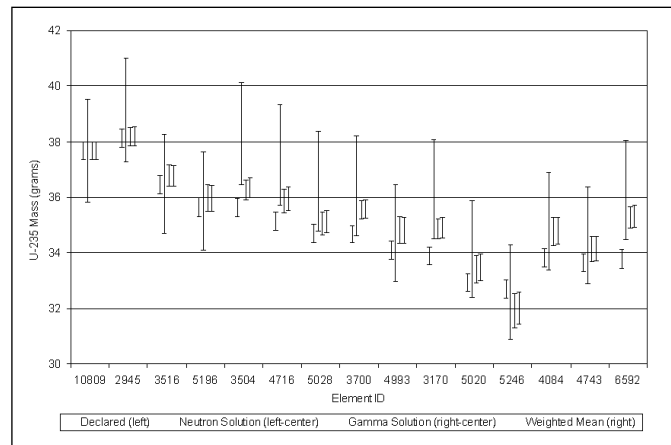

with regard to their trends relative to the declared U-235 mass value. An example of this supporting trend can be seen in Figure 10. Note that for elements 3170 and 6592 the gamma and neutron U-235 solution are both larger (> 1 sigma separation) than the declared U-235 mass. Data from past experiments (e.g., ININ) have shown a correlation between individual element burnup and core position, which typically is not taken into account in the facility's calculation of declared U-235 mass. The facility's declared U-235 mass is usually based upon an average core power history.

Table 1 lists the U-235 mass solutions for the UT STD-PLN. neutron, gamma, and weighted mean U-235 solutions are shown. The Weighted Mean U-235 solution is an error-weighted mean of the neutron and gamma U-235 solutions. In addition, the propagated errors in units of grams and percent relative error for each of these solutions are shown. The percent difference relative to the declared U-235 mass values is shown to compare the DEUS solutions to the facility declared values.

Referring to Table 1, note that the neutron and gamma U-235 solutions have a slight positive bias relative to the declared U-235 masses. The neutron U-235 solutions are approximately equal to the declared initial U-235 masses for elements 2945 and 3504. A portion of the neutron U-235 solution bias is most likely due to uncertainties in the declared U-235 mass for the standard of comparison, element 10809. These solutions are strongly dependent on the declared U-235 mass of element 10809 because the MCNP net response function used to calculate the solutions is normalized to the standard of comparison's measured net

counting rate at this declared U-235 mass value. Thus, small changes in the declared U-235 mass for the standard of comparison can bias the results. However, the gamma U-235 solutions from the independent gamma-ray measurements are also positively biased suggesting that the UT elements probably do have more U-235 remaining than was declared.

Figure 11 is a close-up of Figure 9 showing the measured net counting rates for elements 3504, 2945, and 5196. These elements were measured twice to test the precision of the DEUS at UT. The second measurements were conducted on different days than the first measurement such that the fuel was moved from storage and placed in the DEUS for each measurement. All three measured net counting rates reproduced within < ±0.5 percent and demonstrated the excellent precision capabilities (reproducibility) of the DEUS.

Assay Results from the Texas A&M University Nuclear Science Center

DEUS measurements were conducted on TAMU fuel February 24-28, 2003. The assays were performed on three medium-burnup STD-PLN elements; one with the maximum declared burnup of 9.88 g of U-235 (28.2 percent of U-235 consumed). The STD-PLN elements all had an original nominal loading of 35 g of U-235. DEUS measurements were also performed on five FLIP elements one with the maximum declared burnup of 27.04 g of U-235 (22.3 percent of U-235 consumed). The FLIP elements possessed an original nominal loading of 122 g of U-235 and were thought to have an Er content of 1.5 percent by weight. The only non-irradiated element available, a FFCR element 7512F, was used as the standard of comparison.

Figure 11. DEUS net response vs. U-235 mass for UT STD-PLN TRIGA® elements measured twice. Elements 3504, 2945, and 5196 were independently measured for a second time on a different day to quantify the precision of the DEUS. Each measured net counting rate reproduced within < ±0.5 percent relative to the first measurement.
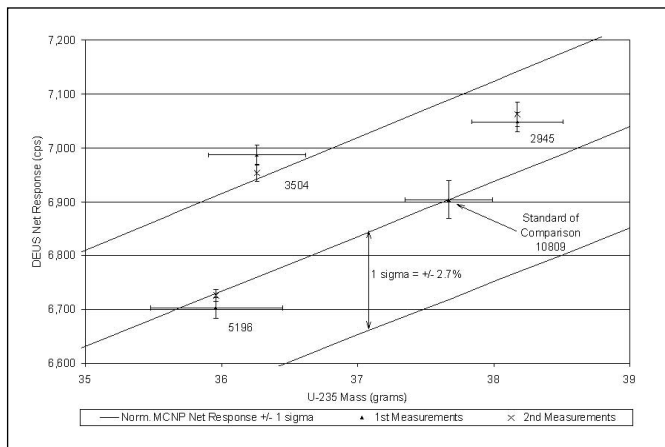
The reactor at TAMU was originally a MTR swimming-pool-type reactor that was authorized to operate at 100 kilowatts thermal power. The reactor was first taken critical on December 18, 1961. The reactor was converted from an MTR-type fuel to a TRIGA® reactor with STD-PLN elements and was licensed to be operational on July 31, 1968. The reactor was further modified and licensed by July 1973 to include FLIP elements. At that time, the reactor core contained thirty-five FLIP elements and sixty-three STD-PLN elements. By 1979, the core was again modified to contain only FLIP elements (nominally four FLIP elements per bundle with an equilibrium core size of twenty-four bundles in a quasi-square configuration). Currently, the TAMU reactor operates with ninety FLIP elements. The TAMU elements are stainless-steel-clad with a nominal outer diameter of 3.58 cm and a total length of 76.2 cm. All TAMU fuel elements have a total-uranium loading representing 8.5 percent of the fuel by weight. The TAMU reactor operates at 1 MW (steady state) thermal power and is routinely used in a pulsing mode. The TAMU reactor design is designated a *conversion* TRIGA® reactor. [15]

Table 1. U-235 solutions from DEUS assay of UT STD-PLN TRIGA® fuel elements

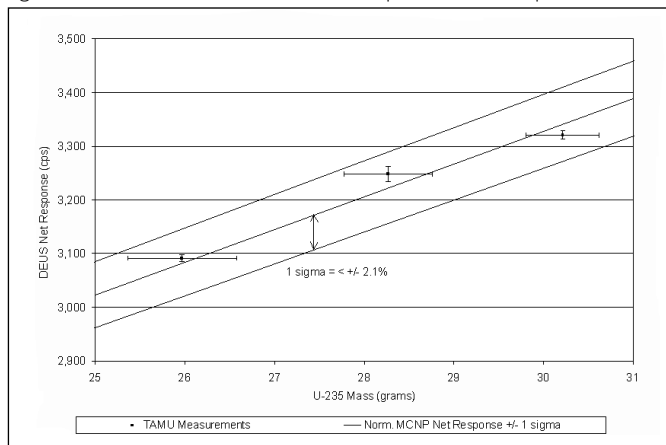| Element ID#	Decl. Initial U-235 (grams)	Decl. Final U-235 (grams)	Neutron U-235 Solution (grams)	Neutron U-235 Solution Error (grams)	% Rel. Error (%)	% Diff. Rel. to Decl. (%)	Gamma U-235 Solution (grams)	Gamma U-235 Solution Error (grams)	% Rel. Error (%)	% Diff. Rel. to Decl. (%)	Wtd. Mean U-235 (grams)	Wtd. Mean U-235 Error (grams)	% Rel. Error %	% Diff. Rel. to Decl. (%)
10809	37.67	37.67	37.1	±1.9	±4.9	0.0	37.7	±0.3	±0.9	0.0	37.7	±0.3	±0.8	0.0
2945	38.84	38.13	39.1	±1.9	±4.8	2.7	38.2	±0.3	±0.9	0.1	38.2	±0.3	±0.9	0.2
3516	39.00	36.47	36.5	±1.8	±4.9	0.0	36.8	±0.4	±1.0	0.9	36.8	±0.4	±1.0	0.9
5196	40.00	35.64	35.9	±1.8	±5.0	0.6	36.0	±0.5	±1.3	0.9	36.0	±0.5	±1.3	0.9
3504	38.00	35.63	38.3	±1.8	±4.8	7.5	36.3	±0.4	±1.0	1.8	36.3	±0.3	±1.0	2.0
4716	39.00	35.12	37.5	±1.8	±4.9	6.9	35.9	±0.4	±1.2	2.1	35.9	±0.4	±1.2	2.3
5028	38.00	34.70	36.6	±1.8	±4.9	5.4	35.1	±0.4	±1.2	1.0	35.1	±0.4	±1.1	1.2
3700	37.00	34.67	36.4	±1.8	±4.9	5.0	35.5	±0.3	±1.0	2.5	35.6	±0.3	±0.9	2.6
4993	39.00	34.09	34.7	±1.8	±5.0	1.8	34.8	±0.5	±1.4	2.2	34.8	±0.5	±1.3	2.2
3170	37.00	33.90	36.3	±1.8	±4.9	7.0	34.9	±0.4	±1.0	2.8	34.9	±0.4	±1.0	3.0
5020	38.00	32.93	34.1	±1.7	±5.1	3.7	33.4	±0.5	±1.5	1.4	33.5	±0.5	±1.5	1.6
5246	38.00	32.70	32.6	±1.7	±5.2	-0.3	31.9	±0.6	±1.9	-2.4	32.0	±0.6	±1.8	-2.2
4084	39.00	33.83	35.1	±1.8	±5.0	3.9	34.8	±0.5	±1.4	2.7	34.8	±0.5	±1.4	2.8
4743	38.00	33.63	34.6	±1.7	±5.0	3.0	34.1	±0.5	±1.4	1.4	34.1	±0.4	±1.3	1.5
6592	38.00	33.78	36.3	±1.8	±4.9	7.3	35.3	±0.4	±1.1	4.4	35.3	±0.4	±1.1	4.5

The majority of the burnup for the TAMU elements occurred in the TAMU reactor. The STD-PLN elements were burned up in the TAMU core from 1968-1973. The FLIP elements that were measured by the DEUS resided in the core from as early as 1973 to as late as 1998.[16] Several FLIP elements, measured by the DEUS, were previously irradiation at the Puerto Rico Nuclear Center and were transferred to TAMU after 1976. Elements 7523T and 7526T, which were also measured by the DEUS, were instrumented elements that resided in the TAMU core 16.38 and 24.51 years, respectively. The discussions that follow will highlight the anomalous results recorded by the DEUS for these elements.

At TAMU, a 6.66 μg Cf-252 source (1.54E+7 n/s) was used in the DEUS resulting in background counting rates of 21,000 cps at +1,750 V_{DC} with 290-second counting times. The standard of comparison, element 7512F, produced counting rates of 26,300 cps at +1,750 V_{DC}.

The estimated relative error in predicted exposure rates was ±6 percent for FLIP and ±5 percent for STD-PLN using a reasonably complete power history. The relative errors for the TAMU measured exposure rates are ±6 percent for FLIP and ±3 percent for STD-PLN. The measured exposure rates ranged from 29.6 R/hr (element 5381) to 280 R/hr (element 7526T).

Referring to figures 12 and 13, the MCNP net response function is normalized by the ratio of the measured net counting rate and the MCNP net response of the standard of comparison, element 7512F measured net counting rates ("TAMU Measurements" series) of the TAMU STD-PLN and FLIP elements are plotted in figures 12 and 13 respectively. Errors in measured net counting rates are shown with y-error bars and are

all < ±0.8 percent. All gamma U-235 solutions are within ±4.1 percent of the declared U-235 mass values. Errors in this gamma U-235 solution are shown with x-error bars and are all < ±2.5 percent relative.

Figure 12 shows that the measured net counting rates of the TAMU STD-PLN elements fall within the normalized MCNP net response error bands, similar to the UT STD-PLN measurements. In contrast, Figure 13 shows three elements other than element 7512F that are outside of the error bands. Element 7512F is off the normalized MCNP net response curve because it has a narrow outer diameter 3.45 cm and is of different construction than the other FLIP elements. Since it was the only non-irradiated element at TAMU, it defaulted to being the standard of comparison.

Figure 13. DEUS net response vs. U-235 Mass for TAMU FLIP TRIGA® elements assayed Feb. 24-28, 2003. The MCNP net response is normalized by the ratio of the measured net counting rate and the MCNP net response for the standard of comparison, element 7512F. "TAMU Measurements" are plotted at the gamma U-235 solutions that are all within ±4.1 percent of the declared values. U-235 mass relative errors for the gamma U-235 solutions are all < ±2.5 percent on this plot.
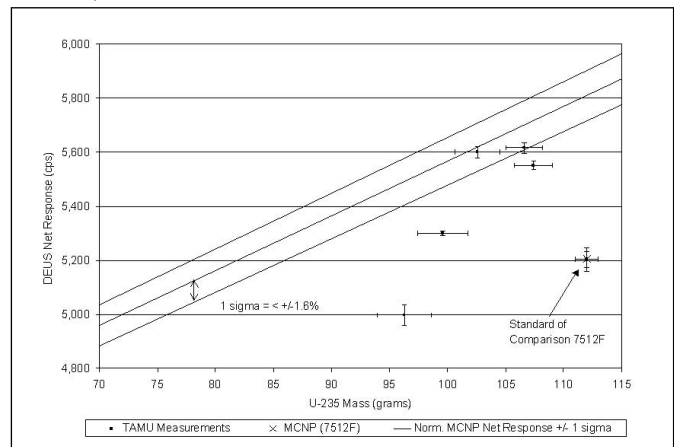

Figure 14. Column-type chart for the TAMU fuel elements similar to Figure 10

Figure 12. DEUS net response vs. U-235 Mass for TAMU STD-PLN TRIGA® elements assayed February 24-28, 2003. The MCNP net response is normalized by the ratio of the measured net counting rate and the MCNP net response for the standard of comparison, element 7512F, shown in Figure 13. "TAMU Measurements" are plotted at the gamma U-235 solutions that are all within ±3.5 percent of the declared values. U-235 mass relative errors for the gamma U-235 solutions are all < ±2.4 percent on this plot.
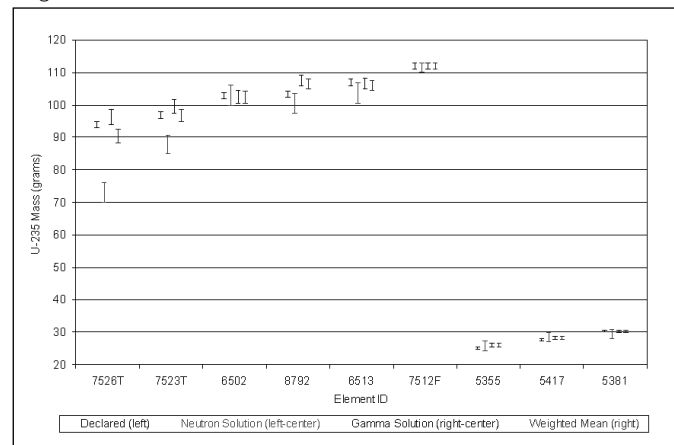
Figure 14 is a column-type chart showing declared U-235 mass with ±0.85 percent relative errors and neutron, gamma, and weighted mean U-235 solutions in grams with associated errors for each TAMU fuel element. The neutron U-235 solution and the gamma U-235 solution overlap at 1 standard deviation for all elements except 8792, 7523T, and 7526T. Elements 7523T and 7526T do not show overlap at even 2 sigma (see specific errors listed in Table 2), and it is quite apparent that the neutron U-235 solutions are significantly low. This effect has been reproduced at TAMU for all DEUS measurements performed on elements 7523T and 7526T.

Table 2 lists the U-235 mass solutions for the TAMU elements assayed. The weighted mean U-235 solution given in Table 2 most closely agrees with the declared U-235 mass values from TAMU. Note that all weighted mean U-235 solutions are within < ±3.9 percent of the TAMU declared values. Even for elements 7523T and 7526T where the neutron U-235 solutions are much lower than the declared values, the weighted mean U-235 solution supports the declared values. In these cases, where an element has undergone excessive burnup (e. g., elements 7523T and 7526T), there is an anomaly in the neutron U-235 solution.

After much effort to reconcile the reduced neutron U-235 solutions for element 7523T and particularly, element 7526T, it became apparent that no systematic errors could be identified in DEUS measurement protocols and analytical methods. The hypothesis emerged that what the interrogating neutrons were revealing was real, and that this may be related to physical changes in the fuel matrix (i.e., fuel damage—especially from reactor pulsing). This viewpoint was supported by the fact that the gamma U-235 solutions in Table 2 show strong agreement (within 2.8 percent) with the declared TAMU U-235 values for elements 7523T and 7526T.

Considering all the distress factors involved in the irradiation process (including reactor pulsing), especially over the 24.5–year lifetime for element 7526T in the TAMU core, it may be difficult to model the irradiated fuel accurately within MCNP. The primary reason is that MCNP fuel models presume a homogenous-mixed solid while highly distressed fuels are actually a multitude of heterogeneous material domains. Quantification of these effects on the DEUS response has been attempted by modeling some of these factors. However, there appears to be no single irradiation distress factor that can describe the discrepancies between the MCNP calculations and measurement results for element 7526T. These discrepancies must be due to a combination of distress factors that are difficult to predict and model.

In order to help resolve the reduced-neutron-response for element 7526T, a destructive assay of FLIP elements 7526T and 6513 (including neutron radiography) has been proposed. As can be seen in Figure 14 and Table 2, element 6513 shows reasonable agreement between the declared U-235 and the measured neutron and gamma U-235 solutions. Hence, destructive assay of both elements provides situations were measurement agreement and disagreement can be compared.

The destructive analysis should provide insight into the neutron response anomaly for element 7526T. An empirical correction to the MCNP net response function may be necessary in situations where FLIP fuel elements exceed a burnup threshold.

Table 2. U-235 solutions from DEUS Assay of TAMU FLIP and STD-PLN TRIGA® Fuel Elements

Element ID#	Decl. Initial U-235 (grams)	Decl. Final U-235 (grams)	Neutron U-235 Solution Error (grams)	Neutron U-235 Solution (grams)	% Rel. Error (%)	% Diff. Rel. to Decl. (%)	Gamma U-235 Solution (grams)	Gamma U-235 Solution Error (grams)	% Rel. Error (%)	% Diff. Rel. to Decl. (%)	Wtd. Mean U-235 (grams)	Wtd. Mean U-235 Error (grams)	% Rel. Error %	% Diff. Rel. to Decl. (%)
FLIP														
7512F	112.00	112.00	112.0	±1.0	±0.9	0.0	112.0	±1.0	±0.9	0.0	112.0	±1.0	±0.9	0.0
6513	121.28	106.90	102.4	±4.4	±4.3	-4.2	106.6	±1.6	±1.5	-0.3	106.1	±1.5	±1.4	-0.7
8792	122.40	103.27	99.2	±4.3	±4.3	-3.9	107.4	±1.6	±1.5	4.0	106.4	±1.5	±1.4	3.0
6502	122.28	102.90	101.6	±4.4	±4.4	-1.2	102.6	±2.0	±1.9	-0.3	102.4	±1.8	±1.8	-0.5
7523T	122.00	96.82	86.8	±4.0	±4.6	-10.3	99.6	±2.2	±2.2	2.8	96.7	±1.9	±2.0	-0.1
7526T	121.00	93.96	71.9	±4.1	±5.8	-23.5	96.3	±2.3	±2.4	2.5	90.4	±2.0	±2.3	-3.8
STD-PLN														
5381	35.00	30.44	29.9	±1.1	±3.8	-1.8	30.2	±0.4	±1.4	-0.7	30.2	±0.4	±1.3	-0.9
5417	35.00	27.74	28.7	±1.1	±3.9	3.4	28.3	±0.5	±1.7	1.9	28.3	±0.5	±1.6	2.1
5355	35.00	25.12	26.1	±1.1	±4.0	3.9	26.0	±0.6	±2.3	3.4	26.0	±0.5	±2.0	3.5

DEUS Response to Various Non-Fissile Materials Substituted for the Fuel Meat within a STD-PLN TRIGA® Fuel Element

In addition to the UT analysis, MCNP calculations were conducted using the UT model to determine the DEUS response to STD-PLN elements that have undergone a clandestine diversion of fuel material. The base case for this situation was UT element 4716, which has a BOL mass of 39 grams of U-235 and 160 grams of U-238 (19.6 percent-enriched). This element also possesses 8.5 percent by weight uranium. In order to simulate diversion of the U-235-bearing fuel material, it was assumed that the element was breached; the fuel material (fuel meat) pieces were removed and replaced with an equivalent size of non-fissile material inside the 0.0508-cm thick cladding, and then resealed. In these calculations, the fuel material was replaced with U-238 metal, beryllium metal, zirconium metal, aluminum 6061, lead, graphite, stainless steel 304, and UZrH with 100 percent U-238. The same algorithm applied to calculate the UT results was applied to these MCNP calculations to determine the neutron U-235 solution for these elements. The results are presented below in Table 3.

Referring to Table 3, note that all neutron U-235 solutions for the fuel elements containing non-fissile materials are negative. This is very significant because it implies that the DEUS can discriminate against non-fissile materials that may be substituted for fuel materials during diversion of special nuclear material. Of equal importance is the fact that the uncertainty is small enough that there is no doubt about the absence of fissile material.

The analysis from the above cases has revealed the following. First, the neutrons from induced U-235 fission in the STD-PLN fuel meat (base case) contribute 87.3 ± 1.1 percent of the DEUS measured net counting rate. Of these fissions, 573 ± 2 occur for a U-235 nucleus for every fission in a U-238 nucleus. The uncertainties noted in the previous two sentences are based on propagated errors from statistical uncertainties associated with relative errors derived by MCNP for the histories of 200 million-600 million source neutrons leaving the Cf-252 neutron source. Given the fact that the induced fission neutrons produce about 87 percent of the measured net counting rate for the base case, and the fact that 99.8 percent of these fissions are due to the fission of U-235 nuclei, the substitution of non-fissile material in the fuel meat produces a pronounced drop in the MCNP net response as demonstrated in Table 3. This pronounced drop, which reduces the MCNP net response below a signal having zero grams of U-235, results in neutron U-235 solutions that are negative. The ability of the DEUS to detect diverted fuel meat is an important feature. This discrimination can be reproduced even if the cladding of the diverted fuel has been irradiated, since the neutron interrogation of the fuel meat independently assays the U-235 that remains. In addition, the independent measured exposure rate can also indicate an anomaly if diversion of the fuel meat has occurred.

Conclusions

The DEUS is a portable nondestructive assay system capable of measuring the U-235 mass remaining in TRIGA® SNF. The DEUS was described and results from DEUS assay of irradiated TRIGA® fuel elements performed at UT and TAMU were presented. These measurements were performed February 24-28, 2003, at TAMU and November 10-14, 2003, at UT. Irradiated fuel elements assayed at TAMU consisted of three 20 percent-

Table 3. Neutron U-235 solution for TRIGA® elements filled with non-fissile materials

Fuel Meat Material	Fuel Meat Density (g/cm³)	MCNP Net Response (n/n₅)	MCNP NET Response Error (%)	Neutron U-235 Solution (g)	Neutron U-235 Solution Error (g)	MCNP Calculated Signal-to-Backround Ratio
39-g U-235	6.08	3.0880E-4	1.16	37.6	±2.0	1.1696
U-238 Metal	18.95	1.1350E-4	3.09	-5.3	±1.4	1.0623
Be Metal	1.85	1.0750E-4	3.25	-6.6	±1.4	1.0590
Zr Metal	6.44	9.8800E-5	3.52	-8.5	±1.5	1.0543
Al 6061	2.70	9.6400E-5	3.61	-9.0	±1.5	1.0529
Natural Pb	11.35	9.1600E-5	3.79	-10.1	±1.5	1.0503
Graphite	1.60	9.0100E-5	3.85	-10.4	±1.5	1.0495
SS-304	7.92	8.1100E-5	4.26	-12.4	±1.5	1.0445
U-238ZrH	6.08	4.3500E-5	7.82	-20.6	±1.6	1.0239

enriched-U-235-by-weight uranium in an UZrH matrix, which are commonly called STD-PLN, and five 70-percent-enriched-U-235-by-weight uranium in an UZrHEr matrix, which are commonly called FLIP. The fourteen irradiated fuel elements assayed at UT were all STD-PLN.

The DEUS performs measurements on fuel elements by means of active neutron interrogation using a Cf-252 source and passive gamma-ray detection using an ionization chamber. The active neutron interrogation measures induced U-235 fission neutrons leaving the TRIGA® SNF, which are stimulated by neutrons exiting the Cf-252 source. The passive gamma-ray measurement is performed by the ionization chamber for gamma rays originating from fission products and activation products residing in the TRIGA® SNF.

The DEUS algorithm consists of computing a simulated burnup (based upon facility declarations of remaining U-235 in the fuel) of each measured element in order to predict the measured net counting rate as well as the measured exposure rate. The measured net counting rate of a non-irradiated Standard-of-Comparison element is used to normalize the MCNP net response function.

The neutron U-235 solutions for the UT STD-PLN fuel have percent relative errors of approximately ±5 percent and showed a disagreement with the declared U-235 mass of –0.3 percent to +7.5 percent. The gamma U-235 solutions had percent relative errors of <±2 percent and showed a disagreement with the declared U-235 mass of –2.4 percent to +4.4 percent. Only one element showed neutron and gamma U-235 solutions that were below the declared U-235 mass. The weighted mean U-235 solutions were essentially the same as the gamma U-235 solutions due to their smaller relative errors. The neutron and gamma U-235 solutions both displayed a positive bias that suggests that the UT elements probably do have more U-235 remaining than was declared. However, the degree of the bias was dependent upon the amount of U-235 that actually exists in the standard of comparison, element 10809, which was used to normalize the MCNP net response function.

The neutron U-235 solutions for the TAMU STD-PLN fuel have percent relative errors of ±4.0 percent and showed a disagreement with the declared U-235 mass of –1.8 percent to +3.9 percent. The gamma U-235 solutions for STD-PLN have percent relative errors of <±2.4 percent and showed a disagreement with the declared U-235 mass of –0.7 percent to +3.4 percent. Only one element showed neutron and gamma U-235 solutions that were below the declared U-235 mass. Weighed mean U-235 solutions were within –0.9 percent to +3.5 percent of the declared U-235 masses. A non-irradiated FLIP FFCR, element 7512F, was used as the standard of comparison at TAMU.

The neutron U-235 solutions for the TAMU FLIP fuel have percent relative errors of <±5.8 percent and showed a disagreement with the declared U-235 masses of -1.2 percent to -23.5 percent (with element 7526T showing the anomalous low value).

The gamma U-235 solutions for FLIP fuel displayed percent relative errors of <±2.5 percent and showed a disagreement with the declared U-235 mass of -0.3 percent to +4.0 percent. The weighted mean U-235 solutions showed a disagreement with the declared U-235 mass of –3.8 percent to +3.0 percent.

The reduced-neutron response for elements 7523T and 7526T (particularly 7526T) is thought to be due to fuel meat irradiation damage such that neutron interaction is effectively suppressed. Destructive analysis should provide additional insight into the cause of the reduced-neutron response.

The absolute errors in DEUS U-235 solutions can be reduced if a certified reference standard can be created with a quantified U-235 uncertainty of less than ±0.85 percent. In spite of this weakness, the DEUS can be used to attain ±5 percent uncertainty (68.3 percent confidence level) in determining the mass of U-235 in spent TRIGA®, fuel. The DEUS is also capable of sensing with definitive statistical significance when fissile material has been diverted and replaced with non-fissile material.

John J. King received his B.S. in physics and mathematics from Manchester College in 1973 and M.S. in physics from Ball State University in 1975, followed by an additional year of graduate physics at the University of Notre Dame. He was employed at the Idaho National Engineering Laboratory from 1977 to 1992, working primarily in applied physics. He has spent the previous twelve years working for four small companies, including Global Technologies Incorporated the last five. His expertise varies from nuclear radiation measurements to radiation transport and nuclear criticality calculations, along with human-health risk assessment and safety analysis. He is a member of the Health Physics Society and the INMM.

Gary N. Hoggard served six years in the U.S. Naval Nuclear Propulsion Program (submarines) prior to completing an internship with the Duke University Radiative Capture Group at Triangle Universities Nuclear Laboratory and receiving his B.S. in physics from Idaho State University in 1999. He is the chief technology officer for Global Technologies Incorporated and is a member of the INMM.

authors wish to express their appreciation to all the students and other facility staff who had the unique opportunity to assist in the movement of irradiated TRIGA® fuel.

The support of Idaho National Engineering and Environmental Laboratory personnel must be acknowledged: James W. Sterbentz for the ORIGEN TRIGA® reactor cross-section sets; and Lance Cole, Douglas Toomer, and Brion Bennett for their efforts to pursue transport and destructive analysis of the two FLIP elements located at TAMU.

Finally, the efforts of Terri Towler of GTI to ship the DEUS equipment to the above facilities are appreciated.

References

1   U.S. DOE. 1996. Final Environmental Impact Statement, Proposed Nuclear Weapons Nonproliferation Policy Concerning Foreign Research Reactor Spent Nuclear Fuel, Appendix B: Foreign Research Reactor Spent Nuclear Fuel Characteristics and Transportation Casks, *DOE/EIS-0218F, Volume 2,* p. B-3.

2   General Atomics Web site—http://triga.ga.com.

3   Fouquet, D. M., J. Ravzi, and W. L. Whittemore. 2003. TRIGA Research Reactors: A Pathway to the Peaceful Applications of Nuclear Energy, *Nuclear News,* 46-56.

4   Tomsio, N. 1986. Characterization of TRIGA Fuel, *GA Project 3442, GA-C18542,* pp. 1-1 to 3-31.

5   2003. Monte Carlo N-Particle Transport Code System, *Versions 4B2, 4C, and 5, CCC-710, Radiation Safety Information Computational Center.*

6   Beddingfield, D. H., H. O. Menlove, and N. H. Johnson. 1999. Neutron Proportional Counter Design for High Gamma-Ray Environments, *Nuclear Instruments and Methods in Physics Research A 422,* 35-40.

7   Personal communication with Michael Krause. October 2003. Reactor Supervisor, University of Texas Nuclear Engineering Teaching Laboratory.

8   1991. Oak Ridge Isotope Generation and Depletion Code-Matrix Exponential Method, *Version 2.1, CCC-371, Radiation Safety Information Computational Center.*

9   1996. Kernel Integration Code System for General Purpose Isotope Shielding Analyses, *Version 2.1, CCC-636, Radiation Safety Information Computational Center.*

10   Personal communication with J. W. Sterbentz. February 15, 1999. Lockheed Martin Idaho Technology Company.

11   Sterbentz, J. W. 1997. Radionuclide Mass Inventory, Activity, Decay Heat, and Dose Rate Parametric Data for TRIGA Spent Nuclear Fuels, *INEL-96/0482.*

12   2000. Microcal ORIGIN, Version 6.0, *Microcal Software Inc.*

13   Stuart, Jr., N. W. and J. H. Fallet. 1979. Material Flow and Inventory data for a U-Zr-Hydride Fuel Element Fabrication Plant, GA-C15113, General Atomic Project 3293. (only six pages available).

14   Personal communication with Fortunado Aguilar. May 2001. Reactor Chief, ININ.

15   1979. Safety Analysis Report for the Nuclear Science Center Reactor, Texas A&M University.

16   Personal communication with Michael Spellman and Bill Asher. November 2000. Reactor Supervisor and Senior Reactor Operator, respectively, Texas A&M University Nuclear Science Center.

Nuclear Material Protection, Control, and Accounting in China: An Evaluation of the Current System and Recommendations for Improvement

Hui Zhang
Kennedy School of Government, Harvard University, Cambridge, Massachusetts U.S.A.

Abstract

The September 11, 2001, large-scale terrorist attack shows that the threat of nuclear terrorism is real. The acquisition of the capability to explode a nuclear device would be very appealing for terrorists who are bent on causing mass destruction. Indeed, Osama bin Laden has stated that acquiring nuclear weapons is a "religious duty" and there is evidence that Al Qaeda has sought nuclear weapons. Recent seizures of stolen weapons-usable HEU and plutonium make clear that establishing modern, well-designed nuclear material protection, control, and accounting (MPC&A) systems to secure nuclear material everywhere is critical to prevent against nuclear proliferation and nuclear terrorism. In particular, following the collapse of the Soviet Union, it has become clear that to reduce this risk all states with civilian or military nuclear facilities need effective MPC&A systems. The nuclear security crisis in Russia has raised concerns that China might also have some weaknesses in its nuclear controls. China's MPC&A system is thought to be similar to Russia's, which in the past depended chiefly on security personnel and relatively little on radiation detectors or measurements. Since the 1960s, China has established a complete military nuclear fuel cycle, and China is establishing a complete civilian fuel cycle as well. Fissile materials are stored at a number of facilities across the country for this military system. China needs an adequate MPC&A system in both the military and civil sectors to secure and account for its fissile materials. The work will assess the current status of MPC&A in China, analyze existing regulations and administrative systems, and recommend steps for improvement, including international cooperation.

Introduction

China began its nuclear industry for defense purposes in the 1950s. Since the 1960s, China has established a complete military nuclear fuel cycle for plutonium and HEU production. Beginning in 1963 China produced HEU at Lanzhou and Heping gaseous diffusion plants (GDP). Both plants stopped HEU production in 1987. It is estimated that both GDPs produced between fifteen to twenty-five metric tons of HEU.[1] Since the late 1960s, China produced its plutonium at Jiuquan Atomic Energy Complex (closed down in 1984) and Guangyuan plutonium production complex (shut down in 1991). It is recently estimated that China produced between two and five metric tons of plutonium.[1] Approximately one to two tons of plutonium and about 9-13.5 tons of weapons-grade uranium could be contained in about 400 nuclear warheads.[2] Chinese non-weapons uses of HEU and plutonium are very limited. Its nuclear-power submarines are reported to be fueled with LEU.[3] In addition, China is operating two centrifuge enrichment plants at Hanzhong and Lanzhou, which produce LEU for civilian purposes.

In 1979 China's nuclear industry switched its focus to civilian nuclear power. China's first nuclear power reactor, Qinshan-I, went online in 1991. Now China is operating three PWRs providing 2.1 GW of nuclear capacity. Another eight reactors are under construction and will be online before 2005. Since the mid-1980s, China has planned to use a closed fuel-cycle strategy to reprocess the resulting civilian spent fuel.[4] In July 1997 China began the construction of a multi-purpose reprocessing pilot plant (50 tHM/a) at Lanzhou. This plant will start operations soon. Moreover, in May 2000 China started construction on the 25 MWe China Experimental Fast Reactor (CEFR), located near Beijing. It will be in commission around 2005. In short, currently China has little use of weapons-usable fissile material for civilian purpose, except a small amount of HEU to fill its several research reactors. Thus, beyond those HEU and plutonium contained in weapons, the remaining China's weapons-usable fissile material could be mainly contained at approximately a dozen of sites including those HEU and plutonium production facilities, nuclear weapons design and production facilities, and some research reactors. Therefore, HEU and plutonium at these facilities should be adequately secured and accounted for.

China's MPC&A Systems

From the beginning, China's nuclear materials production and management was strictly controlled by the military sector. After China became an International Atomic Energy Agency (IAEA) member in 1984, it established material control and accounting (MC&A) systems in accordance with IAEA safeguard guidelines (INFCIRC/153) and physical protection system based on INFCIRC/225 recommendations. Thus far, no nuclear material

sabotage or thefts had occurred in China.[5] Moreover, China has signed a number of international agreements related to fissile material control. In 1988 China signed an agreement (INF-CIRC/369) with the IAEA to voluntarily place some of its facilities under IAEA safeguards. Currently, China has three facilities under IAEA safeguards: the Qinshan-1 nuclear power reactor, a high-temperature research reactor, and a CEP at Hanzhong.[6] In 1989 China acceded to the 1980 Convention on the Physical Protection of Nuclear Material. In 1994, China formulated the Regulations for Physical Protection of Nuclear Materials in International Transport of the People's Republic of China. In 1998, China signed the Guidelines for the Management of Plutonium that establish requirements for the management and disposition of civil plutonium and other plutonium no longer necessary for defense. China signed an additional protocol with the IAEA in January 1999.

Legal/Regulatory Structure

In 1987, China approved and issued the Regulations for Control of Nuclear Materials of the People's Republic of China (Regulations).[7] China's Ministry of Nuclear Industry (MNI) was authorized to implement the Regulations. In order to facilitate the implementation of the Regulations, in 1990 China approved and issued the Rules for Implementation of the Regulations on Nuclear Materials Control of the People's Republic of China (Rules).[8] The China National Nuclear Corporation (CNNC) established on the ground of MNI in 1988 was authorized to implement the Rules. The State Council charges the CNNC with certain governmental functions in the nuclear issues under the name of the China Atomic Energy Authority (CAEA). The National Office for the Nuclear Material Control (ONC) under CAEA was responsible for the control of nuclear material. Following the government reorganization begun in March 1998, the CAEA was independent from CNNC. Now the CAEA is responsible for the control of nuclear material for the whole country.[9] ONC under the CAEA is responsible to elaborate the rules and regulations, and specifications for the control of nuclear materials; to exercise nuclear materials control nationwide, establishing the nationwide accounting system of nuclear materials, and to check the accounting balance management, physical protection, and secrecy of the licensee.

The current legal framework for China's MPC&A is based on the 1987 Regulations and the 1990 Rules. As stated, the goals of the Regulations are to ensure the safety and lawful uses of nuclear materials; to prevent theft, sabotage, loss, unlawful diversion, and unlawful use; to protect the security of the state and the public; and to facilitate the development of nuclear undertakings. Concrete measures are formulated in the 1990 Rules. As stated, the Rules are applied to the application, renewal, assessment, approval, and issuing of nuclear material licenses; to accounting for and control of nuclear material, and to the physical protection of nuclear material.

The ONC has adopted a licensing system for the control of nuclear material including plutonium, uranium, tritium, and lithium-6. As required, operators of nuclear material facilities must apply for a nuclear material license if it holds more than ten effective grams of U-235 or any quantity of plutonium. The accumulated amounts of allocation or production that are less than specified may be exempted from applying licenses, but must be registered. To get the license, the operator must establish MPC&A systems that meet the regulation guidelines provided by CAEA. After the ONC accepts the application of license, it offers the reviewer comments, and the license is issued after being reviewed and approved by the NNSA for civilian use or the COSTIND (now the new COSTIND) for military use.

The license is valid for three years. The ONC will then thoroughly review the practice of the nuclear material control in each facility every three years. The ONC is responsible for organizing professional experts to inspect nuclear facilities to ensure that effective security and accounting measures for weapons-usable materials are in place.[10] If a facility is found in violation of the regulations, it could receive a warning or penalty, or its license could be revoked depending on the severity of the violation. The extent of punishment is influenced by one of the following factors:
- Producing, using, storing, and disposing of nuclear material without approval or in violation of the provisions of regulations
- Making a report that is not in accordance with the rules or that is false in terms of facts and information
- Rejecting supervision
- Management that is not in accordance with rules that causes an accident

If an accident with a serious consequence occurs, i.e., theft, plundering, or sabotage of nuclear material, it will be investigated to determine if there is criminal responsibility according to the law.

Material Control and Accounting Measures

As the 1990 Rules required, the licensee must establish a material balance system that includes provisions stating that the licensee must divide the nuclear facilities into separate material balance areas in according with their respective feature; the balance will be performed according to the classification of nuclear material, each balance area shall have a complete accounting system, and perform the independent material balance. Also, the licensee must establish nuclear material physical inventory procedures with requirements including conducting a complete and strict physical inventories at least once annually and conducting physical inventory for such material as Pu-239, U-233 and HEU at least twice annually, prescribing a closing time for record and report, and conducting physical inventories during the prescribe time, establishing the physical inventory plan and procedures, and supervising in the course of inventory, ensuring the accuracy and reliability of inventory. Moreover, the licensee must establish a record and reporting system, which requires that the record of nuclear material accounting must be clear, accurate, systematic, and complete, and must be maintained at least for five years.

Since 1991, the nuclear material accounting forms were revised in accordance with international standards (see Table 1).[11] Moreover, in the mid-1990s each facility began using computer systems for material accounting.[12] China is now developing a national computerized accounting system to maintain physical inventory.

Table 1: The main forms used in China for accounting reports

Code of form	Name of form	Notation
NMF-R01	Nuclear Material Transaction Report	Similar to the U.S. DOE/NRC Form-741 (which requests information necessary for documenting and reporting transactions involving nuclear material)
NMF-R03	Nuclear Material Inventory Change Report	Similar to IAEA Form ICR (which provides details of all receipts and shipments of nuclear material in each category)
NMF-R04	Physical Inventory Taking	Similar to IAEA Form PIT (which includes a detailed list of nuclear material existing in a facility's inventory at a given point in time)
NMF-R05	Nuclear Material Balance	Similar to IAEA Form MBR (showing the material balance based on a physical inventory of nuclear material actually present in the material balance area)

Physical Protection Measures

China's legal framework incorporated physical protection standards based mainly on INFCIRC/ 225. Since September 11, China has taken some measures to strengthen physical protections, in particular in its management approach aspects. Moreover, CAEA is considering upgrading its MPC&A regulations.[13] China divides its protection requirements for nuclear material into three categories, based on type, quantity, and harmfulness of the nuclear material. These categories are even stricter than that of IAEA guidelines in terms of the limit of material quantity. Based on China's regulation, the fundamental requirement for using and storing nuclear material include: persons designated for access to nuclear material must be examined, and those unqualified persons should be replaced quickly, regularly inspect the implementation of measures, remove hidden dangers,

stop up the weakness, and ensure security; report to the local public security organ the protection measures of nuclear material and consult and coordinate emergency programs with the organ; security personnel must be strictly trained, equipped with necessary equipment and instruments, and must quickly interfere, stop malevolent action, and promptly report in case of sabotage, plunder, and theft.

Besides the concrete protection measures for nuclear material at fixed sites (see Table 2), the domestic transport of nuclear material has also required some protection measures. For instance, shipments of Category I nuclear material must be accompanied by an armed escort and information on the route, time, starting point, and arrival point kept secret.

Some Concerns About China's MPC&A System

Some security experts are concerned about the potential weaknesses of China's MPC&A system. In general, China's MPC&A system is thought to be similar to Russia's, which in the past depended chiefly on "guards, guns, and gates" instead of application of modern safeguard technologies.[14] The nuclear security crisis in Russia since 1991 has raised concerns that China's MPC&A system would be vulnerable to an insider threat.[15] Moreover, even China regulates its system in accordance with NPT safeguard guidelines, the NPT safeguards was not designed to prevent thieves who want to steal weapons-usable nuclear material and sell it on the black market.

Indeed, the possible theft of fissile material by an insider cannot be ruled out. The approach of nuclear material control that mainly relies on social controls and the loyalty of workers was very effective in China to prevent insider thefts in the past. However, this situation has changed in recent years. For example, two decades ago the central government strictly controlled the flow of people through the strict registered permanent resident system that made constant surveillance of personnel by the public security department easy. There was relatively little difference of workers' wages in varied fields. The people were encouraged to focus on spirit education. All this led to low crime rate and poor criminal technique. Since China's economic reforms launched in 1978, however China's society has become more open and market-oriented, which results in a greater flow of people and a larger gap between rich and poor. All these changes would increase the criminal threat and offer more opportunities for theft and smuggling by criminal elements.

Outside terrorist attacks may someday pose another threat to China's nuclear facilities. The terrorist forces of the so-called East Turkestan, which have close links to international terrorism, have long been recipients of training, financial assistance, and support from international terrorist groups. Recently they have caused a lot of incidences of terror and violence in China with bomb attacks and assassinations. The possibility that these terrorist

Table 2: Categorization of fissile material and physical protection measures for fissile material at fixed sites

	Categorization of fissile material	Physical protection measures
Category I	• 2 kg or more unirradiated Pu; • 5 kg or more HEU	• At least two complete, reliable physical barriers; vault or special security container for storing Category I nuclear material • The technical protection system with alarm and monitoring installations • 24-hour armed guard • Special pass for all people entering the site; Strict control on non-site personnel to access with the procedure of registration, and full time escorted by the site-personnel after access. • Vault is performed by "double men and double lock" system
Category II	• Less than 2 kg but more than 10 g unirradiated Pu • Less than 5kg but more than 1kg HEU • 20 kg or more unirradiated U-235 (10% but less than 20%) • 300 kg or more unirradiated U-235 (enriched to less than 10%; not including NU&DU)	• Two physical barriers with one is complete and reliable; a "strong room" or "solid container" type storage area • Alarms or surveillance protection equipment provided in vital areas • Armed guards or specially assigned persons watching out day and night • Special pass for all people entering the site
Category III	• 10 g or less unirradiated Pu; • 1kg or less but more than 10 g HEU • 1kg or more but less than 20 kg unirradiated U-235 (10% but less than 20%) • 10 kg or more but less than 300 kg unirradiated U-235 (enriched to less than 10%; not including NU&DU)	• One complete and reliable physical barrier • Specially assigned persons for watching or letting nuclear material be placed in security containers

forces might attempt to attack nuclear material facilities in the future must not be excluded. Moreover, China's existing physical protection system for nuclear material (possibly based on INF-CIRC/225 Rev. 2) could not be designed to defeat the September 11-type threat. In addition, China's physical protection regulations could lack vulnerability assessments and realistic test procedures. Indeed, as some Chinese scholars have pointed out, before 1998 the concept of vulnerability analysis of physical protection did not get attention. As they pointed out, before that time there was no evaluation and theoretical analysis about physical protection systems. Such physical protection systems "mainly relied on people (especially the PLA or armed police)."[16]

Finally, an effective MPC&A system needs modern equipment and techniques, such as portal monitors to detect fissile materials or weapons leaving or entering a site and tamper-indicating seals on nuclear material containers. However, these modern MPC&A techniques would be very expensive. As a developing country, China is focusing on economic development. Thus, although China could have recognized the importance of the mixed approach, combining personnel with techniques, China lacks the resources (including money, appropriate equipment, and techniques) needed for effective security and accounting for all its nuclear material facilities.[17] Also, some analysts are further concerned that China's limited financial resources have often caused it to place safety and security as lower priorities compared to other objectives when allocating its financial and personnel resources. In addition, some officials even do not realize the need of stringent MPC&A standards ensuring the security of nuclear material because they are satisfied with the current systems that worked well in the past. Moreover, some scholars are concerned that China's MPC&A regulations could in practice be difficult to enforce.[18] In particular, the decentralization and pursuit of economic interest could encourage nuclear operators to be unwilling to follow the strict nuclear regulations. Meanwhile, economic reform and the decentralization could decrease the ability of the government to control those nuclear facility operators.

Recommendations For Improving China's MCP&A System

China should take necessary steps to develop and install comprehensive, effective, technology-based MPC&A systems to ensure that all its stockpiles of HEU and plutonium are secured and accounted for at standards adequate to defeat the threats it is likely to face. It is recommended here and suggested that the following measures should be taken to improve China's existing MPC&A systems.

Using proven and modern methods and technologies for its MC&A systems. For example, all sites with HEU or separated plutonium should be equipped with portal monitors at every entry/exit point to detect attempts to remove nuclear material. All weapons-usable materials should be stored in containers closed with unique, identifiable, and traceable tamper-indicating seals that would be difficult to break and replace without detection. All areas where weapons-usable fissile materials are stored should be continuously monitored (e.g., with television cameras, motion detectors, and alarms). Each facility doing bulk processing (e.g., fuel fabrication, enrichment, and reprocessing) of weapons-usable materials should conduct detailed and accurate measurements of the material that arrives, the material produced, the in-process inventory, and all of the material lost to scrap and waste. Reliable and accurate measurement methods and equipment for material accounting should be used.

Reexamining and updating its guidelines for physical protection for sites with HEU and plutonium. For example, China should review and upgrade the basis it uses for designing physical protection for nuclear material facilities to ensure that it reflects the threat as perceived after September 11. To protect from outsider attacks, feasible and cost-effective physical protection systems should be developed and used. For example, all sites with weapons-usable fissile material should be equipped with perimeter intrusion detection systems to detect any outside attackers entering the protected area.

Developing vulnerability assessments. A system of regular vulnerability assessment and realistic performance tests should be established to monitor each site's ability to protect itself against the threat it is designed for. For example, a system of regular vulnerability assessment would be designed to find the weakest points in the security system, to identify the highest-priority and most cost-effective security and accounting improvements that could be made, and to consider whether the security system in place would work successfully against the threat it was designed to counter. Moreover, occasional tests should be conducted to examine whether the security system succeeds in blocking a particular attempted theft.

Trained personnel. To ensure that modern MPC&A systems are actually implemented effectively, trained personnel and the safeguards culture is imperative. China should hold regular training programs, not only to improve workers' professional skills, but also to make workers understand that security and accounting for nuclear materials is a matter of the highest national security priority. Moreover, it is necessary to have a program to ensure the reliability of the personnel who operate the system, including security screening.

Strengthen cooperation. Insecure nuclear material anywhere is a threat to everyone, everywhere. International cooperation should be strengthened to secure and account for nuclear material anywhere. This is essential to prevent nuclear terrorism and proliferation. To improve China's MPC&A system as quickly as possible, China needs cooperation with countries with advanced MPC&A safeguards and techniques. The United States and China conducted a lab-to-lab collaborative program from 1995 to 1998, which was designed to help create a "safeguards culture" in China by demonstrating the advantages of a modern MPC&A system.[19] The program held several workshops at Beijing on MPC&A techniques and in 1998 a demonstration facility for modern MPC&A technology was installed at the China Institute of Atomic Energy in Beijing to demonstrate to attending Chinese government and nuclear industry officials how technologies could be integrated in a comprehensive system for protecting nuclear materials. However, the program ceased in the aftermath of the 1999 Cox Committee Report and allegations of Chinese espionage at U.S. nuclear weapons laboratories.

Since September 11, the cooperation between the United States and China on fighting against terrorism should provide an opportunity to restart the lab-to-lab program on MPC&A. Since September 11, U.S. President George W. Bush has stated that keeping weapons of mass destruction out of terrorist hands is his administration's "highest priority." In his 2003 State of Union address, he said, "We will do everything in our power to make sure that day never comes."[20] In practice, the United States has begun exploring MPC&A cooperation with other states outside the former Soviet Union, including China, India, and Pakistan.[2] Congress has moved to authorize MPC&A cooperation with any country where it may be needed. Meanwhile, since September 11, the Chinese government stated clearly that it fights all kinds of terrorism including nuclear terrorism. China believes that every government has the duty to protect against nuclear terrorism and the international community should strengthen the cooperation in activities of anti-nuclear terrorism. As the Chinese official stated, "We look forward to cooperating with other member states and the International Atomic Energy Agency in the protection against nuclear terrorism."[21] In practice, since the lab-to-lab program ended in 1999, China has never given up the chances for international cooperation on nuclear security issues.[22] Recently China was involved in a number of activities on MPC&A safeguards, including a December 2004 IAEA workshop held in Beijing where approaches for securing nuclear material were discussed and in which U.S. experts gave some lectures.

The lab-to-lab program between the United States and China should take a step-by-step approach starting from less sensitive issues. As a first and an important step, China should initiate a program to train Chinese MPC&A operators, managers, and regulators. This could involve seminars, workshops, and site visits to demonstrate the advanced MPC&A techniques and

methods. The U.S. government has accumulated invaluable experience (including successes and mistakes) over the last two decades on improving its MPC&A systems. For example, the United States has developed techniques for comprehensively assessing the vulnerabilities of security and accounting systems for all its nuclear sites, and then fixing those weaknesses.[23] The U.S. experience should be very helpful to China to quickly modernize its nuclear material security and accounting. Moreover, the program should help introduce modern technical standards and norms for improving China's MPC&A system, to develop and apply modern MPC&A techniques and methods, and to establish inspection techniques.

Hui Zhang has been a research fellow of the Science, Technology and Public Policy Program in the Belfer Center for Science and International Affairs at Harvard University's John F. Kennedy School of Government since September 1999. His research includes verification techniques of nuclear arms control, the control of fissile material, nuclear safeguards and nonproliferation, and policy of nuclear fuel cycle and reprocessing. He received his Ph.D. in nuclear physics specializing in nuclear arms control physics from the Beijing Institute of Applied Physics and Computational Mathematics. From 1997-99, he was a postdoctoral fellow at the Center for Energy and Environmental Studies, Princeton University, and in 1998-99, he received a postdoctoral fellowship from the Social Science Research Council, a MacArthur Foundation program on international peace and security. While at Princeton, he worked with professor Frank von Hippel on FMCT verification issues.

Zhang is the author of several technical reports and book chapters, and dozens of articles in academic journals and the print media including Science and Global Security, *and the* Nonproliferation Review. *Zhang gives many oral presentations and talks at international conferences and organizations. Zhang is a member of the Institute of Nuclear Materials Management.*

Acknowledgement

References

1. Albright, David. 1997. *Plutonium and Highly Enriched Uranium 1996.* Oxford University Press.
2. Wright, David, and Lisbeth Ground. 2003. Estimating China's Production of Plutonium for Weapons. *Science & Global Security,* No.1.
3. See, e.g. Albright, et al., *Plutonium and Highly Enriched Uranium 1996;* NRDC Nuclear Notebook, 2001; Chinese Nuclear Force, 2001; Bulletin of Atomic Scientists, No. 5.
4. Norris, Robert. 1994. *Nuclear Weapons Databook Volume V: British, French, and Chinese Nuclear Weapons.* Westview Press.
5. Zhang, Hui. 2001. Economic Aspects of Civilian Reprocessing in China. *Proceedings of the 42nd Annual Meeting of the Institute for Nuclear Materials Management.*
6. See details at CAEA Web site: http://www.caea.gov.cn/controls/hbkszs.htm as of June 16, 2003.
7. See IAEA Annual Reports for 2001: http://www.iaea.org/worldatom/Documents/anrep2001/table_3.pdf.
8. 1987. Regulations for Control of Nuclear Materials of the People's Republic of China. Chinese version is available at CAEA Web site: http://www.caea.gov.cn.
9. 1990. Rules for Implementation of the Regulations on Nuclear Materials Control of the People's Republic of China. The National Nuclear Safety Administration, the Ministry of Energy, and the Commission of Science, Technology, and Industry for National Defense, September 25, 1990. Chinese version is available at CAEA Web site: http://www.caea.gov.cn.
10. See details at CAEA Web site: http://www.caea.gov.cn.
11. Communications with CAEA official at Beijing, June 2003.
12. Zhang, Xingqian. 1998. China's Practice of Nuclear Control, in A Comparative Analysis of Approaches to the Protection of Fissile Materials. *Proceedings of the Workshop at Stanford University,* July 28-30, 1997 (Livermore, CA: LLNL, 1998).
13. Zhu, Qinsheng. 1994. *A Brief Overview on State Systems of China Nuclear Material Control.* CAEA, Office of Nuclear Material Control, June 1994.
14. Communications with CAEA official at Beijing, June 2003.
15. Prindle, Nancy. 1997. "U.S. China on Nuclear Arms and Nonproliferation: Building on Common Technical Interest," in James Brown, ed., *Arms Control Issues for the Twenty-First Century* (Albuquerque, NM: SNL Publication, SAND97-2619, 1997).
16. Busch, Nathan. 2002. China's Fissile Material Protection, Control, and Accounting: The Case for Renewed Collaboration. *Nonproliferation Review,* Fall/Winter 2002.
17. Tang, Dan, Yin Xiangdong, Fang Ni, and Guo Cao. 2002. Physical Protection System and Vulnerability Analysis Program in China. Presentation at the *8th ISODARCO Conference on Arms Control,* Beijing, October 2002.
18. Communications with Chinese nuclear security experts at Beijing, May 2003.
19. Hsu, Wen L. 1999. The Impact of Government Restructuring on Chinese Nuclear Arms Control and Nonproliferation Policymaking. *Nonproliferation Review,* fall 1999.
20. See details, e.g., Prindle, Nancy. 1998. The U.S.-China Lab-to-Lab Technical Exchange Program, *Nonproliferation Review,* Spring/Summer 1998.

21. Bush, George W. 2003. 2003 State of the Union Address. Office of the Press Secretary, Press release, January 28, 2003; available at http://www.whitehouse.gov/news/release/2003/01/20030128-19.html.

22. See details in Bunn, Matthew, Anthony Wier, and John Holdren. 2003. *Control Nuclear Warheads and Materials: A Report Card and Action Plan,* Washington, D.C.: Nuclear Threat Initiative and the Projection Managing the Atom, Harvard University, March 2003. Available at http://www.nti.org/cnwm.

23. 2001. Statement by Ambassador Zhang Yishan on the Issue of Protection against Nuclear Terrorism at the November Board of Governors Session, IAEA Nov. 30, 2001. Available at http://www.fmprc.gov.cn/eng/23960.html.

24. Communications with CAEA expert at Beijing, May 2003.

25. Bunn, Matthew. Measures to Modernize Security and Accounting for Nuclear Materials: Learning from Past U.S. Problems and Solutions. Unpublished paper.

Figure 1.
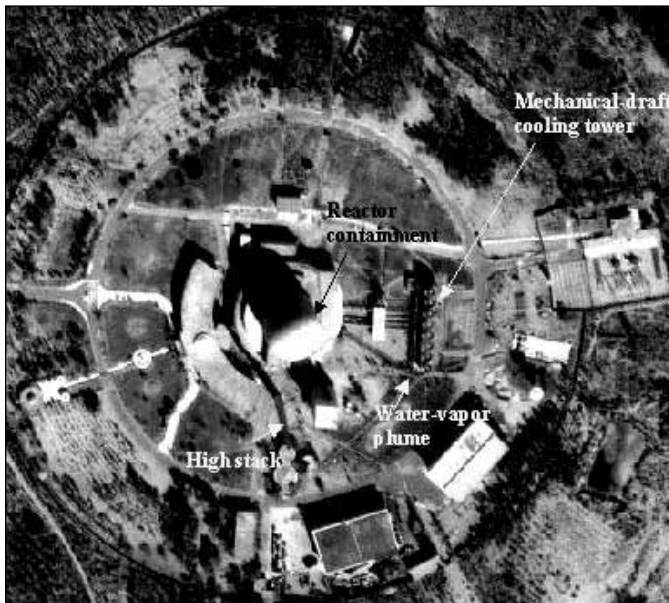
Figure 2a.

Figure 2b.

Figure 3a..

Reprocessing building

Ventilation vent

High stack

Presumed material processing building

High stack

pent fuel ask port

Credit: Space Imaging

Figure 3b..

Reprocessing building

Stack's shadow

Stack

Trucks and casks

Credit: Spaceimaging.com

Figure 4..

Water-vapor plumes

X-330 building

X-333 building

X-326 building
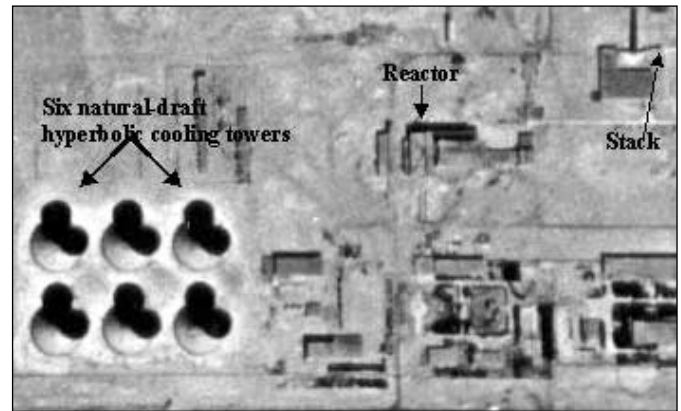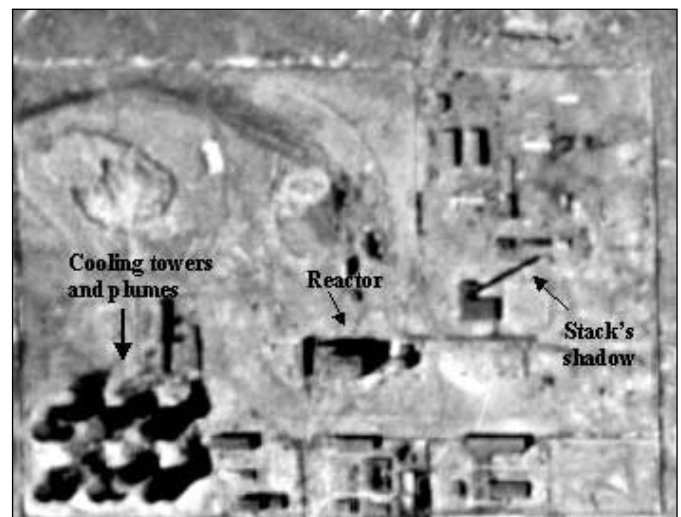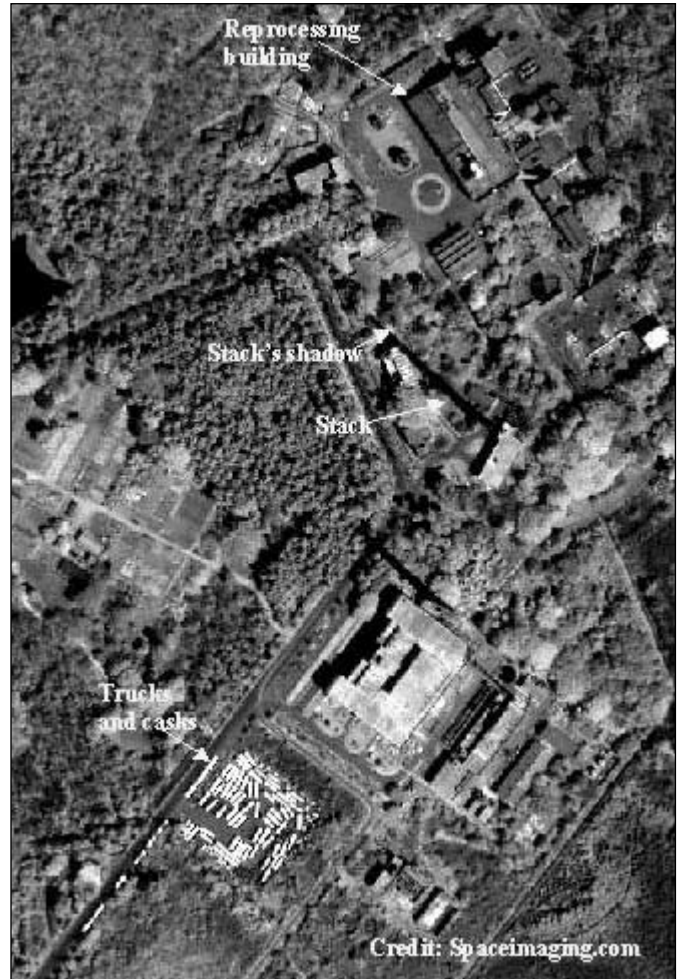
⚛ DOE to Test Licensing Process

In November 2004, the U.S. Department of Energy (DOE) announced awards to two nuclear utility-led consortia under the Nuclear Power 2010 program. DOE will begin the first phase of Nuclear Plant Licensing Demonstration projects with industry teams led by Richmond, Virginia-based Dominion and Chester County, Pennsylvania-based NuStart Energy. These projects are designed to demonstrate the U.S. Nuclear Regulatory Commission (NRC) process for licensing the construction and operation of new Generation III+ nuclear power plants.

The projects will demonstrate the untested combined Construction and Operating License (COL) regulatory process and will enable the power generation companies to make firm business decisions on ordering and building new nuclear power plants.

The projects were proposed by Dominion and NuStart Energy in response to a Nuclear Power 2010 program financial assistance solicitation issued by DOE on Nov. 20, 2003.

⚛ Battelle Energy Alliance Wins Contract for Nuclear Energy and Technology Lab

The U.S. Department of Energy has selected the Battelle Energy Alliance, LLC, to establish the Idaho National Laboratory as the United States' premier laboratory for nuclear energy research, development, demonstration, and education within a decade.

The Idaho National Laboratory will combine the research and development components of the Idaho National Engineering and Environmental Laboratory and Argonne National Laboratory West. The Idaho National Laboratory will begin operating under this new name and contract in February 2005. The term of the contract is ten years and has an estimated value of $4.8 billion. BEA, owned by Battelle Memorial Institute, teamed with several institutions, including Battelle Memorial Institute, BWXT Services Inc., Washington Group International, the Electric Power Research Institute, and the Massachusetts Institute of Technology.

The Idaho National Laboratory will conduct science and technology across a wide range of disciplines. As a multi-program laboratory, the INL will establish strong programs in areas such as materials, chemistry, environment, and computation and simulation. The lab will also play a key role in ensuring the nation's security by applying its technical expertise to helping protect the country's critical infrastructure and preventing the spread of nuclear material.

The laboratory will also lead the establishment of the Center for Advanced Energy Studies, a collaboration of the DOE, the state of Idaho, the laboratory, and universities in Idaho and across the country

A second major contract at the Idaho site will focus on completing the cleanup mission in Idaho. This procurement is ongoing.

⚛ DOE Extends Acceptance Policy for Spent Nuclear Fuel from Foreign Research Reactors Under GTRI

The United States has extended a policy that has enabled it to recover nearly 500 kilograms of uranium-235—enough to build about twenty crude nuclear weapons—in U.S.-origin highly-enriched uranium (HEU) used to fuel foreign research reactors. The U.S. Department of Energy's (DOE) decision to extend the period for spent fuel acceptance will provide additional time for research reactors to convert from HEU to low-enriched uranium (LEU) fuel.

The current acceptance policy, established by DOE and the State Department in 1996, permits the United States to accept certain eligible spent fuel that is irradiated by May 2006, and returned to the United States by May 2009. A revised record of decision, signed by National Nuclear Security Administration (NNSA) Administrator Linton Brooks on November 22, 2004, extends the irradiation deadline to May 2016, and the acceptance deadline to May 2019.

Some countries with eligible fuel have not used their fuel as rapidly as projected or have made alternative fuel processing arrangements, and there have been technical delays in the development of LEU alternatives. The acceptance policy is a cornerstone of the DOE Global Threat Reduction Initiative (GTRI), which focuses on minimizing, and, where possible, eliminating the use of HEU in civil applications by converting research reactors to LEU and securing, returning or recovering vulnerable nuclear material. Since 1996, the acceptance program has successfully conducted thirty shipments involving twenty-seven countries, resulting in the safe return of more than 6,300 spent nuclear fuel assemblies.

Research reactors have important medical, agricultural, and industrial applications. Under the Atoms for Peace program established in the 1950s, the United States provided reactor technology to further other countries' research into peaceful uses of atomic energy.

⚛ Two Universities Get Grant for Cooperative Nuclear Ed Program

The U.S. Department of Energy (DOE) has awarded a $375,000 grant to two universities in Ohio to establish a collaborative nuclear engineering program. The partnership between Wilberforce University, a historically black university in Wilberforce, Ohio, and Ohio State University in Columbus, Ohio, one of the nation's premier engineering universities, has been selected through a competitive award process to provide new educational opportunities for undergraduate engineering and science students at Wilberforce University.

The DOE grant, awarded over three years, will allow Wilberforce University to establish an undergraduate minor in nuclear engineering and several outstanding Wilberforce students will enroll in the master's and doctoral program in nuclear engineering at Ohio State University. Under this program, students will learn about the technical and scientific issues associated with nuclear science and engineering and gain the opportunity to enter

one of the highest-paying technical careers in the United States.

This new partnership will involve a significant effort on the part of the faculty members and administrators from both institutions. The program will involve the establishment of a new set of core courses to support the Wilberforce minor degree program, and a distance education initiative. The program will emphasize both nuclear engineering and health physics. The students entering this program will have greater access to Department of Energy (DOE) national laboratories, research programs, and educational assets.

This is the fifth partnership that DOE has helped to establish under the nuclear engineering education program. Under the DOE University Partnership Program, more than fifty students at minority-serving institutions have entered studies in nuclear science and technology.

News Briefs

⚛ Aussies Distribute Anti-Radiation Drugs

An Australian newspaper reported in November 2004 that the Australian government began distributing drugs intended to combat radiation as part of a plan to defend against radiological attack. The government is also distributing radiation detection equipment to Australian states.

⚛ Sandia Chief Proposes Regional Nuclear Alliances

In a commentary in the journal *Nature,* Sandia President and Director C. Paul Robinson proposed that collective security agreements involving nuclear and non-nuclear states could help better protect countries against nuclear threats. The security agreements would be similar to the North Atlantic Treaty Organizaiton (NATO). The proposal is based on the Baruch Plan, originally proposed by Bernard Baruch in the mid-1950s.

March 10–13, 2005
Reasearch Reactor Fuel
Management (RRFM) 2005
Hilton WestEnd Hotel
Budapest, Hungary
Sponsor:
   European Nuclear Society
Contact:
   Dionne Bosma
   Phone: +32 (0)2 505 30 54
   E-mail: dionne.bosma@euronuclear.org
   Web site: http://www.rrfm2005.org

April 17–21, 2005
Monte Carlo 2005: The Monte Carlo
Method: Versatility Unbounded in a
Dynamic Computing World
Chattanooga, Tennessee, U.S.A.
Sponsor:
   American Nuclear Society
   Web site: http://meetingsandconferences.
   com/MonteCarlo2005

May 8–11, 2005
Waste Management,
Decommissioning and
Environmental Restoration for
Canada's Nuclear Activities
Crowne Plaza Hotel, Ottawa,
Ontario, Canada
Sponsor:
   Canadian Nuclear Society
Contact:
   Canadian Nuclear Society
   E-mail: cns-snc@0n.aibn.com
   Web site:
   http://www.cns-snc.ca/waste_05.html

March 16–18, 2005
International Conference on
Nuclear Security:
Global Directions for the Future
Sponsor:
   International Atomic Energy Agency
Contact:
   Web site: http://www.pub.iaea.org/
   MTCD/Meetings/Announcements.
   asp?ConfID=136

June 5–9, 2005
ANS Annual Meeting
Town & Country Hotel and Resort
San Diego, California, U.S.A.
Sponsor:
   American Nuclear Society
Contact:
   American Nuclear Society
   Web site: http://www.ans.org

July 7–8, 2005
Workshop on Developing Physical
Protection Specialists
Phoenix, Arizona, U.S.A.
Sponsor:
   INMM Physical Protection
   Technical Division
Contact:
   David Lambert
   865-574-3900
   E-mail: lambertld@ornl.gov

July 10–14, 2005
46th INMM Annual Meeting
JW Marriott Desert Ridge
Spa and Resort
Phoenix, Arizona, U.S.A.
Contact:
   INMM
   847-480-9573
   Fax: 847-480-9282
   E-mail: inmm@inmm.org
   Web site: http://www.inmm.org

August 7–11, 2005
ANS Topical on Decommissioning,
Decontamination and Reutilization
Hyatt Regency Hotel
Denver, Colorado, U.S.A.
Sponsor:
   American Nuclear Society
   Web site: http://ddrd.ans.org/index_
   meetings.html

October 30 – November 2, 2005
Changing the Safeguards Culture
Hotel LaFonda
Santa Fe, New Mexico, U.S.A.
Sponsor:
   INMM International Safeguards
   Technical Division, INMM Southwest
   Chapter and ESARDA
   Contact: Jim Larrimore
   Phone: 858-509-9604
   E-mail: larrimor1@cs.com

December 11–14, 2005
European Nuclear Conference
(ENC) 2005
Palais des Congres
Versailles, France
Sponsor:
   French Nuclear Society (SFEN)
Contact:
   Silvie Delapace
   Phone: +33 (0) 1 53 58 32 16
   E-mail: enc2005@sfen.fr
   Web site: http://www.sfen.fr